

Copyright
by
Sydney Ilima Ramirez
2015

**The Dissertation Committee for Sydney Ilima Ramirez Certifies that this is the
approved version of the following dissertation:**

**Mechanism of transmissible gastroenteritis virus nsp1-mediated
translation inhibition**

Committee:

Shinji Makino, D.V.M., Ph.D., Supervisor

Roberto Garofalo, M.D.

Barry Rockx, Ph.D.

Bert Semler, Ph.D.

John Wiktorowicz, Ph.D.

David Niesel, Ph.D., Dean, Graduate School

**Mechanism of transmissible gastroenteritis virus nsp1-mediated
translation inhibition**

by

Sydney Ilima Ramirez, B.S.

Dissertation

Presented to the Faculty of the Graduate School of
The University of Texas Medical Branch
in Partial Fulfillment
of the Requirements
for the Degree of

Doctor of Philosophy

**The University of Texas Medical Branch
May, 2015**

Dedication

Jude 1:25 (KJV): “To the only wise God our Saviour, be glory and majesty, dominion and power, both now and ever. Amen.”

Acknowledgements

I appreciate the assistance and support of all those who helped to make this work possible, including my committee members, the Experimental Pathology Graduate Program, especially Dr. Jere McBride and Paula Gabriles, the UTMB M.D.-Ph.D. combined degree program, in particular Dr. Lawrence Sowers and Claiborne Fant, and the UTMB School of Medicine and Graduate School of Biomedical Sciences.

I would like to thank my Ph.D. mentor, Shinji Makino, for the opportunity to work in his laboratory. I would also like to thank all of the members of the Makino laboratory, both past and present, for their assistance in completing my dissertation research, especially Drs. Krishna Narayanan, Kumari Lokugamage, and Cheng Huang.

Without the love and encouragement of my friends and family, I would not have been able to complete this work. I thank my parents for believing in me, for encouraging me to further my education, and for sacrificing their time and work in order to help me. I cannot express how much my husband and our daughter, who have endured late nights and other trials for my sake, have helped me and cheered me on, or how grateful I am for them. Thank you all.

Mechanism of transmissible gastroenteritis virus nsp1-mediated translation inhibition

Publication No. _____

Sydney Ilima Ramirez, Ph.D.

The University of Texas Medical Branch, 2015

Supervisor: Shinji Makino

The non-structural protein 1 (nsp1) proteins of several coronaviruses share a common property to inhibit host gene expression, but use different mechanisms to exert this function. Unlike the nsp1 protein of SARS coronavirus, a group 2b betacoronavirus, the nsp1 protein of transmissible gastroenteritis virus (TGEV), an alphacoronavirus, inhibits the expression of host genes without associating with the 40S ribosomal subunit or inducing the endonucleolytic cleavage of mRNAs. Nsp1 of TGEV strongly inhibits the translation of capped mRNAs, as well as certain internal ribosome entry site (IRES)-containing mRNAs, in HeLa S10 extract but not in rabbit reticulocyte lysate or wheat germ extract. In this dissertation the mechanism of TGEV nsp1-mediated translation inhibition is further elucidated. Immunofluorescence analysis showed that TGEV nsp1 protein localizes to both the nucleus and cytoplasm of expressed cells. TGEV nsp1 can enter the nucleus via passive diffusion because its molecular weight (~9 kDa) is below the passive diffusion exclusion limit of the nuclear pore complex. Both TGEV infection and TGEV nsp1 protein expression inhibit cellular protein synthesis. TGEV nsp1 expression strongly inhibits the expression of reporter genes from transfected reporter plasmids. However, it fails to inhibit the translation of exogenous reporter mRNAs

directly introduced into the cytoplasm. These data, along with other findings discussed in this dissertation suggest that TGEV nsp1 uses one or more factors associated with mRNA-protein complexes that originate in the cell nucleus to inhibit mRNA translation.

TABLE OF CONTENTS

List of Figures	x
List of Abbreviations	xiii
Chapter 1: Introduction	1
Eukaryotic translation	1
Why target protein synthesis?	4
Coronaviruses	7
CoV nsp1	12
Alpha-CoV nsp1	15
TGEV nsp1 (p9).....	16
Beta-CoV nsp1	18
SARS-CoV nsp1	20
Summary (comparison of TGEVp9 & SARS-CoV nsp1)	23
Chapter 2: The effect of TGEV p9 in different cell-free <i>in vitro</i> translation systems	26
Background.....	26
Cell-free <i>in vitro</i> translation systems	26
Initial studies on the effect(s) of TGEV p9.....	29
Materials & methods.....	32
Plasmid & RNA constructs	32
Restriction digestion protocols	33
<i>In vitro</i> transcription protocol	33
Recombinant protein preparation & purification	34
Cell culture.....	36
Protocols for making HeLa S10 [+/- nuclease] & HeLa S100	36
RRL protocol	37
HeLa S10 protocol	38
RRL + HeLa S100 protocol	38
RRL + HeLa S10 protocol	39
Modifications to original <i>in vitro</i> translation protocols	39
Protocol for pre-incubation of protein in HeLa S10	39

Protocol for in vitro translation in HeLa S10 +/- micrococcal nuclease treatment	40
WGE protocol	41
WGE + HeLa S10 protocol	41
48S Complex SGC analysis	41
Results.....	43
Discussion	67
Chapter 3: Subcellular localization of p9.....	70
Background.....	70
Materials & methods.....	75
Cell culture.....	75
Plasmid constructs	75
Transfection protocol	75
Antibodies	76
Confocal immunofluorescence microscopy & image analysis	76
Results.....	78
Discussion	80
Chapter 4: Effect of p9 on nuclear vs. cytoplasmic mRNAs.....	83
Background.....	83
Materials & methods.....	91
Plasmid constructs	91
RNA constructs.....	92
Antibodies	93
Plasmid transfection protocol	93
Electroporation protocol	94
Reporter assays	95
Metabolic labeling protocol	95
SDS-PAGE, CCB staining, autoradiography, and WB protocols	96
Results.....	98
Discussion	108

Chapter 5: Overall Discussion	111
References.....	116

List of Figures

Figure 1: SARS-CoV nsp1 and TGEV p9-mediated translation inhibition in RRL	43
Figure 2: SARS-CoV nsp1 and TGEV p9-mediated translation inhibition in HeLa S10 extract	44
Figure 3: TGEV p9-mediated suppression of HCV IRES-driven translation in RRL	45
Figure 4: TGEV p9-mediated suppression of EMCV IRES-driven translation in RRL.....	46
Figure 5: TGEV p9-mediated suppression of HCV IRES-driven translation in HeLa S10 extract	47
Figure 6: TGEV p9-mediated suppression of EMCV IRES-driven translation in HeLa S10 extract	48
Figure 7: TGEV p9-mediated translation inhibition in WGE.....	49
Figure 8: TGEV p9-mediated translation inhibition in WGE + S10	50
Figure 9: TGEV p9-mediated translation inhibition in WGE.....	51
Figure 10: SARS-CoV nsp1 and TGEV p9-mediated translation inhibition in RRL	52
Figure 11: TGEV p9-mediated translation inhibition in RRL	53

Figure 12: TGEV p9-mediated translation inhibition in RRL	54
Figure 13: TGEV p9-mediated translation inhibition in RRL + HeLa S10.....	55
Figure 14: TGEV p9-mediated translation inhibition in HeLa S10.....	56
Figure 15: Effect of HeLa S10 extract pre-treatment on TGEV p9-mediated translation inhibition in RRL	57
Figure 16: TGEV p9-mediated translation inhibition in nuclease-treated HeLa S10 extract.....	58
Figure 17: TGEV p9-mediated translation inhibition in nuclease-untreated HeLa S10 extract	59
Figure 18: TGEV p9-mediated translation inhibition in HeLa S10 extract.....	60
Figure 19: SGC analysis of 48S complex formation in the presence of SARS-CoV nsp1 and TGEV p9	61
Figure 20: Confocal microscopic analysis of the subcellular localization of TGEV p9 in expressed cells [Adapted from Narayanan et al., 2014]	78
Figure 21: Effect of TGEV p9 on the translation of nuclear-derived rLuc reporter mRNA	98
Figure 22: Effect of TGEV p9 on the translation of nuclear-derived ALA reporter mRNA	99
Figure 23: Effect of TGEV p9 on the translation of cytoplasmic GLA mRNA	100
Figure 24: Effect of TGEV p9 on the translation of cytoplasmic m7 rLuc RNA..	101

Figure 25: Effect of TGEV p9 on the translation of cytoplasmic TGEV m6 102

Figure 26: Effect of TGEV p9 on the translation of cytoplasmic TGEV m7-V5.. 104

List of Abbreviations

3CL ^{pro}	CoV 3C-like protease
5' cap	5'-7-methylguanosine cap
ACE-2	angiotensin-converting enzyme 2
ATCC	American Type Culture Collection
ATP	adenosine triphosphate
BCoV	bovine CoV
BSA	bovine serum albumin
CAT	chloramphenicol acetyltransferase
CCB	colloidal Coomassie blue
CCoV	canine CoV
CMV	cytomegalovirus
CoV	coronavirus
cpm	counts per minute
Crm-1	chromosome region maintenance 1 (aka Exportin 1)
CrPV	cricket paralysis virus
C-terminus	carboxy terminus
CTP	cytidine triphosphate
DAPI	4', 6-diamidino-2-phenylindole, dihydrochloride
Ddx 18	ATP-dependent RNA helicase DDX18
DHX29	ATP-dependent RNA helicase DHX29
DMEM	Dulbecco's modified Eagle medium

DTT	dithiothreitol
E (protein)	envelope (protein)
ECL	enhanced chemiluminescence
EDTA	ethylenediaminetetraacetic acid
eEF	eukaryotic elongation factor
EGTA	ethylene glycol-bis(2-aminoethylether)-N,N,N',N'-tetraacetic acid
eIF	eukaryotic initiation factor
EJC	exon junction complex
EMCV	encephalomyocarditis virus
eRF	eukaryotic release factor
FBS	fetal bovine serum
FIPV	feline infectious peritonitis virus
fLuc	firefly luciferase
GMP-PNP	Guanosine 5'-[β,γ -imido]triphosphate trisodium salt hydrate
GST	glutathione S-transferase
GTP	guanosine triphosphate
HCoV	human CoV
HCV	hepatitis C virus
HEK	human embryonic kidney
HEPES	4-(2-Hydroxyethyl)piperazine-1-ethanesulfonic acid
His	histidine
hnRNP	heterogeneous nuclear ribonucleoprotein particle
HRI	heme-regulated eIF2 α kinase

HRP	horseradish peroxidase
HRV	human rhinovirus
HSV	herpes simplex virus
HSV-TK	HSV thymidine kinase
IAV	influenza A virus
ICP27	mRNA export factor
IFN- β	interferon beta
IGR	intergenic region
IPTG	isopropyl-beta-D-thiogalactopyranoside
IRES	internal ribosome entry site
ISG15	IFN-stimulated gene 15
ISRE	IFN-stimulated response element
IVT	<i>in vitro</i> translation
Kaps	karyopherins-beta
kb	kilobase
KCl	potassium chloride
kDa	kilodalton
KOAc	potassium acetate
LB	Luria-Bertani
M (protein)	matrix (protein)
m6	TGEV mRNA 6
m7	TGEV mRNA 7
MEM	minimum essential medium

MERS-CoV	Middle East respiratory syndrome CoV
Met-tRNA ⁱ	methionyl-transfer RNA
MgOAc	magnesium acetate
MHV	murine hepatitis virus
mRNA	messenger RNA
mRNP	messenger ribonucleoprotein particle
MWCO	molecular weight cut-off
N (protein)	nucleocapsid (protein)
NaCl	sodium chloride
NCBI	National Center for Biotechnology Information
ncRNA	non-coding RNA
NE	nuclear envelope
NES	nuclear export signal
NIH	National Institutes of Health
NLS	nuclear localization signal
NMD	nonsense-mediated decay
NMR	nuclear magnetic resonance
NPC	nuclear pore complex
nsp1	non-structural protein 1
N-terminus	amino terminus
Nups	nucleoporin proteins
NXF1	nuclear RNA export factor 1
NXT1	NTF2-like export factor 1

OD	optical density
ORF	open reading frame
p9	TGEV nsp1
p15	NTF2-like export factor 1
PABP	poly(A)-binding protein
PBS	phosphate-buffered saline
PBST	PBS Tween-20
PEDV	porcine epidemic diarrhea virus
PIC	pre-initiation complex
PKR	protein kinase R
PL1 ^{pro}	CoV papain-like protease 1
PL ^{pro}	CoV papain-like protease
pre-mRNA	precursor mRNA
pro	protease
PTB	polypyrimidine tract-binding protein
PV	poliovirus
PVDF	polyvinylidene fluoride
RBC	red blood cell
RBP	RNA-binding protein
RLB	reporter lysis buffer
rLuc	<i>Renilla</i> luciferase
rpm	rotations per minute
rpS6	ribosomal protein S6

RRL	rabbit reticulocyte virus
rRNA	ribosomal RNA
RVFV	Rift Valley fever virus
S (protein)	spike (protein)
SARS-CoV	severe acute respiratory syndrome CoV
SDS-PAGE	sodium dodecyl sulfate polyacrylamide gel electrophoresis
SGC	sucrose gradient centrifugation
ST	swine testis
SV40	simian (vacuolating) virus 40
TAP	nuclear RNA export factor 1
TBP	TATA-binding protein
TGEV	transmissible gastroenteritis virus
Tris HCl	Tris(hydroxymethyl)aminomethane hydrochloride
tRNA	transfer RNA
tRNA _i	initiator tRNA
TRS	transcription-regulating sequence
UTMB	The University of Texas Medical Branch
UTP	uridine triphosphate
UTR	untranslated region
vhs	virion host shutoff protein
v/v	volume/volume
WB	Western blot
WGA	wheat germ agglutinin

WGE	wheat germ extract
WHO	World Health Organization
x g	g-force
Xrn1	5'-3' exoribonuclease 1
YB-1	Y-box binding protein 1

Chapter 1: Introduction

Proteins are crucial cellular elements that carry out numerous functions, e.g. enzymes that catalyze reactions needed for cellular respiration and other essential processes, chaperones (proteins that aide other proteins in proper folding and subcellular localization), proteins involved in intracellular transport, proteins involved in cytoskeleton formation, maintenance, and function, which aid in cell division, cell structure, motility, and other processes, as well as cellular pumps, cellular receptors and signal transducers, regulators of the cell cycle, regulators of apoptosis, and regulators of the immune response—cytokines, chemokines, etc.—protein hormones, etc. (Walsh and Mohr, 2011). A single gene can encode multiple polypeptides or proteins via alternative splicing and other mechanisms (Mitchell and Parker, 2014). Messenger RNA (mRNA) acts as the intermediary between the blueprint (DNA code) and effector (protein), and its biogenesis and processing is highly regulated (Mitchell and Parker, 2014). However, it has been discovered that mRNA concentration correlates poorly with protein concentration, and that regulation of protein synthesis accounts for much of the regulation of gene expression (Mitchell and Parker, 2014). Proteins are clearly important players in performing, maintaining, and regulating cellular functions. In order to replicate, viruses rely upon the host protein synthesis machinery (Walsh and Mohr, 2011). Thus, viruses must commandeer the host machinery for the synthesis of viral proteins while avoiding or overcoming the host response to infection (Walsh and Mohr, 2011).

EUKARYOTIC TRANSLATION

In cells, translation is the process whereby proteins are synthesized. Eukaryotic translation occurs in three stages (in order): initiation, elongation, and termination (Jackson et al., 2010; Mohr and Sonenberg, 2012; Parsyan et al., 2009; Svitkin et al., 2009). Initiation is the most regulated of the three stages of translation, thereby making it the rate limiting stage (Jackson et al., 2010; Svitkin et al., 2009). Translation initiation is defined as translation events that occur up to 80S subunit formation. Cap-dependent translation requires 12 eukaryotic initiation factors (eIFs), a messenger ribonucleoprotein particle (mRNP), an initiator transfer RNA (tRNA_i), and the 40S and 60S ribosomal subunits, and may require additional accessory factors (e.g. PABP, DHX29) depending upon the specific features of the mRNA being translated, e.g. based on the level of secondary structure present in the 5' end of the mRNA (Jackson et al., 2010). Energy sources, including adenosine triphosphate (ATP) and guanosine triphosphate (GTP) are also needed (Hinnebusch, 2014). Studies designed to identify the minimal eukaryotic translation initiation factors (eIFs) required for (*in vitro*) translation have found that the eIFs 2, 3, 1, 1A, 4A, 4B, and 4F can efficiently promote 48S complex formation on mRNAs containing 5'-untranslated regions (UTRs) without significant secondary structure (Parsyan et al., 2009). Translation of mRNAs that undergo internal ribosome entry site (IRES)-mediated translation initiation requires fewer to none of the eIFs or auxiliary factors necessary for cap-mediated translation initiation (Jackson et al., 2010).

In eukaryotic cells, the endogenous DNA genetic code of the host is used as a template for transcription of mRNA in the nucleus, which is then exported with the help of proteins and other host molecules that recognize structural elements on the mRNA (e.g. 5' cap and 3' poly(A) tail), forming an mRNP complex, a dynamic complex that changes in composition as the mRNA travels along its journey to its cytoplasmic site of translation (Mitchell and Parker, 2014; Muller-McNicol and Neugebauer, 2013). Initiation of eukaryotic cap-dependent translation occurs when the eIF2-GTP-initiator methionyl-transfer RNA (Met-tRNA_i) ternary complex, eIF1 and 1A, eIF3, and eIF5

come together with the 40S ribosomal subunit to form the 43S pre-initiation complex (PIC), which attaches to the mRNA (Hinnebusch, 2014). The PIC is recruited to the 5' end of host mRNAs close to the 5'-7-methylguanosine cap (5' cap) with the help of the poly(A)-binding protein (PABP) and the eIFs 3, 4B, 4H, and 4F (Hinnebusch and Lorsch, 2012). The eIF4F complex is comprised of multiple eIFs: eIF4A, an RNA helicase, eIF4E, the cap-binding protein, and eIF4G, a scaffold protein with binding domains for the other components of eIF4F, as well as PABP, eIF3 and RNA (Hinnebusch and Lorsch, 2012). The interactions of eIF4G with RNA, the cap-binding protein eIF4E and PABP, allow eIF4G to direct the formation of a circular, "closed-loop" structure in which the 5' cap and poly(A) tail of the mRNA are brought in close proximity to one another and work synergistically to stimulate translation (Hinnebusch and Lorsch, 2012; Mitchell and Parker, 2014; Sonenberg and Hinnebusch, 2009; Svitkin et al., 2009).

Once associated with the mRNA, the PIC scans the mRNA (5' to 3') until it reaches the first (AUG) start codon, where the 48S initiation complex is formed and the AUG initiation codon is complementarily base paired with the anticodon of the Met-tRNA_i; this scanning step is not required in cap-independent (e.g. IRES-dependent) translation (Hinnebusch, 2014; Hinnebusch and Lorsch, 2012). Joining of the 60S ribosomal subunit occurs following two consecutive GTP hydrolysis steps that lead to the removal of the eIFs from the 48S complex and the formation of the 80S initiation complex (Kapp and Lorsch, 2004). Elongation then occurs, as the ribosome moves downstream of the translation initiation start site and tRNAs charged with the appropriate amino acids help to build the nascent polypeptide chain together with the help of the ribosome, which has peptidyl transferase activity, as well as eukaryotic elongation factors (eEFs) like eEF1A, eEF1B, and eEF2 (Mohr and Sonenberg, 2012). Eventually, a termination (or stop) codon is reached and recognized by the eukaryotic release factor (eRF) eRF1, and the polypeptide chain is released (Mohr and Sonenberg, 2012; Walsh

and Mohr, 2011). Additionally, the nascent polypeptide can undergo co- or post-translational modifications (Chen and Shyu, 2014; Mitchell and Parker, 2014).

WHY TARGET PROTEIN SYNTHESIS?

There are numerous pathogens capable of interfering with cellular protein synthesis which function at multiple levels (Mohr and Sonenberg, 2012; Walsh and Mohr, 2011; Walsh et al., 2013). Some pathogens are obligate intracellular parasites and rely exclusively upon the host protein synthesis machinery and its regulation to make their own proteins (Mohr and Sonenberg, 2012; Walsh and Mohr, 2011; Walsh et al., 2013). Pathogens are also recognized as “non-self” by the host immune system and are targeted by the cell for destruction (Mohr and Sonenberg, 2012). Thus, in many cases, pathogens must mount a defense to counter the host immune response to ensure their long-term survival (Mohr and Sonenberg, 2012). Sometimes this involves a “counter-attack” by the pathogen (e.g. the pathogen makes its own factors that compete with, inactivate, or otherwise nullify the effect of the host defense factors) (Mohr and Sonenberg, 2012; Walsh and Mohr, 2011; Walsh et al., 2013). Other times, it involves a change in the regulation or even the shut-off of host protein synthesis (Mohr and Sonenberg, 2012; Walsh and Mohr, 2011; Walsh et al., 2013). For obligate intracellular parasites, there is the potential for a difficult balancing act that occurs involving the need of the pathogen to avoid or limit the host immune response and compete with the host cell for the cellular machinery, while at the same time keeping the cell alive and healthy long enough for the pathogen to undergo replication and the other processes needed to ensure its survival (Mohr and Sonenberg, 2012). The pathogen’s ability to affect cellular processes, e.g. protein synthesis, is not only dependent upon the lifespan of the pathogen within a given cell, it is also dependent upon the arsenal of effectors that the pathogen has available to it (encoded in its genome and applicable to the particular infection scenario)

(Mohr and Sonenberg, 2012). In the end, the successful pathogen is the one that is able to access the host machinery to the extent that it needs for the sake of its own processes while evading or overcoming the host's attempt to neutralize or destroy it (Mohr and Sonenberg, 2012). The successful pathogen must reproduce or replicate efficiently before killing or exiting the host cell, thereby increasing the numbers of pathogen present in the host that can then go on to infect other cells or be transmitted to another organism or to the host's offspring (Mohr and Sonenberg, 2012).

Viruses are obligate intracellular parasites that rely on the host cell machinery to carry out the processes necessary for viral transcription, translation, and replication (Mohr and Sonenberg, 2012; Walsh and Mohr, 2011; Walsh et al., 2013). RNA viruses are especially reliant upon the host cell machinery due to their relatively small genomes, which encode a relatively small number of essential genes (Walsh et al., 2013). Studying viral proteins can provide insight into normal cell physiology by observing the effect(s) of viral proteins on normal cellular processes or functions (Walsh and Mohr, 2011; Walsh et al., 2013). The replication of many viruses has been shown to suppress host gene expression; this suppression can occur at multiple levels, including host protein synthesis (Castello, et al., 2011; Clark et al., 1993; Das and Dasgupta, 1993; Everly et al., 2002; Huang et al., 2011; Kamitani et al., 2006; Kempf and Barton, 2008; Kundu et al., 2005; Le May et al., 2008; Mohr and Sonenberg, 2012; Smiley, 2004; Tadeo et al., 2006; Ventoso et al., 1998; Walsh and Mohr, 2011; Walsh et al., 2013). In some cases, viral proteins have been shown to be directly responsible for suppressing host gene expression (Castello, et al., 2011; Clark et al., 1993; Das and Dasgupta, 1993; Everly et al., 2002; Kamitani et al., 2006; Kempf and Barton, 2008; Kundu et al., 2005; Le May et al., 2008; Mohr and Sonenberg, 2012; Smiley, 2004; Tadeo et al., 2006; Ventoso et al., 1998; Walsh and Mohr, 2011; Walsh et al., 2013). Studying the strategies used by viruses to suppress host gene expression can provide useful knowledge for the development of new or more effective ways to diagnose and treat, or to prevent, viral illnesses by identifying

viral effectors involved in virus replication and/or transmission that could be targets for the design of such diagnostic or therapeutic interventions (Walsh and Mohr, 2011; Walsh et al., 2013).

Viral mRNAs must compete with host mRNAs for the host translation machinery (Mohr and Sonenberg, 2012; Walsh and Mohr, 2011; Walsh et al., 2013). Thus, inhibition of host translation can give viral mRNAs a competitive advantage over host mRNAs for access to the host translation machinery (Mohr and Sonenberg, 2012; Walsh and Mohr, 2011; Walsh et al., 2013). Specific inhibition of antiviral gene expression can also aid in viral evasion or suppression of the host antiviral immune response (Mohr and Sonenberg, 2012). Therefore, viral proteins that inhibit host gene expression act as viral virulence factors and can contribute to viral pathogenesis (Mohr and Sonenberg, 2012; Walsh and Mohr, 2011; Walsh et al., 2013). Examples of viral proteins that have been shown to suppress host gene expression include the virion host shutoff (vhs) protein of herpes simplex virus-1 (HSV-1) and HSV-2, the NSs protein of Rift Valley fever virus (RVFV), the 2A^{pro} and 3C^{pro} of polio virus, and the nonstructural protein 1 (nsp1) of the severe acute respiratory syndrome coronavirus (SARS-CoV) (Castello, et al., 2011; Clark et al., 1993; Das and Dasgupta, 1993; Everly et al., 2002; Kamitani et al., 2006; Kempf and Barton, 2008; Kundu et al., 2005; Le May et al., 2008; Smiley, 2004; Tadeo et al., 2006; Ventoso et al., 1998). The HSV vhs protein is an mRNA-specific RNase that interacts with the host initiation factor eIF4H to cleave both viral and host mRNAs, leading to a global reduction in host protein synthesis, including the production of proteins involved in the innate and adaptive immune response (Everly et al., 2002; Smiley, 2004; Tadeo et al., 2006). This makes vhs an important HSV virulence factor for evasion and suppression of the host antiviral immune response (Hinkley et al., 2000; Koppers-Lalic et al., 2001; Samady et al., 2003; Suzutani et al., 2000; Tigges et al., 2006; Trgovcich et al., 2002). The vhs protein also plays an important role in viral replication by regulating HSV gene expression (Smiley, 2004). The observation that mutant viruses

carrying a deletion(s) of the vhs gene are severely attenuated in the HSV mouse model demonstrates the significance of the vhs protein to viral virulence and efficient viral replication (Smiley, 2004). The RVFV NSs protein blocks general transcription, leading to the suppression of host gene expression, and dampening the host innate immune response by inhibiting interferon beta (IFN- β) mRNA transcription (Le May et al., 2008) and promoting PKR degradation (Habjan et al., 2009; Ikegami et al., 2009). The poliovirus (PV) protein 2A^{pro} cleaves the host initiation factor eIF4G, inhibiting (host) cap-dependent translation inhibition, and the PV 3C^{pro} protein cleaves the host transcription factor TATA-binding protein (TBP), shutting off host transcription (Castello, et al., 2011; Clark et al., 1993; Das and Dasgupta, 1993; Kempf and Barton, 2008; Kundu et al., 2005; Ventoso et al., 1998). The SARS-CoV nsp1 protein suppresses host gene expression by inactivating the 40S ribosomal subunit and by modifying the 5' end of capped host mRNAs (Kamitani et al., 2009). SARS-CoV nsp1 alters the host antiviral immune response by suppressing the expression of IFN, as well as antiviral signaling pathways (Narayanan et al., 2008; Wathelet et al., 2007).

CORONAVIRUSES

Coronaviruses (CoVs) are members of the order Nidovirales, family Coronaviridae, subfamily Coronavirinae, genus Coronavirus (de Groot et al., 2011; Gorbalenya et al., 2004; Snijder et al., 2003; Woo et al., 2010; Woo et al., 2012). Coronaviruses are currently assigned to one of four different genera: Alpha-, Beta-, Gamma-, or Deltacoronavirus (de Groot et al., 2011; Gorbalenya et al., 2004; Snijder et al., 2003; Woo et al., 2010; Woo et al., 2012). Previously, these genera were more commonly referred to as groups I to IV. Coronaviruses are positive-sense, single-stranded RNA viruses. The CoV genome is the largest of all the RNA viruses, and is on the order of 30 kilobases in size (range 27-32 kb) (Lee et al., 1991; Lomniczi, 1977;

Lomniczi and Kennedy, 1977). Like all viruses, CoVs are obligate intracellular parasites that utilize the host cellular machinery for viral replication (Mohr and Sonenberg, 2012; Walsh and Mohr, 2011; Walsh et al., 2013). CoVs are known to infect a wide range of mammalian species (Alpha- and Beta-CoVs), including humans, as well as avian species (Gamma- and Delta-CoVs), primarily causing respiratory and/or enteric diseases in susceptible hosts (Jansson, 2013; Weiss and Navas-Martin, 2005).

The species-specificity and host range of a particular CoV is generally limited by the receptor-binding domain(s) of the virus' spike (S) protein, as CoVs typically enter host cells via receptor-mediated endocytosis, which requires a specific interaction between the CoV S protein receptor-binding domain(s) and the cellular receptor (de Groot et al., 2011; Graham et al., 2013; Weiss and Navas-Martin 2005). However, mutations or RNA recombination that alter the CoV receptor-binding domain and its usage of or affinity for a particular receptor can potentially alter the CoV host range (Enjuanes et al., 2005; Graham et al., 2013; Weiss and Navas-Martin 2005). Following entry via receptor-mediated endocytosis, viral proteins and RNA are synthesized (Graham et al., 2013; Narayanan et al., 2014; Weiss and Navas-Martin 2005). CoV transcription and translation occur in the cytoplasm (Weiss and Navas-Martin 2005). The CoV genomic RNA has a 5' cap and 3' poly(A) tail; thus, it resembles host mRNA, and the incoming virus genome can immediately be used for the translation of viral proteins (Narayanan et al., 2014; Nicholson and White, 2014; Weiss and Navas-Martin 2005). The genomic RNA is also used as a template for the synthesis of full-length negative-sense viral RNA, which can in turn be used as template to make additional copies of the viral genome, as well as subgenomic, negative-sense viral RNAs made by discontinuous transcription, which are then used as templates for a set of 3' coterminal nested subgenomic mRNAs (Enjuanes et al., 2005; Nicholson and White, 2014; Weiss and Navas-Martin 2005). These subgenomic mRNAs share an identical 5' leader sequence that is derived from the 5' end of the CoV genomic RNA and contains a transcription-

regulating sequence (TRS) at its 3' end, as well as a common 3' terminal sequence, due to discontinuous transcription of their negative-sense templates (Enjuanes et al., 2005; Nicholson and White, 2014). Because CoV mRNAs are formed as a nested set of RNAs and the translation of viral proteins requires individual mRNAs for the translation of each of the viral proteins, the CoV mRNAs can contain the open reading frames (ORFs) of multiple viral proteins (Weiss and Navas-Martin 2005). However, typically only the most 5' ORF of such RNAs is used for translation, e.g. the 5' end of genomic length RNA is used to synthesize nsp1 (Enjuanes et al., 2005; Nicholson and White, 2014; Weiss and Navas-Martin 2005). Once sufficient amounts of the CoV nucleocapsid (N) protein and the other CoV structural proteins have been made, virus assembly and budding can occur, and the newly formed virus particles can traffic through the cell's secretory pathway to exit the cell via exocytosis (Weiss and Navas-Martin 2005).

Of note, the CoV open reading frame 1 (ORF1) comprises approximately two-thirds of the CoV genome (Brian and Baric, 2005; Narayanan et al., 2014; Weiss and Navas-Martin, 2005). A ribosomal frameshift signal is located within this most 5' CoV ORF, subdividing the ORF1 into the overlapping ORFs, ORF1a and ORF1b (Bredenbeek et al., 1990; Brian and Baric, 2005; Gorbalenya, 2001; Huang et al., 2011a; Jansson, 2013; Lee et al., 1991; Narayanan et al., 2014; Ziebuhr, 2005). ORF1 encodes all of the viral non-structural proteins (nsp) in the form of two precursor polyproteins, 1a and 1ab (pp1a and pp1ab) (Narayanan et al., 2014; Weiss and Navas-Martin 2005; Ziebuhr, 2005). The viral proteinases papain-like proteinase (PL^{pro}) and 3C-like proteinase (3CL^{pro}) that cotranslationally process the pp1a and pp1b to form the individual mature non-structural proteins are encoded by the ORF1 as well (Weiss and Navas-Martin 2005). Alpha- and Beta-CoVs encode 16 nonstructural proteins, which are sequentially numbered based on their position (from amino-terminus (N-terminus) to carboxy-terminus (C-terminus)), in the ORF1 precursor polyproteins and are translated in the same order in which they are numbered (Ziebuhr, 2005). Thus, nsp1, the most 5' (N-

terminal) encoded protein and first PL^{pro} cleavage product to be released from the ORF 1a polyprotein, is the first protein made in alpha and beta CoV-infected cells (Ziebuhr, 2005). The Gamma- and Delta-CoVs encode 15 nsp proteins, as they lack nsp1 (Snijder et al., 2003; Woo et al., 2010; Ziebuhr, 2005; Ziebuhr et al., 2007). The nsps are also referred to as the replicase proteins or replicase-transcriptase complex. Many of the nsps perform crucial roles in CoV RNA replication and transcription, as demonstrated by the prediction that the enzymatic activities and functional domains of these proteins are conserved among the different CoV genera (Bhardwaj et al., 2004; Cheng et al., 2005; Fan et al., 2004; Imbert et al., 2006; Ivanov et al., 2004a; Ivanov et al., 2004b; Lee et al., 1991; Minskaia et al., 2006; Saikatendu et al., 2005; Snijder et al., 2003; Subissi et al., 2014; Thiel et al., 2003; Weiss and Navas-Martin, 2005; Ziebuhr, 2005). Despite extensive research, the biological functions of the nsps and the roles that they play in the viral life cycle have not been fully elucidated. The structural proteins S, N, matrix (M), and envelope (E) are all encoded downstream of ORF1, along with additional accessory proteins, which vary in number and function depending upon the particular CoV (Graham et al., 2013; Weiss and Navas-Martin, 2005).

CoVs of significant public health interest to human or agricultural health can be found in all four CoV genera. Alpha-CoVs of note include the human CoVs (HCoV) HCoV-229E and HCoV-NL63, and the veterinary CoVs canine coronavirus (CCoV), feline infectious peritonitis virus (FIPV), transmissible gastroenteritis virus (TGEV), and porcine epidemic diarrhea virus (PEDV) (Drexler et al., 2010; Drosten et al., 2003; Isaacs et al., 1983; Ksiazek et al., 2003; Larson et al., 1980; Narayanan et al., 2014; Vabret et al., 2008; Vabret et al., 2003; Wertheim et al., 2013; Zaki et al., 2012). Important human Beta-CoVs include HCoV-OC43 and HCoV-HKU1, and important veterinary Beta-CoVs include murine hepatitis virus (MHV), bovine coronavirus (BCoV), and numerous bat CoVs (Drexler et al., 2010; Drosten et al., 2003; Graham et al., 2013; Isaacs et al., 1983; Ksiazek et al., 2003; Larson et al., 1980; Narayanan et al., 2014; Vabret et al., 2003;

Vabret et al., 2008; Wertheim et al., 2013; Zaki et al., 2012). In the past, CoVs appeared to be of greater importance for veterinary health than human health, as known HCoVs typically caused only mild, self-limited upper respiratory illnesses in humans (Falsey et al., 1997; van der Hoek et al., 2006). Recently, however, two highly pathogenic HCoVs have emerged—SARS-CoV and Middle East respiratory syndrome CoV (MERS-CoV); both Beta-CoVs (Graham et al., 2013; Narayanan et al., 2014). Between the years of 2002 to 2003, the SARS-CoV was reported to have infected approximately 8,000 people from 29 countries across the world, killing nearly 800 of them, for an approximate 10% case-fatality rate (Drosten et al., 2003; Ksiazek et al., 2003; Perlman and Dandekar, 2005; Perlman and Netland, 2009; Rota et al., 2003; van Boheemen et al., 2012). The MERS-CoV emerged in Saudi Arabia in 2012, and the extent to which it will cause disease locally or spread globally is not yet known (Graham et al., 2013; Zaki et al., 2012). As of March 20, 2015, the World Health Organization (WHO) announced an official count of 1075 laboratory-confirmed cases of MERS-CoV and a minimum of 404 related deaths, for an approximate case-fatality rate of 37% (<http://www.who.int/csr/don/20-march-2015-mers-saudi-arabia/en/>).

The emergence of the SARS-CoV and MERS-CoV viruses has illustrated the potential for the transmission to humans of zoonotic CoVs capable of causing severe disease (Drosten et al., 2003; Graham et al., 2013; Ksiazek et al., 2003; Narayanan et al., 2014; Perlman and Dandekar, 2005; Perlman and Netland, 2009; Rota et al., 2003; van Boheemen et al., 2012). Recent evidence has suggested that bats are a natural reservoir for CoV and may be involved in the cross-species transmission of numerous mammalian CoVs (Carrington et al., 2008; Chan et al., 2013; Chu et al., 2008; Gloza-Rausch et al., 2008; Graham et al., 2013; Poon et al., 2005; Reusken et al., 2010; Tang et al., 2006). The most closely related CoVs to both SARS-CoV and MERS-CoV are bat CoVs (group 2C and 2B bat CoVs, respectively) (Graham et al., 2013). Although the connection between bats and the zoonotic transmission of these two viruses to humans is not fully

known, it is believed that, in the case of SARS-CoV, that a bat CoV may have been transmitted to civet cats in China, mutating along the way such that the SARS-CoV S protein receptor-binding domain(s) was able to progressively bind bat, then civet cat, then human ACE-2 with high affinity, thereby making the SARS-CoV virus permissive for replication in bats, then civet cats, then humans, respectively (Graham et al., 2013). Alternatively, there may have been direct transmission of SARS-CoV from bats to humans (Graham et al., 2013). Bats have also been implicated as being a reservoir for MERS-CoV, although the connection between bats and humans is less well established than for SARS-CoV (Graham et al., 2013). Camels are also thought to play a role in MERS-CoV transmission, although it is unclear what role camels may play in spreading or acting as a reservoir for MERS-CoV (Graham et al., 2013).

CoV nsp1

The SARS-CoV and MERS-CoV epidemics have spurred recent research in the field of coronavirology, in particular the identification of viral factors that contribute to CoV virulence and/or pathogenesis and can act as potential targets for vaccine or antiviral drug development (Graham et al., 2013; Narayanan et al., 2014). One such viral factor is the CoV nsp1 (Narayanan et al., 2014). The CoV nsp1 is a novel modulator of host and viral gene expression shared by the Alpha- and Beta-CoVs. Analysis of the nsp1 primary structure has failed to identify any cellular or any other viral homologs to this CoV-specific protein in The Protein Data Bank or NCBI Protein database (Connor and Roper, 2007; Jansson, 2013). As described earlier, nsp1 is the first viral protein to be expressed in both Alpha- and Beta-CoV-infected cells (Jansson, 2013). Unlike many of the other nsps (e.g. nsp3-16), which appear to have a high degree of conservation in their primary sequences and functional domains across the different CoV genera, the nsp1 primary sequence is poorly conserved even among CoVs of the same genus and is considered a

CoV genus-specific marker (Connor and Roper, 2007; Jansson, 2013; Snijder et al., 2003; Thiel et al., 2003). To illustrate the variation in the nsp1 amino acid sequence observed within CoVs of the same genus, let us compare the nsp1 proteins of multiple Alpha-CoVs and Beta-CoVs. The human Alpha-CoVs HCoV-229E and HCoV-NL63 share 60% nsp1 amino acid sequence homology, HCoV-229E and porcine epidemic diarrhea virus 52%, HCoV-229E and TGEV 32%, TGEV and porcine respiratory CoV 97%, and TGEV and FIPV 93% (Huang et al., 2011a; Narayanan et al., 2014). The Beta-CoV SARS-CoV nsp1 shares only 20.6% amino acid sequence similarity with the nsp1 of MHV, 17.3% with BCoV, and 92.2%, 19.7% and 30.9% with the bat strains Rm1, 133 and HKU9-1, respectively (Narayanan et al., 2014; Tohya et al., 2009). The size of nsp1 also differs both between the Alpha- and Beta-CoVs as well as within the Beta-CoV subgroups; Alpha-CoVs encode an nsp1 protein of significantly smaller size than any of the Beta-CoVs (Almeida et al., 2007; Connor and Roper, 2007; Jansson, 2013; Narayanan et al., 2014; Tohya et al., 2009).

A study examining the crystal structure of the TGEV nsp1 (p9) found that, despite their lack of amino acid sequence homology, TGEV p9 and the N-terminus of the SARS-CoV nsp1 protein, share a common fold—a long alpha helix situated on the rim of a six-stranded beta-barrel—implying that the nsp1 protein was probably not independently acquired by the two CoV genera (Jansson, 2013). The study also noted that important structural differences between the Alpha- and Beta-CoV nsp1s might explain the differences in nsp1-mediated 40S-ribosomal subunit-independent translation inhibition mechanisms for the nsp1s of these two CoV genera (Jansson, 2013). The combined alignment of the sequences of nsp1s of various Alpha- and Beta-CoVs showed little conservation between the structure of the nsp1s of Alpha- and Beta-CoVs; as reflected by the TGEV nsp1 and SARS-CoV nsp1 N-terminus three-dimensional alignment and surface electrostatics (Jansson, 2013; Narayanan et al., 2014). Thus, little to no information about the biological function of the nsp1s or the mechanism(s) of nsp1-

mediated translation inhibition could be inferred from either the nsp1 structural or sequence alignment data alone (Jansson, 2013). Jansson also noted that the multiple, highly conserved regions shared by the Alpha-CoVs and the specific conserved regions shared by the Beta-CoVs, may be more related to the structural stability of the nsp1s than to their functions (Jansson, 2013; Narayanan et al., 2014).

As Gamma- and Delta-CoVs lack this protein, nsp1 is clearly not the sole factor that determines CoV virulence or contributes to CoV pathogenesis (Jansson, 2013; Narayanan et al., 2014). However, nsp1 has received substantial attention as a virulence factor for both Alpha- and Beta-CoVs (Narayanan et al., 2014). A growing body of research suggests that the nsp1s of different Alpha- and Beta-CoVs have similar biological functions, promoting viral replication by suppressing the expression of host genes, including those involved with the host antiviral innate immune response, and modulating the expression of viral genes, though their mechanisms of action may differ (Huang et al., 2011a; Jansson, 2013; Kamitani et al., 2009; Kamitani et al., 2006; Narayanan et al., 2014; Tohya et al., 2009). There is evidence in the literature demonstrating that the nsp1s of numerous pathogenic Alpha-CoVs—e.g., TGEV, 229E, and Beta-CoVs—e.g., MHV, SARS-CoV, and multiple bat CoVs, can suppress host gene expression (Huang et al., 2011a; Jansson, 2013; Kamitani et al., 2006; Kamitani et al., 2009; Narayanan et al., 2014; Tohya et al., 2009; Zust et al., 2007). Data published regarding the replication of these viruses indicates that viral replication also causes inhibition of host protein synthesis (Huang et al., 2011a; Kamitani et al., 2006; Narayanan et al., 2014).

The best evidence of the role of nsp1 in viral virulence comes from MHV. It was demonstrated that a virulent wild-type strain of MHV could be attenuated, and used as a type of live-attenuated vaccine, following the deletion of 99 nucleotides from the nsp1 coding sequence (Narayanan et al., 2014; Zust et al., 2007). This deletion mutant virus replicated at levels similar to that of its wild-type counterpart in cultured (murine) cells,

but at severely attenuated growth levels in wild-type mice (Huang et al., 2011a; Narayanan et al., 2014; Zust et al., 2007). However, in type I IFN receptor-deficient mice, the growth of the MHV deletion mutant virus was comparable to that of wild-type MHV, indicating that MHV nsp1 plays a role in antagonizing the murine type I IFN system (Huang et al., 2011a; Narayanan et al., 2014; Zust et al., 2007). Additional evidence supporting the role of nsp1 as a major virulence factor for MHV comes from a study showing that another deletion mutant of MHV was also attenuated in mice compared to its wild-type counterpart, despite demonstrating similar growth kinetics in murine cells (Lei et al., 2013; Narayanan et al., 2014). The amino acid sequence deleted from the MHV nsp1 in this second study is considered to be relatively well conserved, and is present in SARS-CoV nsp1 as well (Lei et al., 2013; Narayanan et al., 2014).

Alpha-CoV nsp1

The molecular pathogenesis of Alpha-CoVs is poorly understood, and a limited number of studies have been published that describe the biological functions of the Alpha-CoV nsp1s (Narayanan et al., 2014). The available data indicate that nsp1 of HCoV-229E and HCoV-NL63, as well as TGEV may play an important role(s) in Alpha-CoV pathogenesis, as these nsp1s have been shown to suppress host gene expression (Huang et al., 2011a; Jansson, 2013; Narayanan et al., 2014; Wang et al., 2010; Zust et al., 2007). All three of the nsp1s mentioned above have been found to inhibit the expression of constitutive, e.g., Simian (vacuolating) virus 40 (SV40), HSV thymidine kinase gene (HSV-TK) and/or cytomegalovirus (CMV), promoter-driven reporter genes in mammalian cell lines (Huang et al., 2011a; Narayanan et al., 2014; Wang et al., 2010; Zust et al., 2007). Additionally, in mammalian cells, HCoV-229E nsp1 and HCoV-NL63 nsp1 can suppress reporter gene expression driven by inducible promoters of innate immune genes, e.g. interferon (IFN)-beta and IFN-stimulated gene 15 (ISG15) (Wang et

al., 2010; Züst et al., 2007). The nsp1 of HCoV-229E and HCoV-NL63 have been shown to associate with the 40S ribosomal subunit component ribosomal protein S6 (rpS6) (Jansson, 2013; Wang et al., 2010; Züst et al., 2007). According to the literature and unpublished data from our laboratory, the TGEV nsp1 protein does not co-immunoprecipitate with rpS6 under the same or even less stringent conditions as the SARS-CoV nsp1 protein (Huang et al., 2011a; unpublished). This may point to a possible difference between the mechanism(s) of TGEV and HCoV-229E and HCoV-NL63 nsp1-induced translation inhibition. As the Alpha-CoVs can be subdivided into the subgroups 1a and 1b, and TGEV is classified as a member of subgroup 1a, while HCoV-229E and HCoV-NL63 are members of subgroup 1b, it is possible that 40S ribosome binding is a subgroup 1b specific phenotype not present in subgroup 1a Alpha-CoV nsp1s (Graham et al., 2013). Perhaps, subgroup plays an important role in determining the translation inhibition mechanism(s) utilized by a particular CoV nsp1. However, it should be noted that the biological function(s) and mechanism(s) of action have not been fully clarified for any of the Alpha-CoV nsp1s yet.

TGEV_{NSP1} (P9)

The best-characterized Alpha-CoV nsp1 is likely the “p9” protein of TGEV. The TGEV nsp1 is an approximately 9 kDa, 108-amino acid-long protein (Almeida et al., 2007; Galan et al., 2005; Huang et al., 2014; Jansson, 2013; Narayanan et al., 2014). In cells infected with the alphacoronavirus HCoV-229E, PL1^{pro} cleaves the site between the nsp1 and nsp2 proteins to release the 9 kDa nsp1 (Galan et al., 2005; Herold et al., 1998; Narayanan et al., 2014; Ziebuhr et al., 2001). The observation that a change in amino acid position 108 within the ORF1a of TGEV altered the cleavage efficiency of PL1^{pro} at this site, led to the prediction that TGEV nsp1 is processed in the same manner as the HCoV-229E nsp1 (Galan et al., 2005; Jansson, 2013; Narayanan et al., 2014).

Recombinant TGEV p9 can be made in *E. coli* as a soluble glutathione S-transferase (GST) fusion protein (Huang et al., 2011a; Jansson, 2013). TGEV p9 is the only alphacoronavirus nsp1 for which the complete crystal structure has been solved (Jansson, 2013). Structural data for the nsp1s is limited, and only the nuclear magnetic resonance spectroscopy structure for the N-terminus of the SARS-CoV nsp1 is available for comparison with the crystal structure of TGEV p9 (Almeida et al., 2007; Jansson, 2013; Narayanan et al., 2014). The TGEV p9 structure is defined by an irregular six-stranded beta-barrel flanked by an alpha-helix and many of the conserved residues form the hydrophobic core of the beta-barrel fold, suggesting that this domain plays a greater role in the structural stability of the protein than in its function (Jansson, 2013; Narayanan et al., 2014). In contrast, two highly conserved areas that map to the surface of TGEV p9 were highlighted as potentially important for the interaction of TGEV nsp1 with other proteins (Jansson, 2013; Narayanan et al., 2014).

TGEV p9 has predominantly been studied in cell-free *in vitro* translation systems, e.g. rabbit reticulocyte lysate (RRL), and HeLa S10 and S100 extracts, or as expressed protein in cell culture (Huang et al., 2011a; Narayanan et al., 2014). TGEV p9 has been shown to efficiently inhibit host and reporter gene expression in mammalian cells, without binding to the 40S ribosomal subunit, modifying mRNA, or affecting the stability of mRNA to promote mRNA degradation (Huang et al., 2011a; Jansson, 2013; Narayanan et al., 2014). In HeLa S10 extract and in RRL supplemented with 20% HeLa S10 extract or S100 post-ribosomal supernatant (derived from HeLa S10 extract via centrifugation), TGEV p9 has been shown to inhibit cap-dependent as well as encephalomyocarditis virus (EMCV) IRES-mediated and hepatitis C virus (HCV) IRES-mediated translation, but to be unable to inhibit cricket paralysis virus (CrPV) IRES-mediated translation (Huang et al., 2011a). No inhibition of any of the listed RNA templates was observed in RRL alone (Huang et al., 2011a; Jansson, 2013; Narayanan et al., 2014). It was proposed that the observed pattern of p9 activity indicated that there is

no factor present in RRL that inactivates p9, but that there may be a host factor(s) absent in RRL but present in HeLa S10 and HeLa S100 extracts and cultured cells necessary for the translation inhibition activity of p9 (Huang et al., 2011a; Jansson, 2013; Narayanan et al., 2014). It was also suggested that TGEV p9 targets the initiation stage of translation (Huang et al., 2011a). TGEV p9 will be discussed in greater detail in later sections.

Beta-CoV nsp1

The nsp1s of the Beta-CoVs: SARS-CoV, several bat CoVs, and MHV have been shown to inhibit host gene expression (Huang et al., 2011a; Kamitani et al., 2006; Narayanan et al., 2008; Narayanan et al., 2014; Tohya et al., 2009; Zust et al., 2007). Both the SARS-CoV and MHV nsp1s can suppress reporter gene expression in human embryonic kidney (HEK) 293 cells (Huang et al., 2011; Jansson, 2013; Kamitani et al., 2006; Lokugamage et al., 2012; Narayanan et al., 2008; Narayanan et al., 2014; Zust et al., 2007). Several bat Beta-CoVs have nsp1s capable of suppressing host gene expression, including interferon production, without modifying or degrading host mRNAs (Tohya et al., 2009; Narayanan et al., 2014). The MHV nsp1 also suppresses host gene expression and has been demonstrated to play an important role in viral virulence and pathogenicity by interfering with the host type I IFN response (Huang et al., 2011a; Narayanan et al., 2014; Zust et al., 2007). Recombinant MHV lacking a full-length, wild-type nsp1 gene is highly attenuated in wild-type mice, but in IFN receptor-deficient mice viral replication and spread are restored to normal levels (Huang et al., 2011a; Narayanan et al., 2014; Zust et al., 2007).

The Beta-CoV genus is subdivided into four different lineages or subgroups, labeled A through D (Graham et al., 2013; Narayanan et al., 2014). Members of all of the Beta-CoV lineages or subgroups include important human and veterinary CoVs, e.g. HCoV-OC43, HCoV-HKU1, MHV and BCoV in lineage A (subgroup 2A), SARS-CoV

and a closely related bat CoV, Rm1, in lineage B (subgroup 2B), MERS-CoV and several bat CoVs, e.g. HKU4-1, 133 and HKU5-5 in lineage C (subgroup 2C), and the bat CoV strains, HKU9-1 to 4 in lineage D (subgroup 2D) (Almeida et al., 2007; Graham et al., 2013; Narayanan et al., 2014; Tohya et al., 2009). As mentioned earlier, the size of the Beta-CoV nsp1s varies among the different Beta-CoV lineages/subgroups, with the estimated amino acid lengths (and molecular weights) of the nsp1s as follows: 245 amino acids for lineage A (referred to as “p28” due to its approximate molecular weight in kDa), 180 amino acids for lineage B (20 kDa), 195 amino acids for lineage C, and 175 amino acids for lineage D (Almeida et al., 2007; Jansson, 2013; Narayanan et al., 2014; Tohya et al., 2009).

Many similarities can be noted between the nsp1s of the Alpha-CoVs and Beta-CoVs (Narayanan et al., 2014). As in the case of the Alpha-CoVs HCoV-229E and TGEV mentioned above, nsp1 of the Beta-CoVs MHV, BCoV, and SARS-CoV is released from the pp1a by PL1^{pro} cleavage (Denison et al., 1995; Denison et al., 2004; Narayanan et al., 2014; Prentice et al., 2004). Like the Alpha-CoVs HCoV-229E and HCoV-NL63, MHV nsp1 and SARS-CoV can suppress transient reporter gene expression in mammalian cells driven by both constitutive, e.g., SV40, and inducible promoters, e.g., IFN-beta and IFN-stimulated response element (ISRE) (Kamitani et al., 2006; Narayanan et al., 2008; Narayanan et al., 2014; Zust et al., 2007). The nsp1s of bat Beta-CoVs representative of multiple Beta-CoV lineages were shown to inhibit host protein synthesis and prevent induction of type I IFN and ISG expression, although to differing degrees (Narayanan et al., 2014; Tohya et al., 2009).

Other properties of the Beta-CoV nsp1s may be genus- or lineage-specific, e.g. mRNA modification and degradation. No Alpha-CoV nsp1 has been shown to modify or degrade mRNA. Like SARS-CoV nsp1, the nsp1s of the aforementioned bat Beta-CoVs promoted the degradation of host mRNAs (Narayanan et al., 2014; Tohya et al., 2009). This may have significant implications given the role of bats as the natural reservoir of

several Beta-CoVs, including those closely related to SARS-CoV, and the potential of CoVs circulating in bats to become a source of emerging human CoVs (Graham et al., 2013; Narayanan et al., 2014; Smith and Wang, 2013). These Beta-CoV nsp1s may also have a conserved role(s) in CoV replication. It has been suggested that MHV nsp1 also plays a role in viral replication based on its subcellular localization at different time points during infection and its interactions with other viral proteins, e.g., nsp7 and nsp10 (Brockway et al., 2004; Deming et al., 2007; Narayanan et al., 2014). For both MHV and BCoV, another group 2a Beta-CoV, a long range RNA-RNA interaction between the 5'-UTR and the coding region of nsp1 has been demonstrated; BCoV nsp1 has also been implicated as a player in BCoV replication or translation based on similar protein-RNA interactions between nsp1 and cis-acting replication elements in the BCoV genome 5'-UTR (Guan et al., 2012, Gustin et al., 2009; Narayanan et al., 2014). SARS-CoV nsp1 also binds to an RNA stem-loop in the 5'-UTR of the SARS-CoV genome; an interaction which has been posited to enhance SARS-CoV replication (Narayanan et al., 2014; Tanaka et al., 2012).

Other nsp1 functions or properties may be specific to particular nsp1s. For example, MHV nsp1 has been shown to induce cell cycle arrest and to limit cell proliferation in multiple cell lines of various origins (Chen et al., 2004; Narayanan et al., 2014). The effects of other CoV nsp1s on the cell cycle have not been well studied, and these findings may prove to be MHV-specific, or possibly lineage- or genus-specific.

SARS-CoV NSP1

A great deal of research has gone into characterizing the biological function and mechanism(s) of action of the SARS-CoV nsp1 protein (Narayanan et al., 2014). SARS-CoV nsp1 was the earliest example illustrating the ability of nsp1 to inhibit reporter gene expression in mammalian cells (Kamitani et al., 2006; Narayanan et al., 2014). SARS-

CoV nsp1 was shown to suppress both inducible, IFN-promoter driven, as well as constitutive reporter, gene expression (Kamitani et al., 2006; Narayanan et al., 2014). Based on previously published findings, the SARS-CoV nsp1 protein exhibits a “two-pronged” approach to suppressing host gene expression that involves both mRNA cleavage-independent and -dependent “prongs” (Huang et al., 2011b; Kamitani et al., 2009; Kamitani et al., 2006; Narayanan et al., 2014). SARS-CoV nsp1 tightly associates with the 40S ribosomal subunit, even under conditions that prevent the association of the eIFs and 60S ribosomal subunit with the 40S subunit (Huang et al., 2011a; Kamitani et al., 2009; Narayanan et al., 2014; Merrick, 1979). SARS-CoV nsp1 gains access to host mRNAs by associating with the host 40S ribosomal subunit and can affect multiple stages of translation initiation in a template-specific manner, including preventing 48S initiation complex formation and/or the transition from the 48S complex to the formation of an elongation-competent 80S initiation complex (Lokugamage et al., 2012; Narayanan et al., 2014).

In cells, SARS-CoV nsp1 also appears to recruit a cellular endonuclease to the site of translation, thereby promoting template-dependent but nucleotide sequence non-specific endonucleolytic RNA cleavage in the 5'-UTR of capped (host) mRNAs, which results in the accelerated degradation of the truncated mRNA by the host Xrn1 mediated 5'-3' exonucleolytic mRNA decay pathway (Gaglia et al., 2012; Narayanan et al., 2014). Similarly, *in vitro* in RRL or HeLa extract, SARS-CoV nsp1 can bring about the endonucleolytic cleavage of capped mRNAs as well as mRNAs carrying different type I and type II picornavirus IRES structures (Huang et al., 2011b; Narayanan et al., 2014). However, SARS-CoV nsp1 is unable to cleave other mRNA templates, e.g. those carrying the CrPV, HCV or classical swine fever virus IRES, or the SARS-CoV 5'-end leader sequence (Huang et al., 2011b; Narayanan et al., 2014). It was proposed that the differences observed in the ability of SARS-CoV nsp1 to induce cleavage in different mRNA species might be related to differences in the translation initiation factors required

by each of these mRNA species to undergo translation (Huang et al., 2011b; Narayanan et al., 2014). However, the mechanism of SARS-CoV nsp1 mRNA cleavage has yet to be fully explained. SARS-nsp1 has not been shown to possess nuclease activity, and the cellular nuclease that it is believed to recruit has not yet been identified (Huang et al., 2011b; Kamitani et al., 2009; Narayanan et al., 2014). Regardless of the susceptibility of a particular mRNA species to SARS-CoV nsp1-mediated cleavage, SARS-CoV nsp1 is able to inhibit translation by inactivating the 40S ribosome (Lokugamage et al., 2012; Narayanan et al., 2014). It was found that a mutant SARS-CoV nsp1 unable to cleave mRNA was able to inhibit the translation of nsp1 cleavage-resistant mRNA templates to the same extent as the wild-type SARS-CoV nsp1 (Lokugamage et al., 2012; Narayanan et al., 2014).

Specific amino acids and domains have been identified that are crucial for the cleavage-dependent and independent functions of SARS-nsp1 (Huang et al., 2011b; Kamitani et al., 2009; Lokugamage et al., 2012; Narayanan et al., 2014). By mutating two amino acid residues, K164 and H165, in the C-terminus of the SARS-CoV nsp1 to alanine, an nsp1 incapable of binding the 40S ribosomal subunit was generated, which lacked both the cleavage-independent and –dependent translation inhibition activities of wild-type SARS-CoV nsp1 (Narayanan et al., 2008; Narayanan et al., 2014). This study illustrated the importance of 40S binding for all SARS-CoV nsp1 functions, including nsp1-mediated evasion of the host innate immune response, which will be described in more detail below (Narayanan et al., 2008; Narayanan et al., 2014). Based on the identification of positively charged residues exposed on the surface of the nuclear magnetic resonance (NMR) structure of the SARS-CoV N-terminus that were believed to play a role in SARS-CoV nsp1-mediated mRNA degradation, the amino acids R124 and K125 of wild-type SARS-CoV nsp1 were substituted for alanine to generate a “cleavage-deficient” SARS-CoV nsp1 mutant with only cleavage-independent activity, thus demonstrating the divisibility of the functions of the SARS-CoV nsp1 protein (Almeida

et al., 2007; Lokugamage et al., 2012; Narayanan et al., 2014). Substitution of the R124 amino acid alone with alanine was shown to have no impact on the translation inhibition activity of SARS-CoV nsp1, but to be sufficient to eliminate the interaction between SARS-CoV nsp1 and mRNA containing the SARS-CoV 5'-UTR (Narayanan et al., 2014; Tanaka et al., 2012). This study also suggested that SARS-CoV nsp1 may play a role in SARS-CoV replication, as mentioned in the previous section (Narayanan et al., 2014; Tanaka et al., 2012).

Amino acid residues in the SARS-CoV nsp1 protein that are important for nsp1-mediated alteration of the host innate immune response have also been identified, supporting the role of nsp1 as potential viral virulence factor in CoV pathogenesis. SARS-CoV nsp1 inhibits virus- and IFN-dependent antiviral signaling pathways, thereby preventing activation of IFN-inducible genes (Kamitani et al., 2006; Narayanan et al., 2014; Wathelet et al., 2007). The R124 and K125 amino acid residues in SARS-CoV nsp1 are not only important for SARS-CoV nsp1-mediated mRNA cleavage, but for SARS-CoV nsp1-mediated suppression of the host antiviral response as well (Narayanan et al., 2014; Wathelet et al., 2007). In IFN-competent cells, the replication of a mutant SARS-CoV encoding an nsp1 with the amino acid substitutions R124S and K125E was strongly attenuated (Narayanan et al., 2014; Wathelet et al., 2007). Extensive mutational analysis of the SARS-CoV nsp1 has led to the belief that distinct but overlapping regions of the protein are involved in the host gene expression and antiviral signaling pathway inhibition functions of the protein via their individual interactions with specific host factors (Jauregui et al., 2013; Narayanan et al., 2014).

Summary (comparison of TGEVp9 & SARS-CoV nsp1)

As TGEV p9 and SARS-CoV nsp1 will be discussed and compared throughout this dissertation, the information that has been published regarding TGEV p9- and SARS-

CoV nsp1-mediated suppression of host gene expression will be briefly summarized here to highlight that TGEV p9 and SARS-CoV nsp1 use different mechanisms to suppress host gene expression.

It appears that the biological function of inhibiting host gene expression is conserved among the nsp1 proteins of Alpha- and Beta-CoVs (Huang et al., 2011a; Jansson, 2013; Narayanan et al., 2014). Both SARS-CoV nsp1 and TGEV p9 can inhibit the translation of a variety of mRNA transcripts (Huang et al., 2011a; Narayanan et al., 2014). However, the mechanisms that these two nsp1 proteins use to suppress host gene expression appear to be different (Huang et al., 2011a; Jansson, 2013; Narayanan et al., 2014). SARS-CoV nsp1 must tightly associate with the 40S ribosomal subunit to exert both its mRNA cleavage-independent and -dependent functions (Huang et al., 2011a; Kamitani et al., 2009; Narayanan et al., 2014). SARS-CoV nsp1 endonucleolytically cleaves capped mRNAs and mRNAs carrying either a type I or type II picornavirus IRES in a nucleotide sequence non-specific manner, leading to the degradation of said mRNAs via cellular Xrn1-mediated mRNA decay (Huang et al., 2011b; Kamitani et al., 2009; Narayanan et al., 2014). Although SARS-CoV nsp1 is unable to modify mRNAs carrying the CrPV, HCV, or classical swine fever virus IRES, it is able to inhibit the translation of such mRNAs through inactivation of the 40S ribosomal subunit (Kamitani et al., 2009; Narayanan et al., 2014).

TGEV p9, however, does not bind to the 40S ribosomal subunit under the same conditions that the SARS-CoV nsp1 protein is able to bind, nor does it modify the mRNA transcripts that the SARS-CoV nsp1 protein is able to modify (Huang et al., 2011a; Jansson, 2013; Narayanan et al., 2014). There is little conservation between the SARS-CoV nsp1 structure and that of TGEV p9 (Jansson, 2013). SARS-CoV nsp1 is significantly larger than p9 and contains a domain with the K164 and H165 residues shown to be important for both the 40S ribosome binding and mRNA modification functions of SARS-CoV nsp1, which is absent in p9 (Kamitani et al., 2009; Huang et al.,

2011a; Jansson, 2013; Narayanan et al., 2014). The absence of a “KH” domain, like that present in SARS-CoV nsp1, may explain why p9 lacks the ability to modify mRNAs.

Another notable difference between SARS-CoV nsp1 and TGEV p9 is that SARS-CoV nsp1 is able to efficiently inhibit translation of the aforementioned mRNAs in RRL, HeLa S10, or RRL supplemented with HeLa extract, but TGEV p9 can only efficiently inhibit translation in HeLa S10 extract or RRL supplemented with HeLa extract (Huang et al., 2011a; Jansson, 2013; Narayanan et al., 2014). This difference in activity suggests that some factor(s) in HeLa cell extract enhances the activity of TGEV p9, and that this factor may be necessary for p9 activity, just as the 40S ribosome is necessary for SARS-CoV nsp1 activity (Huang et al., 2011a; Jansson, 2013; Narayanan et al., 2014).

Chapter 2: The effect of TGEV p9 in different cell-free *in vitro* translation systems

BACKGROUND

Cell-free *in vitro* translation systems

A number of *in vitro* translation systems are commercially available, including eukaryotic RRL, wheat germ extract (WGE), and HeLa cell extract systems (Anderson et al., 1983; Mikami et al., 2006a; Mikami et al., 2006b; Soto Rifo et al., 2007; Van Herwynen and Beckler, 1995). Alternatively, the same types of cellular extracts for *in vitro* translation can be made by established laboratory protocols (Anderson et al., 1983; Barton et al., 1995; Mikami et al., 2006b; Pelham and Jackson, 1976; Todd et al., 1997; Van Herwynen and Beckler, 1995). Regardless of their source, these cellular extracts are designed with the goal of optimizing *in vitro* translation efficiency when the appropriate amounts of the factors needed for *in vitro* translation are present (Anderson et al., 1983; Barton et al., 1995; Mikami et al., 2006b; Mikami et al., 2008; Pelham and Jackson, 1976; Todd et al., 1997; Van Herwynen and Beckler, 1995). Cell-free extracts contain all of the macromolecular components of the cellular translation machinery (e.g. ribosomes, tRNAs, eIFs, eEFs and termination factors) and are supplemented with the amino acid mixture(s), ATP and GTP energy sources, creatine phosphate and creatine kinase, cation co-factors, and other factors needed to promote efficient, high-yield translation of exogenous mRNA transcripts when incubated at an appropriate temperature to sustain enzyme activity (Anderson et al., 1983; Barton et al., 1995; Mikami et al., 2006b; Mikami et al., 2008; Pelham and Jackson, 1976; Todd et al., 1997; Van Herwynen and Beckler, 1995).

Cell-free RRL can be used to synthesize proteins from exogenous mRNAs from cells or transcribed *in vitro*, even at low concentrations of RNA, at rates similar to intact

reticulocytes (Pelham and Jackson, 1976). RRL can be used to synthesize full-length proteins from either capped or uncapped mRNA transcripts with similar efficiency, indicating that the 5'-cap is not essential for translation in RRL (Mikami et al., 2006b). The relative lack of cap- and poly(A) tail-dependence for translation in RRL has been attributed to the relatively low abundance of general RNA-binding proteins (RBPs) versus eIF4F in RRL (Svitkin et al., 2009). Reticulocytes are nearly mature red blood cells (RBCs) or erythrocytes (Ji et al., 2011). As a part of the maturation process that will ultimately generate RBCs, the hemoglobin-producing “factories” needed by the mammalian host, immature mammalian RBCs, referred to as different stages of normoblasts or erythroblasts, extrude their nuclei to become polychromatic erythrocytes (aka reticulocytes) prior to becoming fully mature erythrocytes (Ji et al., 2011). Although reticulocytes lack a nucleus, the translation machinery, together with levels of mRNA sufficient to maintain globin synthesis during the short life span of the RBC, is retained (Ji et al., 2011; van Zalen et al., 2015).

Background translation can be eliminated by treating RRL to eliminate endogenous globin mRNA using a calcium-dependent micrococcal nuclease, which can later be inactivated via calcium ion chelation by ethylene glycol-bis(2-aminoethylether)-N,N,N',N'-tetraacetic acid (EGTA) (Ehrenfeld and Brown, 1981; Pelham and Jackson, 1976). RRL is made via the hypotonic lysis of washed and packed rabbit reticulocytes from rabbits that have been made anemic via injection of acetylphenylhydrazine or another chemical treatment prior to blood collection, followed by centrifugation to remove cell debris and other undesirable material (Pelham and Jackson, 1976). Commercially available RRL is treated with hemin, an inhibitor of the heme-regulated eIF2 α kinase (HRI), an enzyme which, during heme deficiency, can inhibit translation via hyperphosphorylation of the alpha-subunit of eIF2 (Han et al., 2001; Huang et al., 2011a). However, TGEV p9 has not been shown to induce eIF2 hyperphosphorylation (Huang, et al., 2011a). Both Ambion and Promega RRL were tested in our laboratory.

However, no difference was found between the two lysates in terms of nsp1 function. Ambion RRL was used for all of the experiments described in this dissertation, unless otherwise noted.

Like RRL, cell-free WGE can be used to translate exogenous mRNA isolated from cells and tissue or transcribed *in vitro* (Anderson et al., 1983; Mikami et al., 2006a; Mikami et al., 2006b; Mikami et al., 2008; Van Herwynen and Beckler, 1995). Background incorporation is low in WGE due to the low levels of endogenous mRNA present (Anderson, et al., 1983; Van Herwynen and Beckler, 1995). Unlike RRL, WGE can be used to translate mRNA from RNA samples containing small fragments of double-stranded RNA or oxidized thiols, compounds which inhibit translation in RRL (Van Herwynen and Beckler, 1995). The presence of a 5' cap structure can enhance the translation activity of *in vitro* transcribed mRNA templates in WGE; *in vitro* translation activity in WGE is typically more cap-dependent than in RRL (Van Herwynen and Beckler, 1995). WGE is made simply by mechanically processing wheat germ in the presence of an extraction buffer and then centrifuging the extract to remove cell debris, followed by chromatographic separation of the supernatant to remove undesired pigments and endogenous amino acids (Anderson et al., 1983). WGE from Promega was used for all of the experiments described in this dissertation.

Post-translational modifications to proteins do not occur in all cell-free systems (Mikami et al., 2006a). No protein glycosylation occurs in WGE or in RRL to which canine microsomal membranes have not been added, and adding canine microsomal membranes to RRL decreases the overall protein yield (Mikami et al., 2006a; Van Herwynen and Beckler, 1995). Unlike RRL and WGE, HeLa extract is made from a human cell line and is capable of producing full-length human protein products with the proper post-translational modifications (Mikami et al., 2006a). Like WGE, *in vitro* translation activity in HeLa extract is enhanced by the presence of a 5' cap, and translation is much more cap-dependent in HeLa extract than in RRL (Mikami et al.,

2006b; Van Herwynen and Beckler, 1995). The HeLa S10 cytoplasmic extract used in our laboratory is made using a protocol from the lab of Bert Semler, PhD, at the University of California, Irvine (Barton et al., 1995; Huang et al., 2011a; Todd et al., 1997). This protocol was found to be best suited for the *in vitro* translation experiments being carried out in our laboratory, in terms of reporter protein accumulation (based on luciferase reporter assays) as well as nsp1 function. Using this protocol, HeLa cells were maintained in suspension culture and harvested during the logarithmic growth phase via centrifugation. The cells were osmotically swelled in a hypoosmolar lysis buffer before being mechanically lysed. The cellular debris as well as the nuclear pellet was removed by centrifugation. Like the commercially-made RRL (Ambion; Promega) and WGE (Promega) that was used for the experiments described herein, the HeLa S10 extract made in our laboratory was treated with a calcium ion-dependent micrococcal nuclease, followed by EGTA chelation, to remove host nucleic acids (unless otherwise noted) (Ehrenfeld and Brown, 1981; Pelham and Jackson, 1976).

Initial studies on the effect(s) of TGEV p9

Initial studies of TGEV p9-mediated translation inhibition showed that in HEK 293 or swine testis (ST) cells co-transfected with a reporter plasmid and a plasmid expressing C-terminal myc-tagged p9, reporter gene expression was inhibited compared to a negative control (Huang et al., 2011a). Western blot analysis demonstrating that accumulation of p9 was low in expressed cells relative to accumulation of the control protein, suggested that TGEV p9 (like SARS-CoV nsp1) inhibits its own expression (Huang et al., 2011a). TGEV p9-mediated suppression of endogenous host gene expression was also demonstrated in transfected HEK 293 cells, where host protein synthesis was decreased in p9-expressing controls compared to cells expressing a negative control (Huang et al., 2011a). TGEV infection in ST cells, which support TGEV

replication, was also shown to inhibit host gene expression and decrease host protein synthesis versus mock infection (Huang et al., 2011a).

In vitro translation studies in cell-free systems were also conducted to further characterize TGEV p9 (Huang et al., 2011a). Studies showed that unlike SARS-CoV nsp1, TGEV p9 does not cleave mRNA or promote its degradation (Huang et al., 2011a). These studies also suggested that TGEV p9, unlike SARS-CoV nsp1, can only inhibit translation in HeLa S10 extract, and not in RRL (Huang et al., 2011a). However, TGEV p9-mediated inhibition was not attributed to hyperphosphorylation of eIF2 α or consequent activation of HRI (Huang et al., 2011a). Thus, it was hypothesized that HeLa extract and 293 cells contain a factor(s), not found in RRL, which is necessary for p9 activity (Huang et al., 2011a). Additionally, it was demonstrated that RRL does not have a factor capable of inactivating p9 as p9 was able to inhibit translation in a mixture of RRL and HeLa S10 or S100 extract (Huang et al., 2011a). As the *Renilla* luciferase (rLuc) and *Photinus* (firefly) luciferase (fLuc) reporter proteins used in these studies do not require post-translational modifications to be functional, it is unlikely that differences in the abilities of the different cell-free *in vitro* translation systems to produce proteins with post-translational modifications explain the variance in the ability of p9 to inhibit translation in the various systems (Matthews et al., 1977).

Unlike cap-, EMCV IRES- and HCV IRES-driven translation, TGEV p9-mediated inhibition of CrPV intergenic region (IGR) IRES-driven translation was not observed in HeLa S10 (Huang et al., 2011). This suggested that p9 targets the initiation stage of translation, as CrPV IGR IRES- driven translation only differs from cap-, EMCV IRES- and HCV IRES- driven translation during the initiation stage, requiring the same factors for the subsequent stages of translation (Huang et al., 2011a; Martinez-Salas et al., 2008; Wilson et al., 2000). Unlike translation initiation of other mRNA transcripts, translation initiation of mRNA transcripts containing the CrPV IGR IRES does not require any of the canonical eIFs; it only requires the 40S and 60S ribosomal subunits,

suggesting that p9 does not inactivate the ribosome (Huang et al., 2011a; Jan and Sarnow, 2002; Martinez-Salas et al., 2008; Wilson et al., 2000). The CrPV IGR IRES can recruit the 40S ribosomal subunit independent of the eIFs, and complex with the 80S monosome in the absence of eIF2, initiator tRNA, eIF5B, or GTP hydrolysis (Jan and Sarnow, 2002; Pestova and Hellen, 2003; Pestova et al., 2004; Spahn et al., 2004). HCV IRES-driven translation requires the eIF2-GTP-Met-tRNAⁱ ternary complex, eIF3, eIF5, and eIF5B for initiation (Fraser and Doudna, 2007; Huang et al., 2011a). EMCV IRES-driven translation requires all of the factors necessary for cap-driven 48S complex formation *in vitro* except for eIF4E, namely, the 40S ribosomal subunit, ATP, the eIF2-GTP-Met-tRNAⁱ ternary complex, eIF4A, eIF4G, and eIF3 (Huang et al., 2011a; Martinez-Salas et al., 2008; Pestova et al., 1996).

Inhibition of EMCV IRES- and HCV IRES-driven translation by TGEV p9 is less efficient than that of inhibition of cap-driven translation, unlike SARS-CoV nsp1, which inhibited translation of all of these transcripts efficiently (Huang et al., 2011a; Kamitani et al., 2009). It was hypothesized that once p9 accesses the RNA template, it inhibits translation by targeting and inactivating one or more of the eIFs. As mentioned above, p9 can inhibit cap-dependent translation and translation driven by the HCV IRES and EMCV IRES, but not by the CrPV IGR IRES in HeLa S10 (Huang et al., 2011). It was further demonstrated that the 5' cap and 3' poly(A) tail of GLA mRNA were not essential for p9 activity in HeLa S10, thus the 5' cap-binding protein eIF4E and the poly(A)-binding protein (PABP) are not necessary for p9-mediated translation inhibition—findings which correlate well with the ability of p9 to inhibit both HCV and EMCV IRES-mediated translation, which do not require eIF4E to initiate translation (Huang et al., 2011a).

While HCV IRES- and EMCV IRES-driven translation initiation require fewer eIFs for 40S ribosomal subunit recruitment than cap-driven translation, CrPV IGR IRES-driven translation initiation requires none of the eIFs for 40S ribosomal recruitment (Jan

and Sarnow, 2002; Pestova and Hellen, 2003; Pestova et al., 2004; Spahn et al., 2004). Out of the mRNA templates whose translation is affected by p9 (capped, HCV IRES-containing, EMCV IRES-containing), HCV has the fewest requirements for translation initiation: eIF2-GTP-Met-tRNA_i ternary complex, eIF3, eIF5, and eIF5B (Fraser and Doudna, 2007; Huang et al., 2011a). Hence, it was believed that one of these eIFs (or the ternary complex) might be targeted by p9 and that targeting leads to translation inhibition (Huang et al., 2011a). If p9 targets the ternary complex or eIF3, formation of the 48S initiation complex should be reduced (Pestova et al., 2000). However, if p9 instead targets eIF5, which catalyzes eIF2 GTP hydrolysis, or eIF5B, which facilitates joining of the 60S ribosomal subunit, formation of the 80S initiation complex should be reduced, but formation of the 48S initiation complex should be unaffected (Pestova et al., 2000).

MATERIALS & METHODS

Plasmid & RNA constructs

For the generation of *in vitro*-synthesized EMCV-fLuc (monocistronic EMCV IRES fLuc RNA), GLA, HCV-rLuc (monocistronic HCV IRES rLuc RNA), and TGEV m7 rLuc mRNA transcripts, the plasmids pT7-IRES-EMCV-FfLuc, pGLA-SV40, HCV16Luc, and pSMART-TGEV m7 rLuc were used, respectively. The pT7-IRES-EMCV-fLuc and pGLA-SV40 plasmids were constructed, as previously described (Huang et al., 2011a; Ikegami et al., 2005; Yi et al., 2000). The pT7-IRES-EMCV-fLuc vector is a pT7-IRES plasmid containing the EMCV IRES sequence between the T7 promoter sequence and fLuc ORF from the pRLHL plasmid (Ikegami et al., 2005; Yi et al., 2000). The pGLA-SV40 plasmid encodes a T7 promoter sequence and the rLuc ORF, flanked by the 5'-UTR of rabbit beta-globin mRNA and a 3' 50-nucleotide-long poly(A) tail sequence in place of the rLuc gene of pRL-SV40 (Promega) (Huang et al., 2011 a; Huang et al., 2011b). As described in the literature, the HCV16Luc plasmid and

specific primers were used to generate the PCR product DNA template for *in vitro* transcription of the HCV-rLuc RNA, carrying the rLuc ORF downstream of a 5'-HCV IRES sequence (Lokugamage et al., 2012). A PCR product encoding the rLuc ORF flanked by the 5' and 3' UTRs of TGEV mRNA 7, along with a T7 promoter sequence and a 22-nucleotide-long long poly(A) tail sequence was cloned into a pSMART vector (Lucigen) to generate the pSMART-TGEV m7 rLuc plasmid, which was made by Krishna Narayanan. The plasmids were linearized, as needed, and used for *in vitro* transcription, as described below.

Restriction digestion protocols

Plasmids were linearized overnight or for a minimum of 3 hours using the appropriate restriction endonuclease (NEB). Following digestion, the restriction enzyme was heat inactivated, if possible, and the linearized plasmid preparation was purified by phenol-chloroform extraction followed by ethanol precipitation.

***In vitro* transcription protocol**

Capped and polyadenylated EMCV-fLuc, GLA, HCV-rLuc, and TGEV m7 rLuc RNAs were generated by linearizing and transcribing the plasmids pT7-IRES-fLuc, pGLA-SV40, transcribing the PCR products generated from the HCV16Luc plasmid, and linearizing and transcribing the plasmid pSMART-TGEV m7 rLuc, respectively. An aliquot of the linearized purified plasmid or purified PCR product (HCV-rLuc RNA) was used to make *in vitro* transcribed RNA. The MEGAScript® kit (Ambion) was used for *in vitro* transcription of the HCV-rLuc RNA, the mMESSAGE mMACHINE® kit (Ambion) for GLA RNA and TGEV m7 rLuc RNA, and the mMESSAGE mMACHINE® T7 Ultra kit (Ambion) for the EMCV-fLuc RNA. Transcription reactions

were allowed to incubate for two to three hours at 37°C before TURBO DNase treatment and polyadenylation (as needed). Otherwise, the kits were used according to the manufacturer's protocol. The *in vitro* transcribed RNA was purified by phenol-chloroform extraction and isopropanol precipitation. The efficiency of the transcription reaction was checked by agarose gel electrophoresis followed by ethidium bromide staining.

Recombinant protein preparation & purification

The full-length TGEV p9 and SARS-CoV nsp1 genes were PCR-amplified with or without the addition of both myc and Histidine (myc/His) epitope tags and cloned into a pGEX vector (GE Healthcare) to yield pGEX-p9 and pGEX-SCoV nsp1-wt, or pGEX-p9-myc/His and pGEX-SCoV nsp1-myc/His, respectively (Huang et al., 2011a; Kamitani et al., 2009). Recombinant proteins for *in vitro* translation experiments were made by transforming Escherichia coli BL21-CodonPlus® (DE3))-RP chemically competent cells (Agilent Technologies) with the above vectors encoding recombinant p9 or SARS-CoV nsp1 GST fusion proteins or the control vector encoding recombinant GST protein alone, with or without terminal myc and histidine (His) epitope tags (Huang et al., 2011a; Kamitani et al., 2009). The cells were grown overnight at 37°C on Luria-Bertani (LB) agar plates containing ampicillin. A single transformed colony was picked and grown in LB medium containing ampicillin overnight at 37°C to generate a starter culture for larger bacterial cultures that were grown at 37°C for approximately three to four hours the following day, until reaching an optical density (OD) value at 600 nm of 0.4-0.6.

When the desired OD value was reached, 0.1 M isopropyl-beta-D-thiogalactopyranoside (IPTG) was added to the cultures to induce protein expression. After three hours, the bacterial cells were collected via centrifugation at 4800 rpm for ten minutes at 4°C. The pellet was washed and collected in cold phosphate-buffered saline

(PBS), then again subjected to centrifugation as described above. The supernatant was discarded, and the bacterial cell pellet was frozen at -80°C. The pellet was later thawed and resuspended in 10 mL per 1 L of bacterial culture of BugBuster® Protein Extraction Reagent (Novagen), and incubated at room temperature for ten minutes before being centrifuged at 4°C for ten minutes at 15,000 rpm. The supernatant was then collected, filtered using a sterile 0.45 µm filter, and placed on ice. The filtered supernatant was then applied to 1.3 mL glutathione sepharose 4B per 1 L of bacterial culture (GE Healthcare) and incubated at 4°C overnight.

The next day, each sample was applied to Poly-Prep Chromatography Column (Bio-Rad) and allowed to flow through the column by gravity. Each column was washed three times with cold PBS, and one time with cold PreScission™ Protease buffer (50 mM Tris HCl, 1 mM EDTA, 150 mM NaCl, 1 mM DTT). Then, each column was capped and 3 mL of cold PreScission™ Protease buffer and 30 µL of PreScission™ Protease (GE Healthcare) were added to each column. The columns were allowed to incubate at 4°C for four hours to allow the PreScission™ Protease to cleave the GST portion of the GST fusion proteins before the sample was eluted from each column by gravity (or by the reduction of glutathione by the elution buffer in the case of the recombinant GST control protein). When preparing the recombinant GST control protein, the PreScission™ Protease steps were omitted. Each eluted sample was stored at -80°C, then dialyzed in cold PBS by applying the sample to a Slide-A-Lyzer® 3,500 kDa molecular weight cut-off (MWCO) dialysis cassette (Thermo Scientific), submerging the cassette in cold PBS, and allowing the cassette to rotate in the PBS (to facilitate dialysis) overnight at 4°C.

After removing each sample from its dialysis cassette, each sample was concentrated using an Amicon Ultra centrifugal filter unit with a 3,000 kDa MWCO (Millipore). The protein concentration of each sample was determined using the Bio-Rad DC Protein Assay with bovine serum albumin (BSA) standards (Bio-Rad). Protein samples were also visualized using polyacrylamide gel electrophoresis (12% gel)

followed by Bio-Safe™ Coomassie blue staining (Bio-Rad). Aliquots of each protein sample were stored at -80°C.

Cell culture

HeLa S3 cells (ATCC) were maintained as a semi-adherent, plated culture in F-12K medium (Gibco) with 10% fetal bovine serum (FBS), then transferred to glass spinner flasks (Bellco) and maintained as a suspension culture in MEM-S medium containing: minimum essential medium (MEM) Eagle Joklik modification powder (Sigma), antibiotic-antimycotic (Omega Scientific), hydrochloric acid, sodium bicarbonate, and water. The MEM-S was supplemented with 10% newborn calf serum (Gibco).

Protocols for making HeLa S10 [+/- nuclease] & HeLa S100

HeLa S10 extract was prepared from HeLa S3 suspension culture cells (ATCC). Cells were harvested during the logarithmic growth phase by centrifugation at 1,000x g for ten minutes at 4°C. The cell pellet was washed twice in ice-cold wash buffer (35 mM HEPES, pH 7.4; 146 mM NaCl, 11 mM glucose) and collected via centrifugation, as described above. The washed cell pellet was resuspended in an equal volume of ice-cold hypotonic buffer (20 mM HEPES, pH 7.4; 10 mM KCL, 1.5 mM MgOAc, 1 mM DTT) and incubated on ice for 15-20 minutes. The cell suspension was then transferred to a chilled glass dounce homogenizer (Wheaton) and mechanically lysed. The cellular lysate was then transferred to a chilled tube, and a volume of ice-cold 10X post-lysis buffer (20 mM HEPES, pH 7.4; 120 mM KOAc, 4mM MgOAc, 5 mM DTT) equal to one-tenth of the lysate volume was added. Cellular debris and nuclei were removed from the extract via centrifugation at 1000x g for ten minutes at 4°C.

The supernatant was collected and centrifuged again at ~12,000x g for 15-20 minutes at 4°C. The supernatant was again removed, and transferred to a new, chilled tube. 10 µL of 0.1 M calcium chloride and 10 µL of 2 mg/mL micrococcal nuclease (NEB) was added for each milliliter of extract, and the extract was incubated at 12-13°C for 15 minutes. 20 µL of 0.2 EGTA per milliliter of extract was added to inactivate the nuclease, and the extract was centrifuged at 12,000x g for 15 minutes at 4°C to remove any precipitates. The supernatant (HeLa S10 extract treated with micrococcal nuclease) was then removed, divided into aliquots, and stored in liquid nitrogen.

HeLa S100 extract, a postribosomal supernatant, was prepared by removing the ribosomes from HeLa S10 extract by centrifugation of the HeLa S10 extract at 100,000 x g for 3 hours at 4°C using a Beckman TLA-120.2 fixed-angle rotor in a tabletop ultracentrifuge (Beckman Coulter). The supernatant (HeLa S100 extract) was stored in liquid nitrogen.

RRL protocol

For *in vitro* translation in RRL, the Ambion Retic Lysate IVT™ Kit (Applied Biosystems) or the Promega Rabbit Reticulocyte Lysate System, Nuclease Treated (Promega) was used. For each standard *in vitro* translation reaction, 17 µL of RRL (Ambion, unless otherwise noted) was mixed with 1 µL of 1mM complete amino acid mixture (Promega), 1.25 µL of 20X Translation Mix -Met (lacking methionine), and 3.75 µL of water. To this p9 or control protein purified from *E. coli* was added, the final reaction volume adjusted to 25 µL as needed, and the mixture was incubated on ice for ten minutes. Subsequently, 0.25 µg of *in vitro* transcribed mRNA was added, and the mixture was incubated at 30°C for ten or 30 minutes.

Following this incubation, 5 µL of each reaction/translation product was added to 100 µL of 1X *Renilla* Luciferase Assay Lysis Buffer (diluted from 5X) from the Promega

Renilla Luciferase Assay System and incubated at room temperature for 10 minutes. Then, 20 μ L of each reaction was combined with 100 μ L of the *Renilla* Luciferase Assay Reagent (prepared by diluting 100X *Renilla* Luciferase Assay Substrate in *Renilla* Luciferase Assay Buffer), and mixed. The rLuc activity for each sample was read with a GloMax® 20/20 Luminometer (Promega) with the luminescence integrated over a 10 second period, with a two second delay. All samples were run in triplicate, and the mean and standard deviation were calculated for each set of samples. The mean levels of p9- and SARS-CoV nsp1-mediated translation inhibition were calculated relative to GST. Statistical significance was determined using Student's t-tests.

HeLa S10 protocol

For *in vitro* translation in HeLa S10 extract, 17.5 μ L of HeLa S10 extract was combined with 2.25 μ L of 10X buffer (155 mM HEPES KOH (Sigma), pH 7.4; 10mM rATP (Promega); 2.5 mM rGTP, rUTP, rCTP (Promega); 600 mM KOAc (Sigma), pH 7.4; 300 mM creatine phosphate (Roche), 4 mg/mL creatine kinase (Roche), water), 2.5 μ L of 1 mM complete amino acid mixture (Promega), and 0.25 μ L of water per reaction. To this, p9 or control protein was added, and the mixture was incubated on ice for 10 minutes. Then, 0.25 μ g of mRNA (0.25 μ g/ μ L) was added, and the tube was incubated at 30°C for an appropriate amount of time (usually 30 minutes).

As with RRL, a 5 μ L aliquot was removed and used for subsequent luciferase activity readings. All samples were typically run in triplicate, with the mean and standard deviation being calculated for each sample set. To determine the relative activity of p9 or SARS-CoV nsp1, the mean percent inhibition relative to the GST control was calculated, and significance was determined using Student's t-tests.

RRL + HeLa S100 protocol

The protocol for RRL supplemented with HeLa S100 extract that was used is the same as the RRL protocol, except that the volume of RRL used per reaction was reduced to 12.5 μL of RRL, and 5 μL of HeLa S100 extract (20% of total reaction volume) was added to each translation reaction. Typically, an incubation time of 30 minutes at 30°C was used. The data suggests that, although a ten-minute incubation is sufficient, the difference between the GST and p9 groups is greater after 30 minutes.

RRL + HeLa S10 protocol

The protocol for RRL supplemented with HeLa S10 extract was the same as that for RRL supplemented with HeLa S100 extract, other than that HeLa S10 extract was used in place of HeLa S100 extract. The data suggests that there is no significant difference in p9 activity in RRL supplemented with HeLa S10 extract versus RRL supplemented with HeLa S100 extract.

Modifications to original *in vitro* translation protocols

Occasionally, the original *in vitro* translation protocols for RRL, HeLa S10, or WGE were modified, e.g. changing the amount of protein used from the standard 1 μg of protein or changing the incubation time of the translation reaction. These variations and their significance are noted or discussed in the appropriate text and/or figure legends.

Protocol for pre-incubation of protein in HeLa S10

To test whether preincubation of p9 in HeLa S10 extract would enhance the activity of p9 in RRL, 5 μL p9 or GST plus 5 μL HeLa S10 extract was incubated for 15 minutes at 30°C. Then, 17 μL of RRL (Ambion), 1 μL of 0.5 $\mu\text{g}/\mu\text{L}$ GST or p9 for

control reactions or 1 μL of GST or p9 preincubation reaction (i.e. 0.5 μg of GST or p9 exposed to HeLa S10 extract) for experimental reactions, plus 2 μL of water was combined. To this mixture, 5 μL of premix, composed of the following: 1.75 μL water, 1.25 μL 20x translation mixture, 1 μL complete amino acid mixture (Promega), and 1 μL RNA (0.25 $\mu\text{g}/\mu\text{L}$) was added to each reaction. The tubes were incubated at 30°C for 10 minutes.

From each reaction, 5 μL was used to measure the rLuc activity. Samples were run in triplicate, and the mean rLuc activity and standard deviation were calculated for each sample set. The average percent inhibition of rLuc activity by p9 was calculated relative to GST. Differences between the levels of rLuc activity for the GST and p9 samples, as well as between the control (standard protocol) and experimental (pre-incubation in HeLa S10) group samples were assessed, and their statistical significance was calculated using Student's t-tests.

Protocol for in vitro translation in HeLa S10 +/- micrococcal nuclease treatment

The protocol for testing the activity of p9 in HeLa S10 extract that was treated or untreated with calcium ion-dependent micrococcal nuclease is the same as for the standard HeLa S10 extract in vitro translation protocol previously described. However, one set of reactions, referred to as “nuclease minus,” used HeLa S10 extract that was not treated with micrococcal nuclease or EGTA during the preparation of the extract.

As usual, 5 μL of each reaction was used to measure the rLuc activity, samples were run in triplicate, and the mean rLuc activity and standard deviation were calculated for each sample set. The activity of p9 was calculated as the average percent inhibition of rLuc activity by p9 relative to GST. The statistical significance of the differences between the levels of rLuc activity observed for the GST and p9 samples, as well as

between the nuclease treated and untreated groups, was determined using Student's and two sample (unequal variance) t-tests, respectively.

WGE protocol

For *in vitro* translation in WGE, the following reagents were combined to yield a 20 μ L total volume: 12.5 μ L WGE (Promega), recombinant GST or p9 protein, and water. This mixture was preincubated at 30°C for ten minutes. Then the following were added to each reaction: 2 μ L complete amino acid mixture (Promega), 2 μ L 1 M KOAc, and 1 μ L RNA (0.25 μ g/ μ L). Then, the tubes were incubated at 25°C for 30 minutes.

From each reaction, 5 μ L was used to measure the rLuc activity. The samples were run in triplicate, and the mean rLuc activity and standard deviation were calculated for each sample set. As with the other *in vitro* translation protocols described above, Student's t-tests were used to establish statistical significance. The activity of p9 was calculated as the mean percent inhibition relative to the GST control.

WGE + HeLa S10 protocol

For *in vitro* translation in WGE supplemented with HeLa S10 extract, the same protocol was used as for WGE alone but with the addition of 5 μ L HeLa S10 extract (20% of final volume). The volume of WGE (12.5 μ L) was not reduced, and the total reaction volume remained unchanged.

48S Complex SGC analysis

Sucrose gradient centrifugation (SGC) analysis was performed in a similar fashion as described previously, but using RRL supplemented with 20% HeLa S100

extract for the *in vitro* formation of 48S ribosomal complexes (Bordeleau et al., 2006; Lokugamage et al., 2012). The RRL supplemented with HeLa S100 extract was incubated with GST or p9 and the other translation reaction components on ice for ten minutes as in a typical RRL plus HeLa S100 extract *in vitro* translation reaction. Guanosine 5'-[β,γ -imido]triphosphate (GMP-PNP) and 200 ng of [α - ^{32}P]UTP-radiolabeled EMCV-fLuc RNA was added to the tubes, and translation was carried out at 30°C for 30 minutes. The samples were subjected to SGC analysis on 10-40% sucrose gradients. The radioactivity of each fraction in counts per minute (cpm) was calculated as a percentage of the total radioactivity for all of the fractions collected from the gradient, and the reduction in the 48S complex formation in the presence of p9 relative to the GST control was calculated (based on a comparison of the total area under the curves by integration).

RESULTS

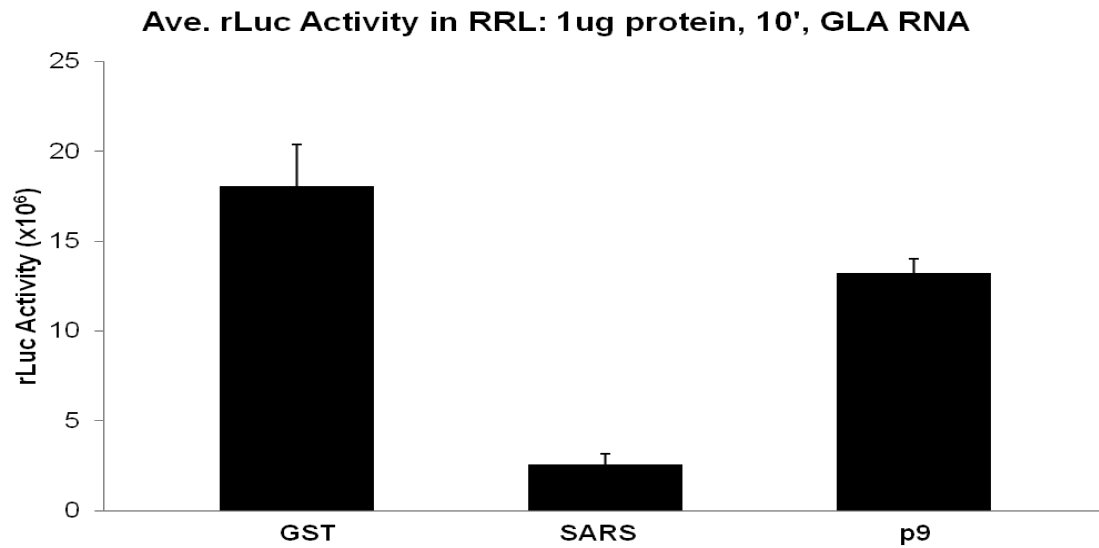


Figure 1: SARS-CoV nsp1 and TGEV p9-mediated translation inhibition in RRL

Capped and polyadenylated GLA mRNA (0.25 μ g RNA) was translated in RRL (Ambion Retic Lysate IVT Kit) for 10 minutes at 30°C in the presence of 1 μ g of purified GST, SARS-CoV nsp1 (SARS), or TGEV p9 (p9). A portion of each translation reaction was used to measure the rLuc activity. The average rLuc activity from triplicate samples is shown. The average rLuc activity for SARS-CoV nsp1 samples was 14% of GST and p9 samples was 73% of GST (86% and 27% inhibition, respectively); $P < 0.01$ for SARS-CoV nsp1, $P < 0.05$ for p9. Error bars represent the standard deviation. The data shown is representative of three or more independent experiments.

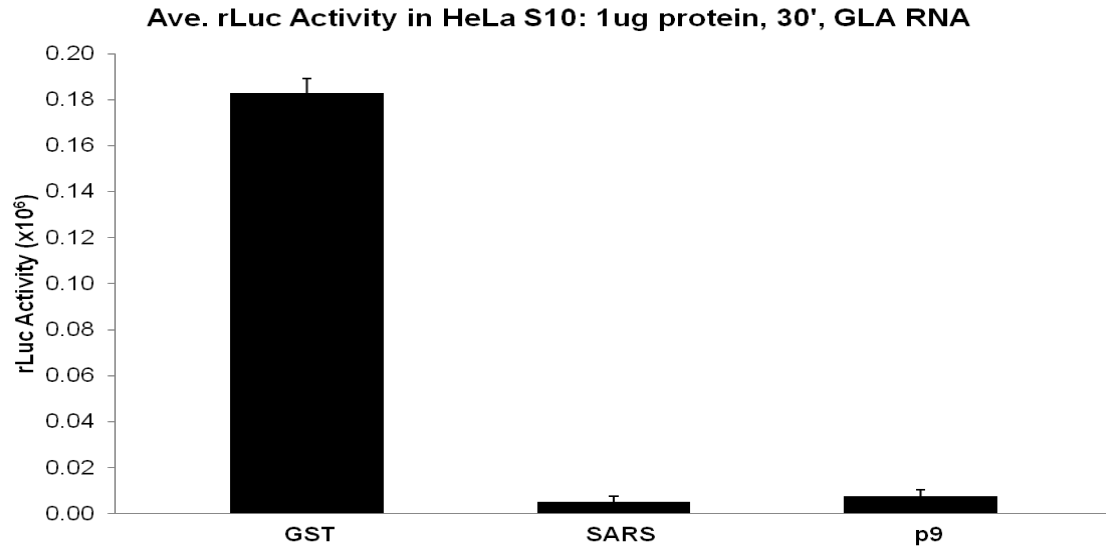


Figure 2: SARS-CoV nsp1 and TGEV p9-mediated translation inhibition in HeLa S10 extract

Capped and polyadenylated GLA mRNA (0.25 μ g RNA) was translated in HeLa S10 extract for 30 minutes at 30°C in the presence of 1 μ g of purified GST, SARS-CoV nsp1 (SARS), or TGEV p9 (p9). A portion of each translation reaction was used to measure the rLuc activity. The average rLuc activity from triplicate samples is shown. The average rLuc activity for SARS-CoV nsp1 samples was 3% of GST and p9 samples was 4% of GST (97% and 96% inhibition, respectively); $P < 0.01$ for both SARS-CoV nsp1 and p9. Error bars represent the standard deviation. The data shown is representative of three or more independent experiments.

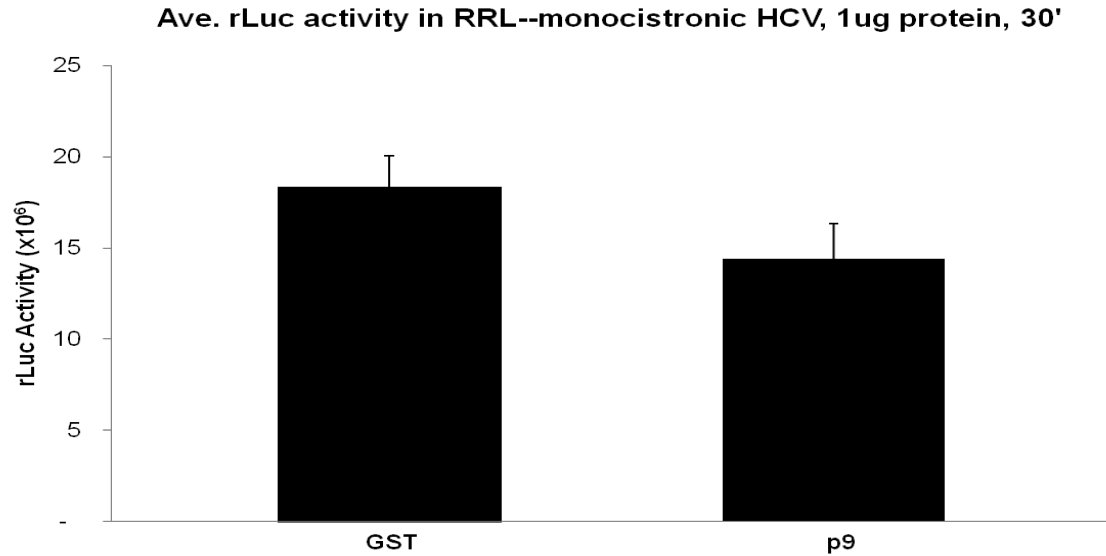


Figure 3: TGEV p9-mediated suppression of HCV IRES-driven translation in RRL

Monocistronic HCV IRES-containing HCV-rLuc mRNA (0.25 μ g RNA) was translated in RRL (Ambion Retic Lysate IVT Kit) for 30 minutes at 30°C in the presence of 1 μ g of purified GST or TGEV p9 (p9). A portion of each translation reaction was used to measure the rLuc activity. The average rLuc activity from triplicate samples is shown. The average rLuc activity for p9 samples was 78% of GST (22% inhibition); $P < 0.05$. Error bars represent the standard deviation. The data shown is representative of three or more independent experiments.

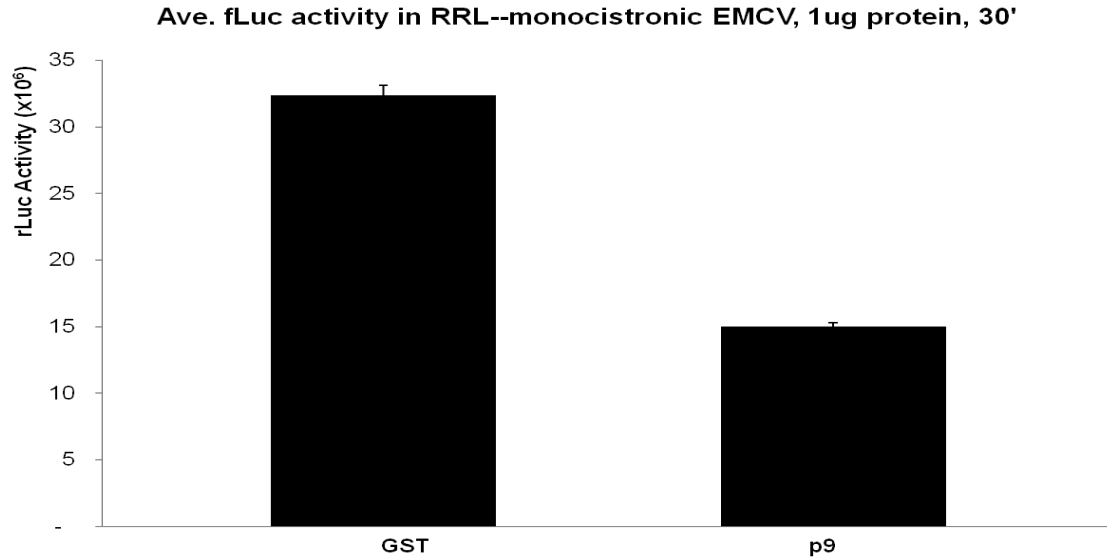


Figure 4: TGEV p9-mediated suppression of EMCV IRES-driven translation in RRL

Monocistronic EMCV IRES-containing EMCV-fLuc mRNA (0.25 μ RNA) was translated in RRL (Ambion Retic Lysate IVT Kit) for 30 minutes at 30°C in the presence of 1 μ g of purified GST or TGEV p9 (p9). A portion of each translation reaction was used to measure the fLuc activity. The average fLuc activity from triplicate samples is shown. The average fLuc activity for p9 samples was 46% of GST (54% inhibition); $P < 0.01$. Error bars represent the standard deviation. The data shown is representative of three or more independent experiments.

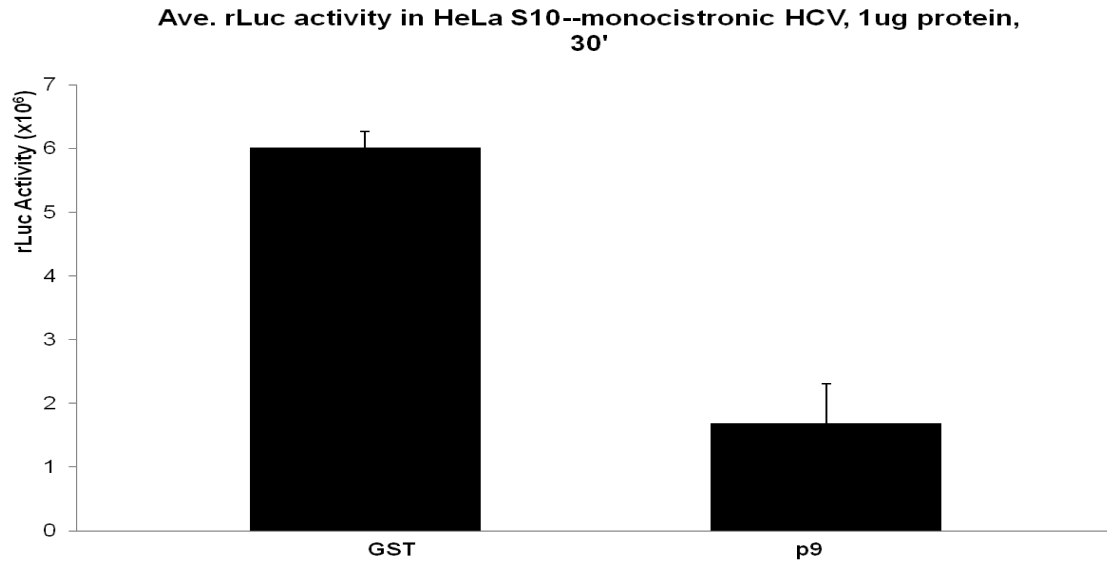


Figure 5: TGEV p9-mediated suppression of HCV IRES-driven translation in HeLa S10 extract

Monocistronic HCV IRES-containing HCV-rLuc mRNA (0.25 μ g RNA) was translated in HeLa S10 extract for 30 minutes at 30°C in the presence of 1 μ g of purified GST or TGEV p9 (p9). A portion of each translation reaction was used to measure the rLuc activity. The average rLuc activity from triplicate samples is shown. The average rLuc activity for p9 samples was 28% of GST (72% inhibition); $P < 0.01$. Error bars represent the standard deviation. The data shown is representative of three or more independent experiments.

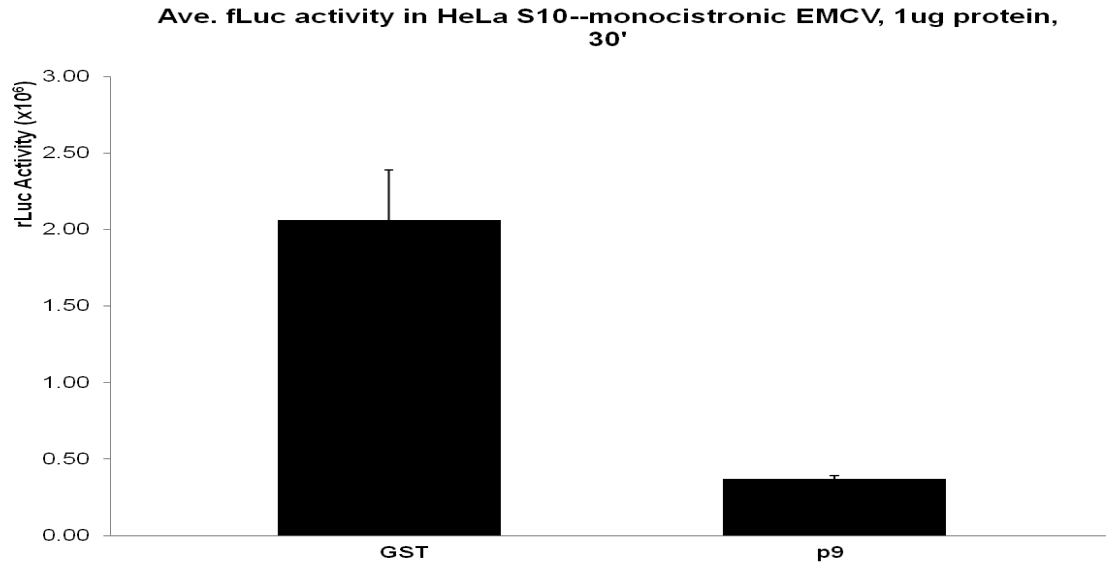


Figure 6: TGEV p9-mediated suppression of EMCV IRES-driven translation in HeLa S10 extract

Monocistronic EMCV IRES-containing EMCV-fLuc mRNA (0.25 μ g RNA) was translated in HeLa S10 extract for 30 minutes at 30°C in the presence of 1 μ g of purified GST or TGEV p9 (p9). A portion of each translation reaction was used to measure the fLuc activity. The average fLuc activity from triplicate samples is shown. The average fLuc activity for p9 samples was 18% of GST (82% inhibition); $P < 0.01$. Error bars represent the standard deviation. The data shown is representative of three or more independent experiments.

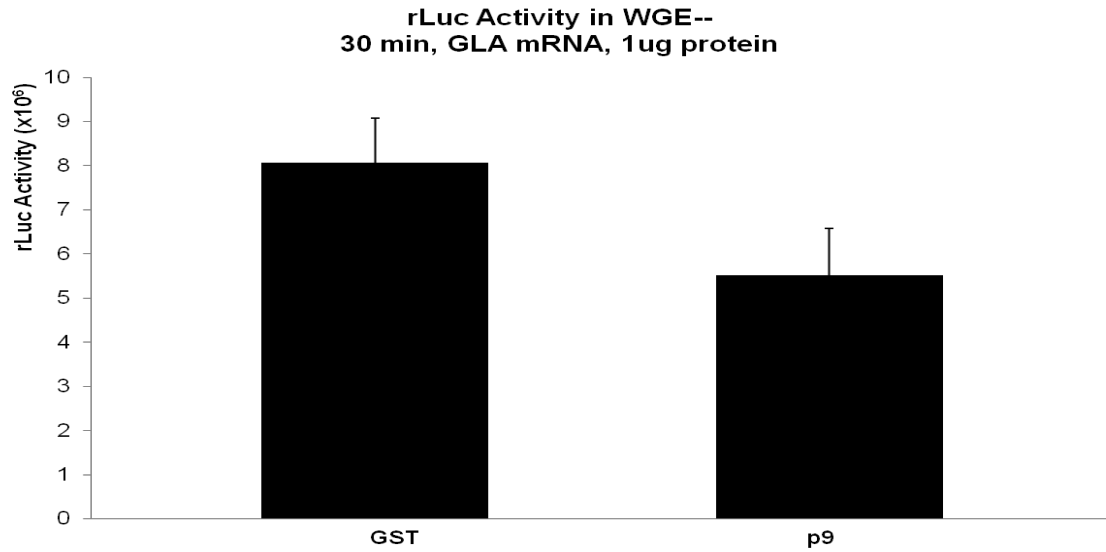


Figure 7: TGEV p9-mediated translation inhibition in WGE

Capped and polyadenylated GLA mRNA (0.25 μ g RNA) was translated in WGE (Promega) for 30 minutes at 30°C in the presence of 1 μ g of purified GST or TGEV p9 (p9). A portion of each translation reaction was used to measure the rLuc activity. The average rLuc activity from triplicate samples is shown. The average rLuc activity for p9 samples was 68% of GST (32% inhibition); $P < 0.05$. Error bars represent the standard deviation. The data shown is representative of three or more independent experiments.

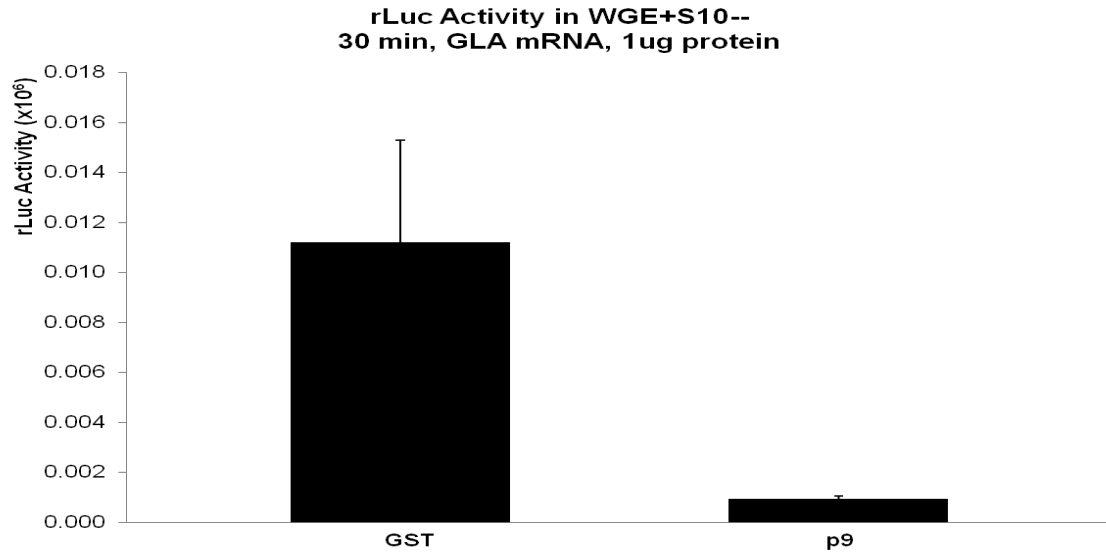


Figure 8: TGEV p9-mediated translation inhibition in WGE + S10

Capped and polyadenylated GLA mRNA (0.25 μ g RNA) was translated in WGE (Promega) supplemented with 20% (v/v) HeLa S10 extract for 30 minutes at 30°C in the presence of 1 μ g of purified GST or TGEV p9 (p9). A portion of each translation reaction was used to measure the rLuc activity. The average rLuc activity from triplicate samples is shown. The average rLuc activity for p9 samples was 8% of GST (92% inhibition); $P < 0.05$. Error bars represent the standard deviation. The data shown is representative of three or more independent experiments.

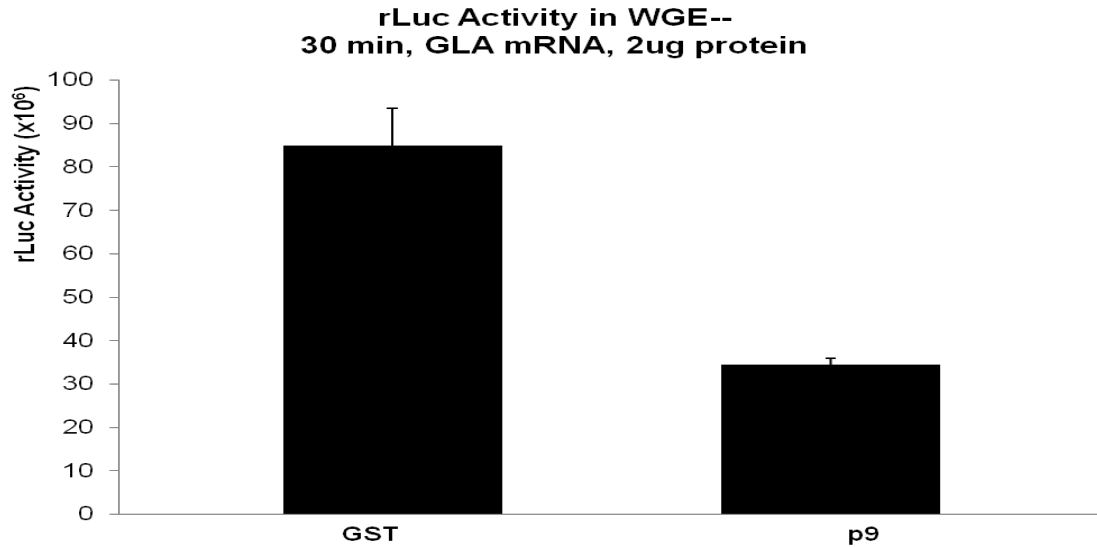


Figure 9: TGEV p9-mediated translation inhibition in WGE

Capped and polyadenylated GLA mRNA (0.25 μ g RNA) was translated in WGE (Promega) for 30 minutes at 30°C in the presence of 2 μ g of purified GST or TGEV p9 (p9). A portion of each translation reaction was used to measure the rLuc activity. The average rLuc activity from triplicate samples is shown. The average rLuc activity for p9 samples was 41% of GST (59% inhibition); $P < 0.01$. Error bars represent the standard deviation. The data shown is representative of three or more independent experiments.

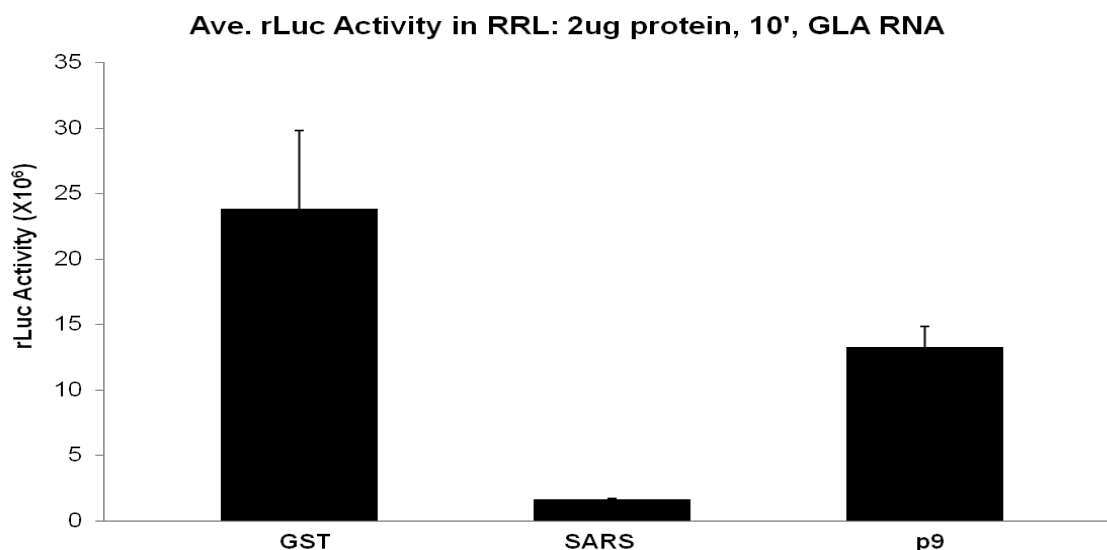


Figure 10: SARS-CoV nsp1 and TGEV p9-mediated translation inhibition in RRL

Capped and polyadenylated GLA mRNA (0.25 μ g RNA) was translated in RRL (Ambion Retic Lysate IVT Kit) for 10 minutes at 30°C in the presence of 2 μ g of purified GST, SARS-CoV nsp1 (SARS), or TGEV p9 (p9). A portion of each translation reaction was used to measure the rLuc activity. The average rLuc activity from triplicate samples is shown. The average rLuc activity for SARS-CoV nsp1 samples was 7% of GST and p9 samples was 56% of GST (93% and 44% inhibition, respectively); $P \leq 0.01$ for SARS-CoV nsp1, $P < 0.05$ for p9. Error bars represent the standard deviation. The data shown is representative of three or more independent experiments.

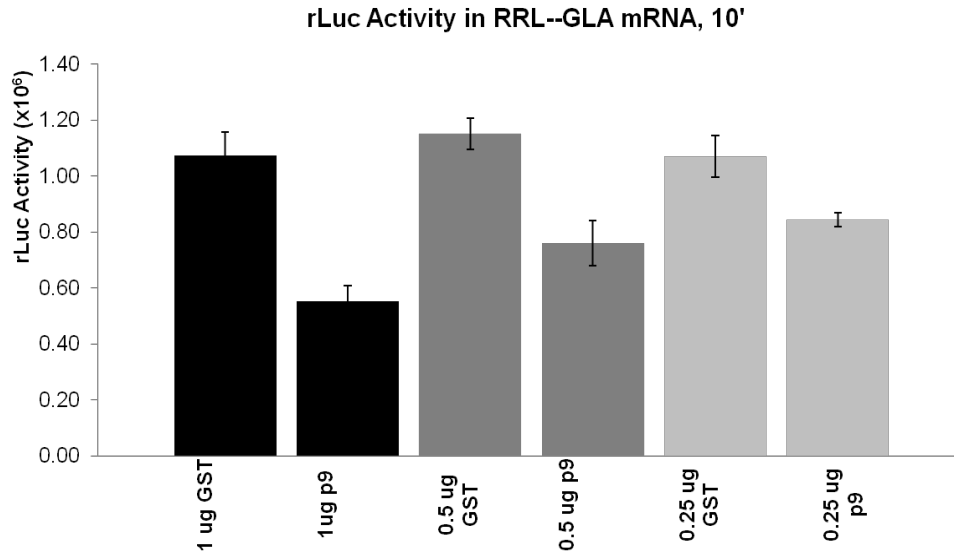


Figure 11: TGEV p9-mediated translation inhibition in RRL

Capped and polyadenylated GLA mRNA (0.25 μ g RNA) was translated in RRL (Ambion Retic Lysate IVT Kit) for 10 minutes at 30°C in the presence of different concentrations (0.25, 0.5, or 1 μ g) of purified GST or TGEV p9 (p9). A portion of each translation reaction was used to measure the rLuc activity. The average rLuc activity from triplicate samples is shown. The average rLuc activity for p9 samples was 79%, 66%, and 52% of GST for 0.25, 0.5, and 1 μ g of p9, respectively (21%, 34%, and 48% inhibition, respectively); $P < 0.01$ for all samples. Error bars represent the standard deviation.

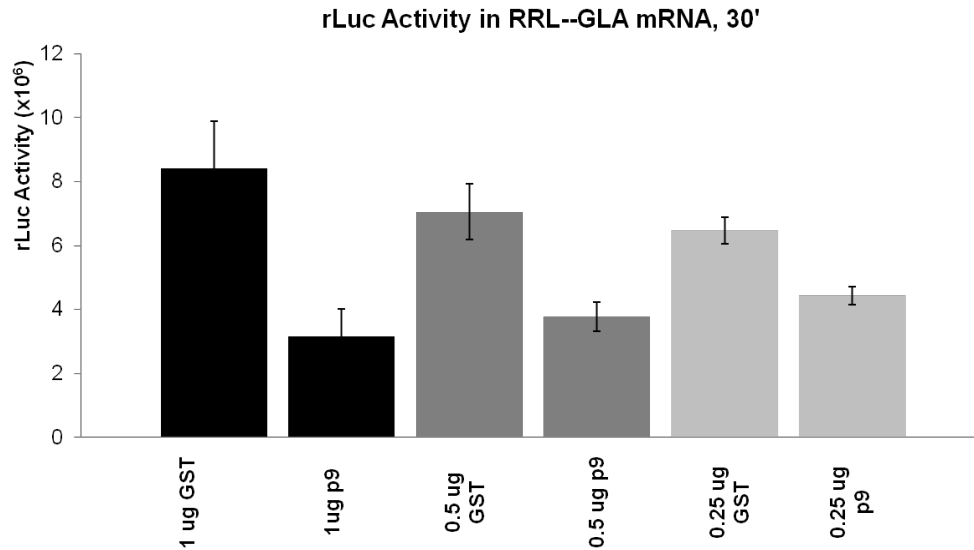


Figure 12: TGEV p9-mediated translation inhibition in RRL

Capped and polyadenylated GLA mRNA (0.25 μ g RNA) was translated in RRL (Ambion Retic Lysate IVT Kit) for 30 minutes at 30°C in the presence of different concentrations (0.25, 0.5, or 1 μ g) of purified GST or TGEV p9 (p9). A portion of each translation reaction was used to measure the rLuc activity. The average rLuc activity from triplicate samples is shown. The average rLuc activity for p9 samples was 69%, 54%, and 38% of GST for 0.25, 0.5, and 1 μ g of p9, respectively (31%, 46%, and 62% inhibition, respectively); $P < 0.01$ for all samples. Error bars represent the standard deviation.

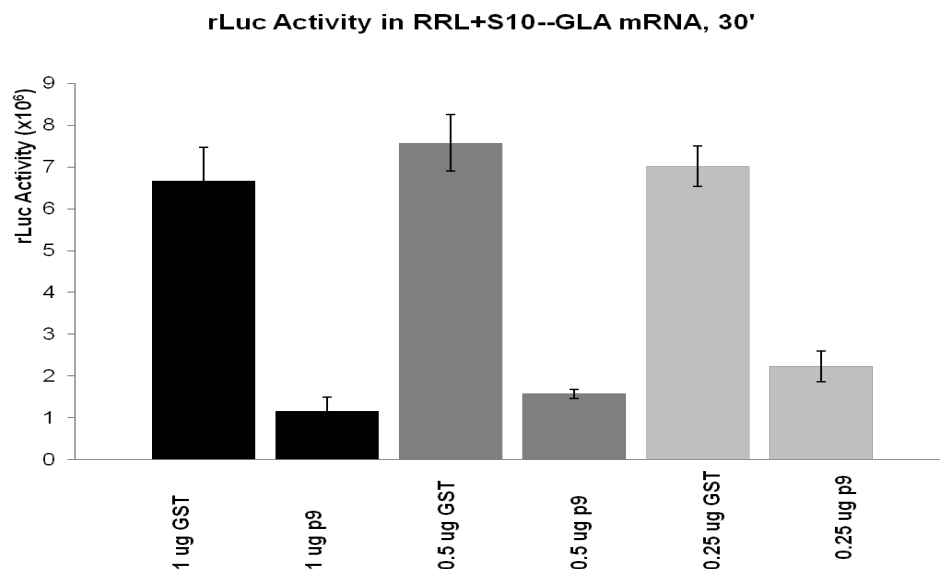


Figure 13: TGEV p9-mediated translation inhibition in RRL + HeLa S10

Capped and polyadenylated GLA mRNA (0.25 μ g RNA) was translated in RRL (Ambion Retic Lysate IVT Kit) supplemented with 20% (v/v) HeLa S10 extract for 30 minutes at 30°C in the presence of different concentrations (0.25, 0.5, or 1 μ g) of purified GST or TGEV p9 (p9). A portion of each translation reaction was used to measure the rLuc activity. The average rLuc activity from triplicate samples is shown. The average rLuc activity for p9 samples was 32%, 21%, and 18% of GST for 0.25, 0.5, and 1 μ g of p9, respectively (68%, 79%, and 82% inhibition, respectively); $P < 0.01$ for all samples. Error bars represent the standard deviation.

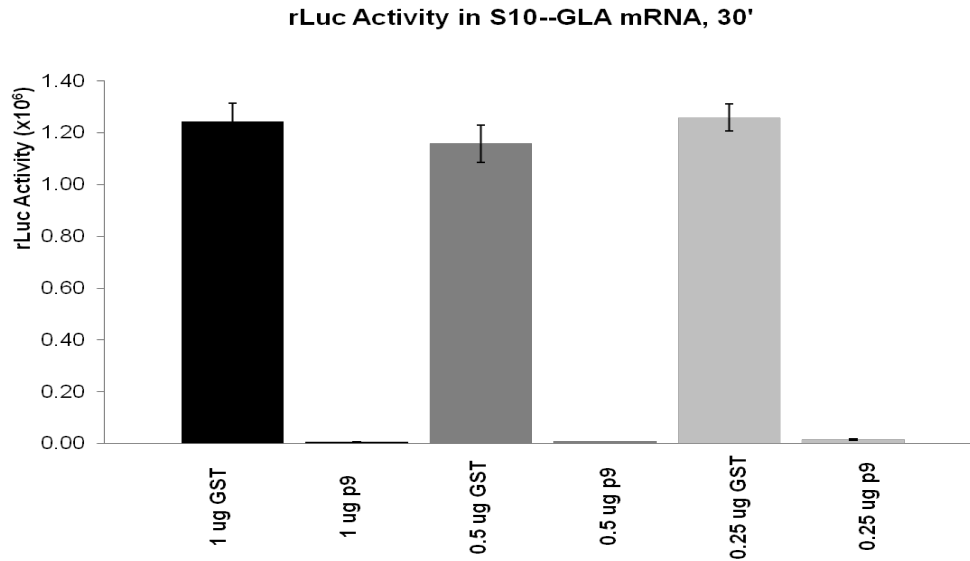


Figure 14: TGEV p9-mediated translation inhibition in HeLa S10

Capped and polyadenylated GLA mRNA (0.25 μ g RNA) was translated in HeLa S10 extract for 30 minutes at 30°C in the presence of different concentrations (0.25, 0.5, or 1 μ g) of purified GST or TGEV p9 (p9). A portion of each translation reaction was used to measure the rLuc activity. The average rLuc activity from triplicate samples is shown. The average rLuc activity for p9 samples was 1% (1.3%), 1% (0.9%), and 0% (0.5%) of GST for 0.25, 0.5, and 1 μ g of p9, respectively (99% (98.7%), 99% (99.1%), and 100% (99.5%) inhibition, respectively); $P < 0.01$ for all samples. Error bars represent the standard deviation.

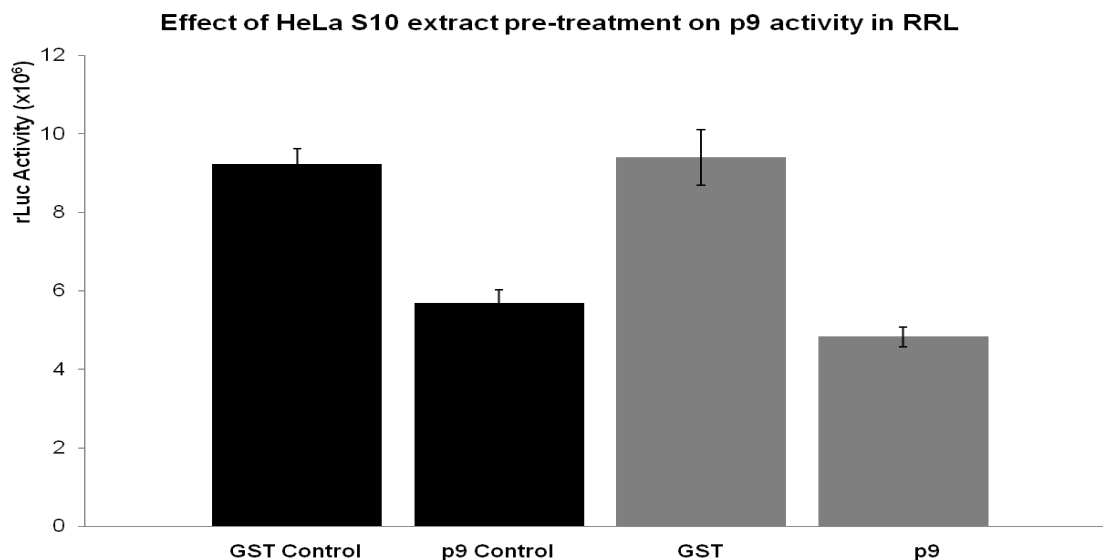


Figure 15: Effect of HeLa S10 extract pre-treatment on TGEV p9-mediated translation inhibition in RRL

Capped and polyadenylated GLA mRNA (0.25 μ g RNA) was translated in RRL (Ambion Retic Lysate IVT Kit) for 30 minutes at 30°C in the presence of 0.5 μ g of purified GST (GST control) or TGEV p9 (p9 control) as described in figure 1 [black bars], or in the presence of 0.5 μ g of purified GST or TGEV p9 (p9) that was first incubated in HeLa S10 extract [gray bars]. A portion of each translation reaction was used to measure the rLuc activity. The average rLuc activity from triplicate samples is shown. The average rLuc activity for control p9 samples was 62% of control GST and pre-treatment p9 samples was 51% of pre-treatment GST (38% and 49% inhibition, respectively); $P < 0.01$ for control and $P < 0.05$ for pre-treatment groups. Error bars represent the standard deviation. The data shown is representative of two independent experiments.

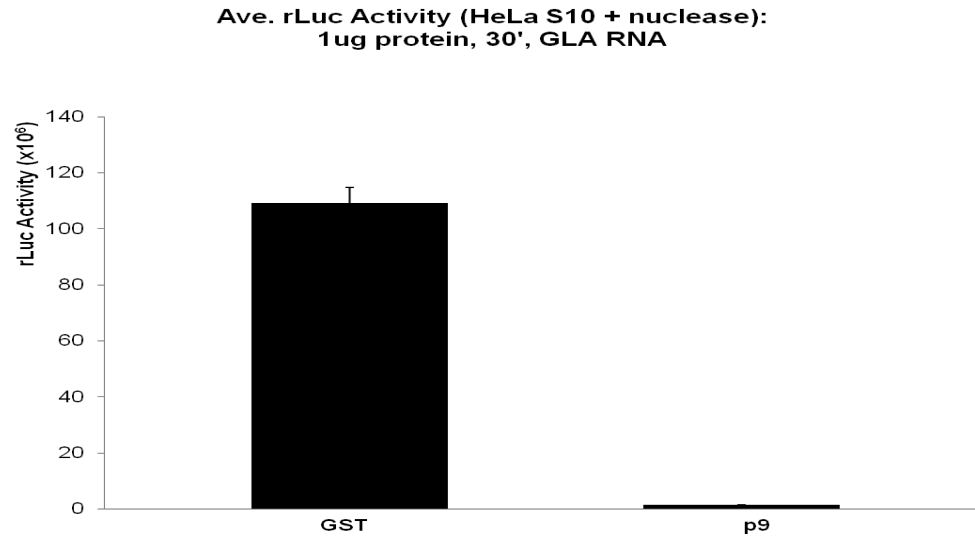


Figure 16: TGEV p9-mediated translation inhibition in nuclease-treated HeLa S10 extract

Capped and polyadenylated GLA mRNA (0.25 μ g RNA) was translated in micrococcal nuclease-treated HeLa S10 extract for 30 minutes at 30°C in the presence of 1 μ g of purified GST or TGEV p9 (p9), as described in Fig. 2. A portion of each translation reaction was used to measure the rLuc activity. The average rLuc activity from triplicate samples is shown. The average rLuc activity for p9 samples was 1% of GST (99% inhibition); $P < 0.01$. Error bars represent the standard deviation. The data shown is representative of three or more independent experiments.

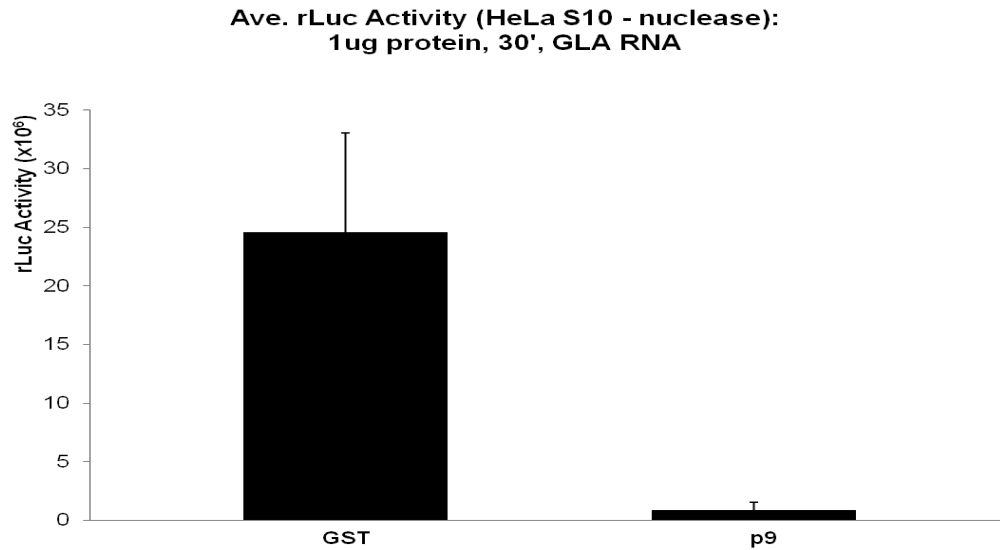


Figure 17: TGEV p9-mediated translation inhibition in nuclease-untreated HeLa S10 extract

Capped and polyadenylated GLA mRNA (0.25 μ g RNA) was translated in HeLa S10 extract untreated with micrococcal nuclease for 30 minutes at 30°C in the presence of 1 μ g of purified GST or TGEV p9 (p9). A portion of each translation reaction was used to measure the rLuc activity. The average rLuc activity from triplicate samples is shown. The average rLuc activity for p9 samples was 6% of GST (94% inhibition); $P < 0.05$. Error bars represent the standard deviation.

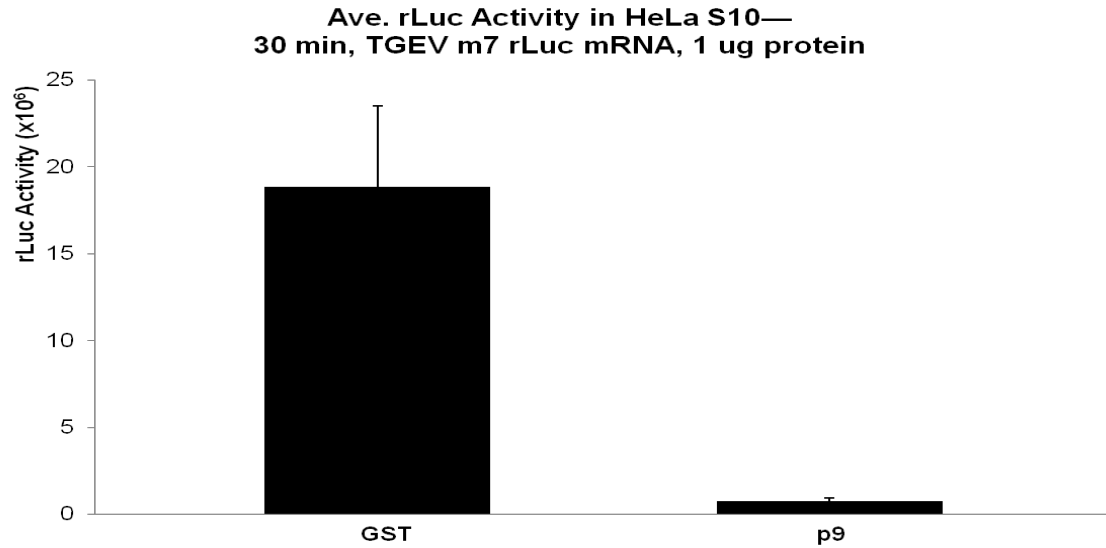


Figure 18: TGEV p9-mediated translation inhibition in HeLa S10 extract

Capped and polyadenylated chimeric TGEV m7-like mRNA (0.25 µg RNA) containing the rLuc ORF flanked by the TGEV 5' and 3' UTRs was translated in HeLa S10 extract for 30 minutes at 30°C in the presence of 1 µg of purified GST or TGEV p9 (p9). A portion of each translation reaction was used to measure the rLuc activity. The average rLuc activity from triplicate samples is shown. The average rLuc activity for p9 samples was 4% of GST (96% inhibition); $P < 0.01$. Error bars represent the standard deviation. The data shown is representative of three or more independent experiments.

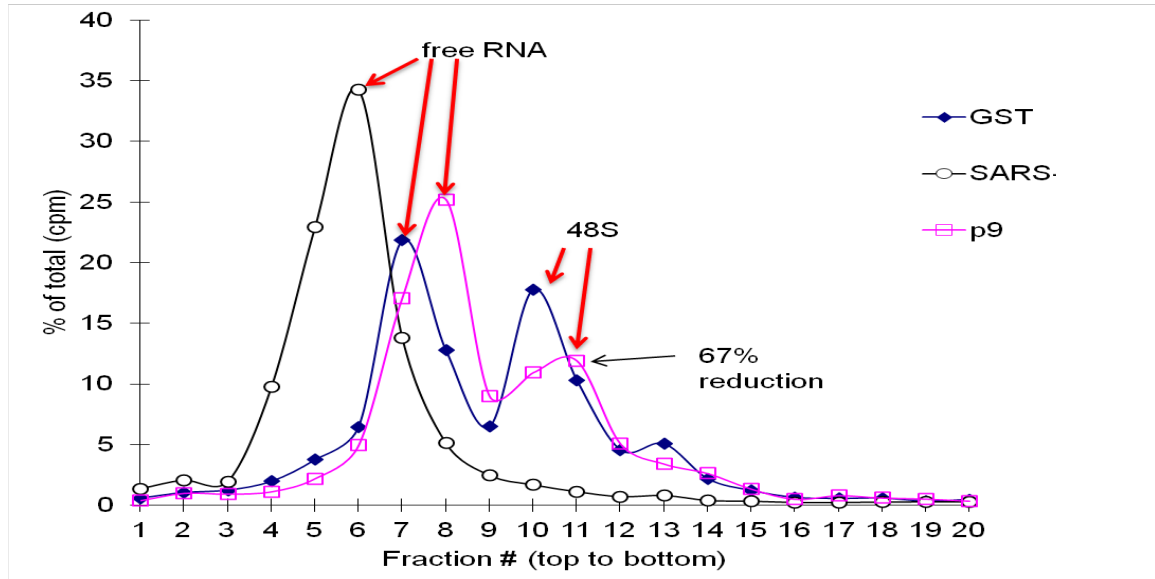


Figure 19: SGC analysis of 48S complex formation in the presence of SARS-CoV nsp1 and TGEV p9

RRL (Ambion Retic Lysate IVT Kit) supplemented with 20% (v/v) concentrated HeLa S100 extract was incubated with GST, SARS-CoV nsp1 (SARS) or TGEV p9 (p9) in the presence of GMP-PNP, then radiolabeled EMCV-fLuc RNA (200 ng RNA) was added, and translation was carried out at 30°C for 30 minutes. The samples were subjected to SGC analysis. The y-axis represents the radioactivity of each fraction as a percentage of the total radioactivity. The reduction in 48S complex formation in the presence of p9 relative to GST is shown (67% reduction).

Although the interaction of p9 and 40S ribosomal subunits was studied using stringent co-immunoprecipitation conditions (high salt buffer and high stringency washing conditions) under which SARS-CoV nsp1 and 40S interactions are maintained, potential p9-ribosome interactions under conditions of low stringency had not been previously studied (Huang et al., 2011a; data not shown). As p9 was demonstrated to share high levels of conservation with the Alpha-CoVs HCoV-NL63 and HCoV-229E, which have been reported to bind to the 40S ribosomal subunit, it was necessary to further assess if ribosome binding played a role in p9-mediated translation suppression (Jansson, 2013; Narayanan et al., 2014; Wang et al., 2010). Polysome profile analysis performed using cultured 293 cells transfected with RNA encoding C-terminal myc-tagged chloramphenicol acetyltransferase (CAT) (negative control), SARS-CoV nsp1, or p9 confirmed that p9 does not associate with the 40S ribosomal subunit even under low stringency conditions (data not shown). Both p9 and CAT were found in the fractions lacking rRNA, while the SARS-CoV nsp1 protein was found in the fractions containing the 40S ribosomal subunit (data not shown). Thus, unlike SARS-CoV nsp1, p9 does not gain access to mRNA templates via direct binding of the 40S ribosomal subunit (Huang et al., 2011a; Jansson, 2013; Narayanan et al., 2014).

Although the published literature states that p9 cannot suppress translation *in vitro* in RRL, it was discovered that this is not entirely accurate, and that p9 can inhibit translation in RRL (Fig. 1), though to a lesser extent than in HeLa extract (Fig. 2) (Huang et al., 2011a). Regardless of the *in vitro* translation system used, p9-mediated translation inhibition was strongest for cap-dependent translation, e.g. GLA mRNA translation (Figs. 1 and 2). In RRL, relatively moderate p9-mediated translation inhibition was also observed for HCV IRES- (Fig. 3) and EMCV IRES- (Fig. 4) driven translation of monocistronic reporter RNA containing the HCV IRES and EMCV IRES, respectively. As with cap-dependent translation, p9-mediated inhibition of both HCV IRES- (Fig. 5) and EMCV IRES- (Fig. 6) dependent translation was stronger in HeLa extract. It should

be noted that the previously published data only examined the effect of p9 on dicistronic RNA constructs encoding two reporter genes, with the synthesis of the 5' reporter gene product driven by cap-mediated translation, and synthesis of the 3' reporter gene product driven by IRES-mediated translation (Huang et al., 2011a).

That p9 is biologically active in RRL was an important finding. It was originally believed that the inability of p9 to inhibit translation in RRL meant that p9 does not directly target the (canonical) eIFs, 40S or 60S ribosomal subunit, all of which are found in RRL, nor bind to mRNA templates and make them translationally inactive (Huang et al., 2011a). However, as inhibition was observed in RRL, albeit to a lesser extent than in HeLa extract, the possibility exists that p9 may target one or more of the translation machinery components mentioned above, though it may do so indirectly (e.g. via a binding partner). Similar levels of inhibition were observed in RRL manufactured by both Promega and Ambion for both p9 and SARS-CoV nsp1, suggesting that SARS-CoV nsp1 and p9 activity was not altered by the RRL system used (data not shown [can compare dissertation figures with Huang et al, 2011a]). Consistent with the published literature, SARS-CoV nsp1 strongly inhibited translation in RRL and HeLa S10 extract, as well as RRL supplemented with HeLa extract (Huang et al., 2011a; Figs. 1, 2, and data not shown, respectively).

In addition to HeLa extract and RRL, p9 activity was tested in WGE and was found to inhibit cap- and IRES-mediated translation at levels similar to those observed for RRL (Fig. 7). This was an unexpected finding as WGE was hypothesized to be more similar to HeLa extract than RRL, and p9 was expected to have similar activity in WGE as in HeLa S10 extract. However, as WGE is a plant extract, it may be that WGE does not contain or utilize all of the same host factor(s) for translation as HeLa extract, or it may simply be more similar to RRL in composition than anticipated. It should be noted that SARS-CoV nsp1, which had never previously been tested in WGE either, was able to strongly inhibit both cap- and IRES-mediated translation in WGE (data not shown), just

as in RRL, HeLa S10 extract, or RRL supplemented with HeLa extract (data not shown). The effect of p9 is strongest in HeLa S10 extract for any given mRNA template (Fig. 2). Similar to RRL supplemented with HeLa extract, an intermediate level of inhibition is observed when WGE is supplemented with HeLa extract (Huang et al., 2011a; Fig. 8).

Although TGEV p9-mediated translation inhibition is most efficient for a given amount of p9 protein and capped mRNA in HeLa extract, the effect of p9 on capped mRNA translation in both WGE (Figs. 9) and RRL (Figs. 10 and 11) can be enhanced by increasing the amount of p9 protein used in the reaction. The activity of p9 in RRL can also be increased by a longer incubation time (Fig. 12). The same is true regarding protein amount and incubation time for RRL supplemented with HeLa extract (Fig. 13). That the addition of an equivalent amount of HeLa S10 or S100 extract similarly enhances p9 activity in RRL, suggests that the presence or absence of HeLa cell ribosomes does not play a significant role in p9-mediated translation inhibition in RRL (data not shown). This may be another indication that p9, unlike SARS-CoV nsp1, does not (directly) rely on ribosomes or the ribosomal subunits to exert its biological activity.

As the experimental conditions (e.g. amount of protein and/or incubation time) used for the control GST reactions were the same as for the p9 reactions, other variables that might explain the enhancement in p9 activity were controlled for as much as possible. In HeLa S10 extract, a longer incubation time or greater amount of p9 protein also favors p9 activity, but the effect is less pronounced as HeLa S10 extract requires a longer incubation period to reach levels of translation activity (measured in terms of rLuc activity) comparable to those seen in RRL, and even a small amount of p9 is sufficient to achieve strong translation inhibition in HeLa S10 (Fig. 14). The findings regarding incubation time seemingly contradict the published findings stating that no change in p9-mediated translation inhibition was observed in either RRL or HeLa S10 extract with a longer incubation (Huang et al., 2011a). However, it might be more appropriate to state that p9 activity was significantly stronger in HeLa S10 extract than RRL for any given

incubation time or concentration of p9 tested. It should also be noted that the enhanced activity of p9 in HeLa S10 extract (or RRL supplemented with S10) versus RRL alone does not appear to be due to a dilution effect (unpublished data; data not shown). The above data suggest that there is a factor(s) in HeLa extract that enhance(s) the activity of p9.

Additional evidence suggesting that there is a factor present in HeLa extract that enhances the activity of p9 is that preincubation of p9 in HeLa S10 extract may enhance its activity in RRL. When p9 protein was preincubated in HeLa S10 extract before being added to RRL, p9-mediated translation inhibition of GLA mRNA was significantly stronger following a 30-minute incubation in RRL than control p9 protein that was directly added to RRL (Fig. 15). The same result was not observed for the GST control protein. The rLuc activity of the GST samples remained statistically unchanged, regardless of whether the GST protein was preincubated in HeLa S10 extract or directly added to RRL (Fig. 15).

The HeLa extract factor(s) responsible for enhancing p9 activity may be associated with host mRNP complexes *in vivo*. During the preparation of HeLa S10 extract, the extract is typically treated with micrococcal nuclease to degrade endogenous nucleic acids, particularly HeLa cell mRNAs (Ehrenfeld and Brown, 1981). This nuclease treatment helps to eliminate background protein synthesis by limiting the translation of HeLa cell mRNAs, thereby promoting the translation of exogenous mRNAs added to the translation reaction (Ehrenfeld and Brown, 1981). By using HeLa S10 extract untreated with nuclease for *in vitro* translation, it was anticipated that the yield of rLuc reporter protein would be lower than in nuclease treated HeLa S10 for both the GST control and p9 samples due to the presence of HeLa mRNAs. However, it was also believed that p9 activity would be decreased in HeLa S10 untreated with micrococcal nuclease, as the host factor(s) responsible for enhancing p9 activity might remain associated with host mRNP complexes in the absence of nuclease treatment, thereby

limiting the amount of this factor(s) available to associate with reporter mRNA-containing mRNP complexes, which would limit p9 access to these complexes. As comparison of Figs. 16 and 17 shows, p9-mediated translation inhibition is decreased in the absence of nuclease treatment. Testing this hypothesis with a two sample t-test (unequal variance) to compare p9 activity in nuclease treated and untreated HeLa S10 extract indicated that there was a statistically significant difference between the two sample sets. Thus, the factor(s) present in HeLa extract that is responsible for the enhancement of p9 activity *in vitro* likely associates with HeLa cell mRNPs in the absence of nuclease treatment.

Another interesting finding was that the TGEV UTRs (including the 5' leader sequence) did not protect a chimeric reporter mRNA from p9-mediated translation inhibition *in vitro* in HeLa extract (Fig. 18). That the TGEV UTRs did not protect mRNA from p9-mediated translation inhibition is not an unprecedented finding. In infected cells, SARS-CoV mRNAs appear to be affected by cleavage-independent SARS-CoV nsp1-mediated translation inhibition even though mRNAs carrying the SARS-CoV 5'-leader sequence are protected from SARS-CoV nsp1-mediated modification (Huang et al., 2011b; Narayanan et al., 2014). However, the role(s) of the CoV UTRs in protecting CoV mRNAs from the biological activity of nsp1, or potentially even enhancing CoV translation or replication, is not fully understood. It has been suggested that the SARS-CoV 5' UTR may do both (Narayanan et al., 2014; Tanaka et al., 2012).

SGC analysis in RRL supplemented with HeLa S100 extract treated with GMP-PNP showed that, in the presence of p9, 48S initiation complex formation was reduced compared to the GST control (Fig. 19). Unfortunately, SGC analysis of 80S complex formation in the presence of p9 was not conclusive (data not shown). This suggests that p9 may target a factor involved in 48S complex formation, although its effect on 80S complex formation is not clear.

DISCUSSION

Among the conserved amino acid residues shared by the nsp1s of the Alpha-CoVs, many are thought to be more important for the structural stability of these proteins rather than their biological function(s) because the representative TGEV p9 amino acid residues are located within the protein's core (Jansson, 2013). However, some of the amino acid residues located on the TGEV p9 surface are relatively well conserved among the Alpha-CoV nsp1s, and these residues may be involved in the interaction of p9 with its protein binding partner(s) or target molecule(s) (Jansson, 2013). This protein(s) or factor(s) may well be the host factor(s) present in HeLa extracts that enhances p9 activity *in vitro* (Huang et al., 2011a).

In vivo, the ability of p9 to suppress host gene expression in both infected and expressed cells has been demonstrated (Huang et al., 2011a). *In vitro*, it was demonstrated that p9 activity is not limited to HeLa S10 extract or RRL supplemented with HeLa extract, and that the translation of a variety of mRNAs can be inhibited by p9, to varying degrees, in RRL and WGE, as well as WGE supplemented with HeLa extract. As p9 activity is strongest in HeLa S10 extract, the previously published hypothesis that RRL does not contain a factor that inactivates p9, but that HeLa extract contains a factor(s) that enhances the activity of p9 remains the leading hypothesis to explain the differences in p9 activity observed across the cell-free *in vitro* translation systems tested (Huang et al., 2011a). That p9 activity in WGE is similar to that in RRL can be added to the body of knowledge regarding the mechanism of p9-mediated translation inhibition, and may provide invaluable insight/clues as to the identity of this factor(s). As HeLa extracts are made from nucleated cells, it was proposed that this host factor(s) may only be found in nucleated cells (Huang et al., 2011a). As WGE extract is derived from nucleated cells, it might be that this factor(s) is specific to nucleated mammalian cells. However, the enhancement of p9 activity observed in WGE supplemented with HeLa

extract suggests that this factor(s) is functional in both mammalian and plant-based systems. Thus, it might not be that this factor is unique to HeLa extract; rather, that it is more abundant and/or otherwise plays a greater role in the regulation of translation in HeLa cell extract.

Preparation of HeLaS10 extract typically includes nuclease treatment to eliminate endogenous HeLa cell mRNAs (Ehrenfeld and Brown, 1981). This nuclease treatment might also release a p9 binding partner(s) from HeLa cell mRNPs. Thus, p9 activity in nuclease-untreated HeLa extract should be diminished as less of this host factor(s) is available to bind with p9. By comparing p9 activity in HeLa extracts prepared with and without micrococcal nuclease treatment, it was possible to determine that p9 activity is statistically greater following nuclease treatment. Since the difference in p9 activity between nuclease treated and untreated HeLa extracts was modest, it might be surmised that a large proportion of the p9 binding partner(s) is unbound or freely dissociable in HeLa extract even in the absence of nuclease treatment.

Based on the results of the *in vitro* experiments with the chimeric m7 rLuc RNA, it appears that the TGEV RNA UTRs do not protect (viral) RNA from p9-mediated translation inhibition. This may occur because the SARS-CoV and TGEV 5' leader sequences or UTRs do not protect CoV mRNA against nsp1-mediated, cleavage-independent translation inhibition, only against nsp1-mediated cleavage, and p9 does not cleave mRNA. Given that TGEV mRNAs, like host mRNAs, have a 5' cap and 3' poly(A) tail and the TGEV RNA UTRs are not protective against p9 activity *in vitro*, then perhaps TGEV mRNAs are subject to p9-mediated translation inhibition *in vivo* as well, unless there is another means by which TGEV mRNAs might be distinguished from host mRNAs or efficiently translated in spite of p9 activity. The ability of p9 to inhibit the translation of the m7 rLuc RNA may be influenced by the *in vitro* environment and the lack of compartmentalization present *in vitro* versus *in vivo* systems. Because CoVs are RNA viruses and viral transcription, unlike host transcription, takes place in the cell

cytoplasm, there is a possibility that the factor(s) that enhances p9 activity in HeLa extract might not be associated with viral mRNAs in TGEV-infected cells and might only be associated with the host, nuclear-transcribed mRNAs. Thus, p9 might be unable to access viral mRNAs in TGEV-infected cells due to the lack of this host factor(s) in viral mRNPs, and there might be no need for the TGEV UTRs to confer protection against p9-mediated translation inhibition *in vivo*.

It was shown that p9 activity was independent of the presence of a 5' cap or 3' poly(A) tail (Huang et al., 2011a). It was therefore presumed that eIF4E and PABP were not essential to p9 activity, and that another factor common to translation initiation of both capped and uncapped, and polyadenylated and non-polyadenylated, mRNAs must be targeted by p9. Based on the preliminary SGC analysis findings shown in Fig. 19, it appears that p9 reduces 48S initiation complex formation. Targeting of the ternary complex or eIF3, would lead to a reduction of 48S complex formation; whereas, targeting of eIF5 or eIF5B, which facilitates joining of the 60S ribosomal subunit, would lead to a reduction in 80S complex formation without affecting 48S complex formation (Pestova et al., 2000). Although the SGC analysis data was not conclusive for 80S complex formation, the reduction in 48S complex formation suggests that p9 does not (directly or indirectly) target eIF5 or eIF5B, but that it may target the ternary complex or eIF3. This finding correlates well with the ability of p9 to inhibit cap-, HCV IRES-, and EMCV IRES-driven translation, as the ternary complex and eIF3 are necessary for translation initiation of mRNAs containing all of the aforementioned structures (Fraser and Doudna, 2007; Huang et al., 2011a; Martinez-Salas et al., 2008; Pestova et al., 1996).

Chapter 3: Subcellular localization of p9

BACKGROUND

One feature that distinguishes eukaryotic cells from prokaryotic cells is the compartmentalization that exists in eukaryotic cells, whereby the cell nucleus is separated from the rest of the cell by the nuclear envelope (NE) (Bjork and Wieslander, 2014; Floch et al., 2014; Natalizio and Wentz, 2013). This also signifies a spatial separation of the nuclear processes, e.g. transcription and splicing, from cytoplasmic processes, e.g. translation, and can also afford eukaryotic cells with finer temporal regulation of these cellular processes (Bjork and Wieslander, 2014; Floch et al., 2014; Natalizio and Wentz, 2013). The NE, which encloses the nucleus, is a double membrane comprised of the inner and outer nuclear membranes, each of which is made up of a phospholipid bilayer (Natalizio and Wentz, 2013). The NE is not an impermeable barrier, and cargo is able to both selectively and non-selectively be transported to and from the cell cytoplasm across the nuclear envelope via the nuclear pore complex (NPC) (Bjork and Wieslander, 2014; Floch et al., 2014; Lange et al., 2007; Natalizio and Wentz, 2013). The NPC consists of multiple copies of approximately 30 different nucleoporin proteins (Nups), which anchor the NPC within the nuclear membrane and provide structural support for the nuclear export receptors, which are responsible for selective transport (import and export) through the nuclear pores, and also comprise part of the non-selective nuclear transport barrier (Bjork and Wieslander, 2014; Lange et al., 2007). Other cellular factors (e.g. nuclear export factors) stably associate with the NPC, and the precise composition of the NPC and its components have been demonstrated to vary between cell types and/or species to impart different NPCs with specific functional adaptations (Bjork and Wieslander, 2014). Although the majority of mRNP nuclear export occurs across the

NPC, alternative means of nuclear transport have been identified (Bjork and Wieslander, 2014; Natalizio and Wentz, 2013).

As mentioned above, the NPC is selectively permeable. Cargo smaller than the NPC passive diffusion limit of ~30-50 kDa or ~5 nm in diameter can freely diffuse through the NPC, whereas larger molecules, e.g. mRNPs, must undergo facilitated transport (Boisvert et al., 2014; Floch et al., 2014; Lange et al., 2007; Natalizio and Wentz, 2013). Cargo must be recognized by soluble nuclear transport receptors of the karyopherin family in order to cross through the central channel of an NPC via facilitated transport (Floch et al., 2014; Lange et al., 2007). Recognition of cargo to be imported into the nucleus is mediated by a nuclear localization signal (NLS), whereas cargo to be exported from the nucleus is mediated via a nuclear export signal (NES), respectively (Floch et al., 2014). A classical NLS is characterized by a series of positively charged amino acid residues, e.g. lysine or arginine, and a protein may contain one or more NLS (Boisvert et al., 2014; Floch et al., 2014; Lange et al., 2007). Proteins may also contain one or more non-classical but functional NLS(s), or be imported into the cell nucleus in the absence of a predictable or identifiable NLS (Boisvert et al., 2014; Floch et al., 2014; Lange et al., 2007). NESs are poorly characterized relative to NLSs, though they usually contain a series of hydrophobic amino acids, typically leucine, interspersed with other amino acid residues (Floch et al., 2014). Non-classical NESs are also known to exist (Floch et al., 2014). Karyopherins-beta (Kaps) can recognize cargo via direct or indirect (mediated by an adaptor protein) binding of NLS or NES sequences (Floch et al., 2014). Kaps involved with nuclear transport are also referred to as importins, exportins, and transportins based on their role in nuclear import, export, or bidirectional transport, respectively (Floch et al., 2014; Lange et al., 2007). Facilitated nuclear transport requires an energy source, which is provided by the Ran-GTPase system (Floch et al., 2014; Lange et al., 2007). This system also maintains the directionality of nuclear transport as a consequence of the Ran gradient present in cells, and the preferential interactions

between Ran-GTP and karyopherins that favors the dissociation of importins from cargos in the nucleus and exportins from cargos in the cytoplasm of cells (Floch et al., 2014; Lange et al., 2007).

Unlike proteins and most other RNA species, the majority of mRNAs do not depend upon Ran- or exportin-dependent pathways for nuclear export (Floch et al., 2014). The export of mRNAs (as mRNPs) is tightly regulated, and mRNP formation is tied to mRNA biogenesis and processing, which serves as a means of quality control to ensure that only fully mature, processed mRNAs are exported from the cell nucleus as part of a properly assembled mRNP complex (Floch et al., 2014). Although selected mRNPs are exported from the nucleus via Crm-1-dependent or other alternative export pathways, the majority of mRNPs are exported via the TAP-p15 (also referred to as NXF1-NXT1) export dimer (in vertebrate cells), which interact with mRNAs by means of various adaptor proteins (Floch et al., 2014; Yarbrough et al., 2014). The directionality of mRNA transport across the NPC is not driven by the Ran gradient either (Floch et al., 2014). Rather, it is driven by the cytoplasmic Ddx18 DEAD box helicase (in vertebrate cells), and possibly by other factors (Floch et al., 2014).

For viruses whose replication requires nuclear import of viral components, the NE and its NPCs are physical barriers that must be overcome (Cohen et al., 2012). Many viruses target the NE, NPC, and nucleocytoplasmic transport pathways as a means of overcoming the barriers to viral replication posed by cellular compartmentalization and to subvert the host antiviral immune response (Cohen et al., 2012; Floch et al., 2014; Yarbrough et al., 2014). In order to replicate their DNA genomes, the majority of DNA viruses must import their genomes into the cell nucleus (Cohen et al., 2012; Kuss et al., 2013). However, viral proteins are still translated in the cell cytoplasm, making it essential for viral mRNAs to be exported from the nucleus to the cytoplasm (Cohen et al., 2012; Kuss et al., 2013; Yarbrough et al., 2014). Once the assembly of new viral particles begins to take place, viral proteins and any other necessary viral constituents

must be imported into the nucleus, and the newly assembled virions must also egress from the nucleus (Cohen et al., 2012). To facilitate the transport of viral components or factors into and out of the nucleus, viruses may need to modulate nuclear selectivity or transport (Cohen et al., 2012; Kuss et al., 2013; Yarbrough et al., 2014). Even for viruses whose replication occurs outside of the nucleus, e.g. in the cell cytoplasm, it may be beneficial to alter the permeability of the NE and/or NPC selectivity or to alter nucleocytoplasmic trafficking, in order to subvert the host antiviral response or gain access to cellular components necessary for efficient viral replication (Cohen et al., 2012; Kuss et al., 2013; Yarbrough et al., 2014).

Viruses use various mechanisms to modulate such cellular processes (Cohen et al., 2012; Kuss et al., 2013; Yarbrough et al., 2014). For example, one of the HSV-1 viral proteins, ICP27, mediates preferential export of HSV-1 mRNAs from the nucleus at the expense of host mRNA export (Kuss et al., 2013; Yarbrough et al., 2014). Proteases from the picornaviruses, such as PV and human rhinovirus (HRV), proteolytically cleave many of the Nups, and potentially target other host proteins, resulting in alterations to NPC permeability and nucleocytoplasmic trafficking, including the mislocalization of cellular NLS-containing proteins and proteins involved in the cellular antiviral response (Yarbrough et al., 2014). It should also be noted that the expression of particular Nups is upregulated by IFNs (Yarbrough et al., 2014). By sequestering host mRNAs in the nucleus, viruses can prevent antiviral proteins from being translated or acquire a competitive advantage over host mRNAs for access to the host translation machinery (Kuss et al., 2013; Yarbrough et al., 2014). Influenza A virus (IAV), adenovirus, and vesicular stomatitis virus block nuclear export of host mRNAs, including mRNAs encoding antiviral proteins (Kuss et al., 2013; Yarbrough et al., 2014). Another strategy used by viruses is to block nuclear import of antiviral factors rather than nuclear export of host mRNAs (Yarbrough et al., 2014). The SARS-CoV ORF6 protein prevents the nuclear import of proteins important for host antiviral signaling pathways by binding to

and sequestering karyopherins, thereby dampening the cellular response to infection (Yarbrough et al., 2014). It is not known if p9 or any other TGEV proteins have an effect on nuclear selectivity or nucleocytoplasmic trafficking.

As the subcellular localization of a protein can provide insight into its biological function(s), identification of the subcellular localization of p9 was believed to be important for understanding p9-mediated suppression of host gene expression. Given that p9 is a small protein with a molecular weight below that of the NPC passive diffusion limit, it was hypothesized that p9 could freely diffuse across the NPC (Floch et al., 2014; Natalizio and Wentz, 2013). It was unknown where the TGEV p9 protein localized in infected cells following expression of the protein in the cell cytoplasm. The nsp1 of both MHV and SARS-CoV were predominantly localized to the cytoplasm of infected cells (Brockway et al., 2004; Kamitani et al., 2006). MHV nsp1 is specifically associated with intracellular membranes, and has been implicated as playing a role in MHV viral replication and virion assembly due to its close proximity to viral replication complex components early during infection, and to virion assembly sites characterized by high concentrations of the MHV M protein late during infection, respectively (Brockway et al., 2004). Studies examining the subcellular localization of SARS-CoV nsp1 in SARS-CoV-infected cells found no spatial separation between SARS-CoV mRNAs and SARS-CoV nsp1, indicating that SARS-CoV mRNAs may be subject to nsp1-mediated translation inhibition (Narayanan et al., 2014). The interaction between the CoV nsp1s and other viral and cellular components necessary for virus propagation in infected cells is evidently complex and not well understood. In particular, the spatial relationship between nsp1 and various components of mRNPs might provide insight into the biological function(s) of nsp1. Additionally, studying the interactions between viruses and the host cell machinery may be used to identify host factors and pathways that contribute to viral processes like replication, thereby providing promising targets for antiviral therapeutics (Cohen et al., 2012; Kuss et al., 2013; Yarbrough et al., 2014). To

this end, the subcellular localizations of the different CoV nsp1s, including p9, warrant more detailed examination.

The immunofluorescence data demonstrating the subcellular localization of p9 in expressed cells, which is described in this chapter, has been published (Narayanan et al., 2014).

MATERIALS & METHODS

Cell culture

HEK 293 cells were grown and maintained in high glucose Dulbecco's minimal essential medium (DMEM) (Gibco) supplemented with 10% FBS and 100 µg/mL kanamycin.

Plasmid constructs

The pCAGGS-TGEV nsp1-myc plasmid expressing TGEV p9 with a C-terminal myc epitope tag was generated by cloning the nsp1 gene ORF of the Purdue strain of TGEV into the multiple cloning site of the pCAGGS vector (Huang et al., 2011a).

Transfection protocol

One day prior to transfection, HEK 293 cells were seeded on Lab-Tek II 4-chamber slides (Nalgene Nunc International) to achieve the desired cell density of ~70-80% confluence at the time of plasmid transfection. DNA complexes for plasmid co-transfection were formed in Opti-MEM I Reduced-Serum Medium (Gibco) by combining the control (pCAGGS) or p9 expression plasmid (pCAGGS-TGEV nsp1-myc) with 3 µL of TransIT-293 Transfection Reagent (Mirus) per 1 µg of DNA, using the transfection

conditions recommended by Mirus for a 24-well plate, and allowing the mixture to incubate at room temperature for 15 minutes. The complexes were added to the cells drop-wise with a micropipette, and distributed evenly by gently tapping the slides. The cells were processed for confocal microscopy as described below.

Antibodies

Rabbits were immunized with purified, full-length, recombinant C-terminal myc epitope-tagged p9 protein made in *E. coli* by the UTMB Protein Synthesis and Biomarker Core Facility to generate polyclonal anti-p9 antibody (ProSci). The recombinant p9 protein was made as described in chapter 2. The GST tag was removed from the p9-GST fusion protein prior to immunization of the rabbits.

Confocal immunofluorescence microscopy & image analysis

HEK 293 cells were grown on Lab-Tek II four-well chamber slides (Nalgene Nunc International) and transfected with pCAGGS-TGEV nsp1-myc or empty pCAGGS plasmid as described above (four chambers per plasmid). At 24 hours post-transfection, the cells were washed with PBS one time then fixed in 4% paraformaldehyde for 15 minutes at room temperature. Next, the cells were washed in PBS for 5 minutes then permeabilized with 0.1% Triton X-100 in PBS for 10 minutes at room temperature. The slides were blocked with 3% bovine serum albumin (BSA) in PBS for 30 minutes at room temperature, then incubated with rabbit polyclonal anti-TGEV p9 primary antibody (ProSci) overnight at 4°C. The next day, the slides were washed three times with PBS for 10 minutes per wash, then incubated with an Alexa Fluor 594-conjugated anti-rabbit secondary antibody (Molecular Probes) in PBS for 1 hour at room temperature, before being counterstained for 1 hour at room temperature with DAPI (Cell Signaling

Technology) in PBS, overlaid with a thin layer of VECTASHIELD HardSet mounting medium (Vector Labs) and mounted and sealed with a coverslip. The slides were examined and images were captured using a Zeiss LSM-510 META confocal laser-scanning microscope with a 100X oil immersion lens in the UTMB Optical Imaging Core. Z-stack acquisition was performed to better determine the subcellular localization of p9 in expressed cells (data not shown). Images were processed with the LSM image browser (Zeiss) and ImageJ (NIH) software programs.

RESULTS

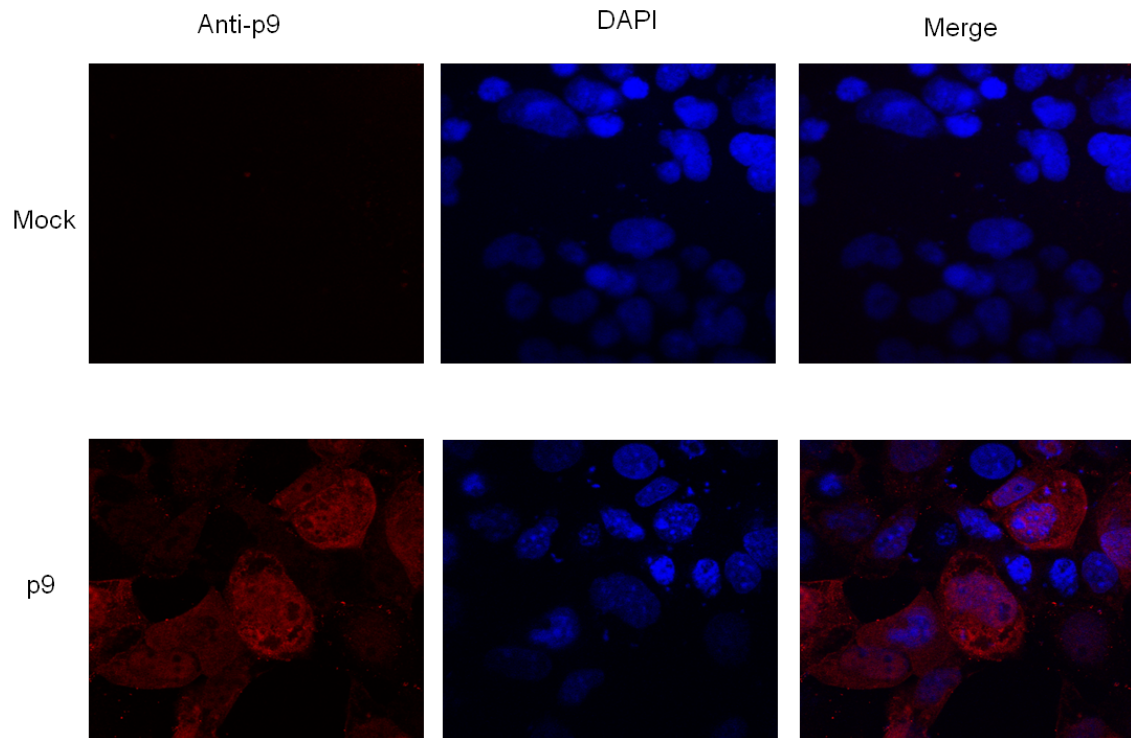


Figure 20: Confocal microscopic analysis of the subcellular localization of TGEV p9 in expressed cells [Adapted from Narayanan et al., 2014]

HEK 293 grown on 4-chamber slides were transfected with empty pCAGGS plasmid (mock; upper row) or pCAGGS plasmid encoding TGEV p9 (lower row). At 24 hours post-transfection, p9 was visualized by immunofluorescence using an anti- p9 primary antibody (ProSci Inc.) and an Alexa Fluor 594-conjugated secondary antibody (Molecular Probes), with DAPI counterstaining (Cell Signaling Technology). Images were captured using a Zeiss LSM 510 confocal laser-scanning microscope (100X) and processed using the LSM image browser (Zeiss) and ImageJ (NIH) software programs. Based on individual images like those shown above and z-stack data, p9 is distributed throughout the nucleus and cytoplasm of expressed cells and undetected in mock-transfected cells (z-stack data not shown).

HEK 293 cells were transfected with a p9 expression plasmid or mock transfected with an empty control plasmid, and immunofluorescence and confocal microscopic analysis, including z-stack acquisition (data not shown), was used to detect expressed p9 and to determine the subcellular localization of transiently expressed p9 (Narayanan et al., 2014). No p9 was detected in mock-transfected cells, demonstrating the specificity of the antibodies used (Fig. 20, upper row; Narayanan et al., 2014). In p9-expressing cells, p9 was distributed throughout the cell nucleus and cytoplasm (Fig. 20, lower row; Narayanan et al., 2014). Similar experiments were undertaken in TGEV-infected ST cells (data not shown). However, although p9 appeared to be present in the nucleus and cytoplasm of TGEV-infected cells, the findings were deemed inconclusive due to non-specific antibody binding in mock-infected ST cells (data not shown). Analysis of the p9 amino acid sequence did not reveal the presence of a canonical NLS (Boisvert et al., 2014; Lange et al., 2007; Narayanan et al., 2014; Shen and Chou, 2010; Wang, X. et al., 2013). It should be noted that viral NLS sequences do not necessarily resemble those of cellular proteins, and that even a large percentage of cellular proteins that localize to the nucleus lack a classical NLS (Boisvert et al., 2014; Floch et al., 2014; Lange et al., 2007). TGEV p9 lacks any significant structural similarity to other proteins listed in the Protein Data Bank, and lacks any known homologues aside from the other CoV nsp1s, none of which have been described to localize to the nucleus (Brockway et al., 2004; Jansson, 2013; Kamitani et al., 2006; Narayanan et al., 2014). Thus, no non-classical NLS sequences have been described for p9 or any other CoV nsp1. Despite the lack of a canonical NLS, p9 might diffuse freely into the cell nucleus due to its relatively low molecular weight (~9 kDa), which is below the passive diffusion limit of the nuclear pore complex (Bjork and Wieslander, 2014; Boisvert, et al., 2014; Floch et al., 2014; Gorlich, 1998; Narayanan et al., 2014; Natalizio and Wente, 2013; Silver, 1991).

DISCUSSION

As p9 does not contain a canonical NLS recognized by bioinformatics pattern recognition software, it might be perceived that p9 is unable to enter the cell nucleus on its own (Shen and Chou, 2010; Wang, X. et al., 2013). However, based on its molecular weight, p9 should be able to passively diffuse through the NPC (Bjork and Wieslander, 2014; Boisvert, et al., 2014; Floch et al., 2014; Gorlich, 1998; Narayanan et al., 2014; Natalizio and Wentz, 2013; Silver, 1991). It could also be that p9 is drawn into the nucleus due to a concentration gradient, similar to that of the Ran-GTPase gradient, due to the relative abundance of the p9 binding partner(s) in the cell nucleus versus the cytoplasm (Floch et al., 2014; Lange et al., 2007). That TGEV p9 is able to enter the nucleus of cells when expressed supports the possibility that p9 interacts with a protein or factor which is present exclusively in the cell nucleus or traffics between the nuclear and cytoplasmic compartments, possibly as part of an mRNP complex (Narayanan et al., 2014).

Because p9 is not limited to a relatively small number of discrete locations within the cytoplasm, it might be that the cytoplasmic distribution of p9 not only corresponds to areas of p9 protein synthesis but also to areas where bound p9 is present in host mRNPs that have been exported from the nucleus and are being trafficked to cytoplasmic translation sites (Narayanan et al., 2014). In the cross-section shown in Fig. 20, expressed p9 is found distributed throughout much of the cell cytoplasm and nucleus, although there are clearly areas in both cellular compartments with no p9. The significance of the specific distribution pattern of p9 within the nucleus or cytoplasm is not known. More detailed imaging of p9 should be undertaken to better describe the distribution pattern(s) of p9 in both expressed and infected cells.

The subcellular localization of p9 *in vivo* in expressed cells appears to correspond well with the *in vitro* findings regarding p9-mediated translation inhibition. It is possible

that *in vivo* expressed p9 targets one (or more) host factor involved with mRNP biogenesis, export or localization, but that *in vitro*, where nuclear processes do not occur and compartmentalization is non-existent, we only observe p9-mediated translation inhibition. As many factors which associate with mRNPs in the cell nucleus play a role in downstream processes, e.g. mRNP localization and/or translation, p9-mediated translation inhibition *in vitro* may be due to the same factor(s) responsible for p9 activity *in vivo* (Eliseeva et al., 2013; Mitchell and Parker, 2014; Muller-McNicoll and Neugebauer, 2013; Natalizio and Wenthe, 2013). For example, PABPs are a well-conserved group of RNA-binding proteins found throughout eukaryotes that associate with eukaryotic mRNAs throughout their “life cycle” and can be found in both the cell nucleus and cytoplasm (Eliseeva et al., 2013). However, the specific number of PABPs present in a cell and their subcellular localization varies from species to species (Eliseeva et al., 2013). Differences in p9 activity in HeLa extract, RRL, and WGE may be due to interspecies variation.

Differences in p9 activity in the different cell-free *in vitro* translation systems may also be due to other differences in the cell type or methods used for the preparation of the lysates or extracts. RRL is made from cells that lack a nucleus and have a relatively low abundance of RBPs and other nuclear factors (Ji et al., 2011; Mikami et al., 2006b; Svitkin et al., 2009). This may explain why p9 activity is low in this cellular lysate. On the other hand, HeLa extract is made from nucleated cells, and the cell nucleus is removed by centrifugation following hypotonic lysis of the HeLa cells (Barton et al., 1995; Huang et al., 2011a; Todd et al., 1997). In HeLa cells transcription continues to occur until the time of extract preparation; whereas, in reticulocytes transcription has ceased prior to lysate preparation and the factors involved with mRNP biogenesis, nuclear export and/or protein synthesis have potentially been lost or had their role(s) altered as a consequence of the enucleation process (Ji et al., 2011; Floch et al., 2014). As low speed centrifugation fails to remove the HeLa ribosomes, initiation factors, or

other translation apparatus components, it is unlikely that nuclear proteins (or other factors) that are not strictly confined to the nucleus at the time of cell lysis are removed from the extract. Therefore, said protein(s) (or other factor(s)) may be left behind to interact with p9 when the extract is used for *in vitro* translation. Thus, the factor(s) responsible for enhanced p9 activity in HeLa extract may be more essential to the regulation of translation in HeLa cell extract than in RRL.

Perhaps a factor(s) associated with the NE or NPC enhances the activity of p9 both *in vivo* as well as in cell-free HeLa extract. The NE and its NPCs are more dynamic and have a different composition in actively dividing cells versus terminally differentiated cells (e.g. twice the number of NPCs in interphase of cell division) (Floch et al., 2014). Another notable difference between HeLa cells and reticulocytes is that HeLa cells are actively dividing, immortalized cells, whereas reticulocytes are nearly terminally differentiated primary cells (Ji et al., 2011). Cellular differentiation may also be an important difference between wheat germ and HeLa cells. Alternatively, the factor(s) that enhances p9 activity in HeLa extract may be absent or function differently in WGE due to its being a plant extract. It has been shown that wheat germ agglutinin (WGA) has a negative effect on nuclear export, binding to the NPC and preventing macromolecular transport across the NPC (Floch et al., 2014). Perhaps, WGA also has an effect on *in vitro* translation carried out in WGE, and WGA competes with p9 for a particular factor(s) or otherwise alters translation in WGE.

Chapter 4: Effect of p9 on nuclear vs. cytoplasmic mRNAs

BACKGROUND

In eukaryotic cells the processes of transcription and translation are physically separated by the nuclear envelope (Bjork and Wieslander, 2014; Floch et al., 2014; Lange et al., 2007; Muller-McNicoll and Neugebauer, 2013; Natalizio and Wente, 2013). Within the nucleus is where mRNA biogenesis begins—there, mRNAs termed precursor mRNAs (pre-mRNAs) until ready for nuclear export, are transcribed and processed post-transcriptionally (Bjork and Wieslander, 2014; Floch et al., 2014; Muller-McNicoll and Neugebauer, 2013; Natalizio and Wente, 2013). From the beginning of their biogenesis, mRNAs are associated with proteins and other host factors, and are more appropriately referred to as mRNPs (Bjork and Wieslander, 2014; Chen and Shyu, 2014; Floch et al., 2014; Mitchell and Parker, 2014; Muller-McNicoll and Neugebauer, 2013; Natalizio and Wente, 2013). These mRNPs are dynamic complexes whose composition changes, or is remodeled, as the mRNA matures and is processed, and different RBPs, as well as other proteins that do not directly bind to the mRNA (e.g. adaptor proteins), and host factors associate with and dissociate from the mRNP complexes as they journey through the cell from biogenesis to degradation (Chen and Shyu, 2014; Mitchell and Parker, 2014; Muller-McNicoll and Neugebauer, 2013; Natalizio and Wente, 2013). It is unknown how many different types of mRNPs exist in any given cell, and it has been speculated that for every mRNA present in a cell, a unique mRNP complex may exist (Mitchell and Parker, 2014). However, it is thought that there may be core components present in all, or at least groups of, related mRNPs (Mitchell and Parker, 2014). Unfortunately, little is known about the composition of individual mRNPs *in vivo* (Chen and Shyu, 2014; Mitchell and Parker, 2014; Muller-McNicoll and Neugebauer, 2013). What follows is a summary of what is known regarding eukaryotic mRNPs.

Eukaryotic mRNPs typically progress through the same basic stages prior to translation: initial assembly during mRNA transcription, co-transcriptional mRNA processing and mRNP remodeling, nuclear export and subcellular localization (Chen and Shyu, 2014; Mitchell and Parker, 2014; Muller-McNicoll and Neugebauer, 2013). Additional remodeling and structural rearrangements occur as the mRNP travels through the cell and prepares to undergo translation (Mitchell and Parker, 2014). Eventually, all mRNAs are degraded and the mRNP complexes are disassembled (Mitchell and Parker, 2014). Given that each mRNP component can influence mRNA biogenesis and function, it is crucial to understand mRNP composition at various times throughout the mRNP “life cycle” in order to understand mRNA and translation regulation, and, ultimately, gene expression (Chen and Shyu, 2014; Mitchell and Parker, 2014; Muller-McNicoll and Neugebauer, 2013). The core components of mRNPs are mRNA, proteins, and non-coding RNAs (ncRNAs), both small and large (Mitchell and Parker, 2014).

Throughout their “lifetime” mRNPs interact with conserved host machinery, which regulates and carries out the key stages of the mRNA “life cycle”: biogenesis, processing, transport, translation and degradation (Mitchell and Parker, 2014; Muller-McNicoll and Neugebauer, 2013). Because interaction with this core host machinery is common to most mRNAs, there is a certain level of uniformity shared by the majority of mRNPs, and it is the degree to which the interactions of specific mRNAs with core host machinery vary that is potentially more telling (Mitchell and Parker, 2014). The individual characteristics of each mRNA, e.g. the primary sequence and structure of the mRNA, cause mRNAs to interact differently with the core host machinery, though in a fashion that permits the core machinery to function properly (Mitchell and Parker, 2014). For example, all mRNAs that contain introns undergo splicing and must interact with the splicing machinery (Mitchell and Parker, 2014; Muller-McNicoll and Neugebauer, 2013). However, mRNAs that undergo alternative splicing interact with a different set of factors than mRNAs that undergo canonical splicing (Mitchell and Parker, 2014). Additionally,

intronless mRNAs and mRNAs that are not spliced must recruit alternative factors for nuclear export than spliced mRNAs (Mitchell and Parker, 2014; Muller-McNicoll and Neugebauer, 2013). Association of core host machinery with mRNAs is typically determined by the presence of common mRNA landmarks, e.g. 5' cap and 3' poly(A) tail, or by other proteins recruited to the mRNP during earlier processing events. Many of the proteins that are deposited on mRNAs during early events have been shown to remain bound to the mRNA and to influence later events (Mitchell and Parker, 2014; Muller-McNicoll and Neugebauer, 2013).

In addition to the binding of mRNAs by the core host machinery, mRNPs involve the interaction of the mRNA with proteins and ncRNAs that bind to specific sequences present in individual mRNAs (Mitchell and Parker, 2014; Muller-McNicoll and Neugebauer, 2013). These sequence-specific factors often bind to mRNAs at the same time as the core machinery and regulate the processing of the specific subclasses of mRNAs with which they interact by recruiting the core machinery, promoting or inhibiting the functions of the core machinery, or modifying the core machinery (Mitchell and Parker, 2014). Sequence-specific mRNA binding proteins can also cause mRNA to interact differently with the core machinery by directly modifying the mRNA structure (Mitchell and Parker, 2014; Muller-McNicoll and Neugebauer, 2013). However, as individual mRNAs interact differently with the core machinery, the effects of sequence-specific regulators can result in different outcomes for individual mRNAs (Mitchell and Parker, 2014).

Not all mRNA-binding proteins bind mRNAs with high sequence specificity or as part of the categorical host machinery (Mitchell and Parker, 2014). Other mRNA-binding proteins display a range of specificity from extremely discerning to not: Pumilio-domain-containing proteins bind specific sequences eight to ten bases long, hnRNP A1 and related hnRNP proteins bind to a numerous mRNAs but with discernable sequence preferences, and certain DEAD-box helicases can act on a wide array of mRNAs

illustrating the of range of mRNA-sequence specificity required by mRNA-binding proteins from high, to medium, to low (Mitchell and Parker, 2014). Therefore, it is important to understand the interactions of individual mRNAs with both the core machinery and specific mRNA-binding proteins, and how such interactions influence mRNP composition (Chen and Shyu, 2014; Mitchell and Parker, 2014; Muller-McNicoll and Neugebauer, 2013).

Protein-mRNA interactions can have mutual effects, and mRNA binding can regulate the enzymatic or nonenzymatic activities of bound proteins, just as the proteins can regulate the mRNAs to which they bind (Mitchell and Parker, 2014). The activation of certain enzymes is dependent upon RNA binding, and this sort of protein-RNA interaction can allow for the exclusive regulation of the mRNP containing the activated enzyme via enzyme-induced modification of components within the mRNP (Mitchell and Parker, 2014). Thus, activation of a protein can be limited to RNA-bound protein, preventing the bulk of the protein within the cell from being activated, even if the concentration of the protein is significantly higher than that of its mRNA binding partner(s) (Mitchell and Parker, 2014).

Numerous proteins and ncRNAs bind to and regulate mRNAs at different times, but mRNP composition at any given time is determined by a four basic parameters: the local context, cellular context, mRNP components deposited during biogenesis, and changes in mRNP make-up and structure during mRNA maturation (Mitchell and Parker, 2014). The local context is made up of the mRNA and the proteins and ncRNAs that are bound to it, and determines the basic affinity with which an mRNA-binding factor binds a particular site on the mRNA (Mitchell and Parker, 2014). The ability and affinity with which a protein or ncRNA binds to a particular mRNA binding site can be affected by one or more of the following factors: the primary mRNA sequence, mRNA structural features, or proteins and ncRNAs bound at or near the binding site (Mitchell and Parker, 2014). Additionally, the cellular context—the cellular concentration of the protein or

ncRNA and the number of competing binding sites for the protein or ncRNA—also regulates mRNA binding. It should be noted that some proteins must be modified post-translationally, e.g. by phosphorylation, in order to enhance their mRNA binding affinity (Chen and Shyu, 2014; Mitchell and Parker, 2014; Muller-McNicoll and Neugebauer, 2013). Thus, the total concentration of a given protein within a cell may not be reflective of the amount of that protein available to bind to mRNAs (Mitchell and Parker, 2014). Proteins within an mRNP can also undergo posttranslational modifications, and these modifications can alter the function(s) of the proteins or the affinity of the proteins for other mRNP components, consequently altering the structure of the mRNP (Chen and Shyu, 2014; Mitchell and Parker, 2014; Muller-McNicoll and Neugebauer, 2013). Post-translational modification of RNA-binding proteins can be used to regulate the binding of such proteins both globally as well as in specific regions of the cell (Chen and Shyu, 2014; Mitchell and Parker, 2014; Muller-McNicoll and Neugebauer, 2013). For example, enzyme gradients can be used as a means of regulating mRNP composition throughout a cell by varying the local concentrations of modification enzymes, and thereby active mRNA-binding proteins, at different locations across a cell (Mitchell and Parker, 2014).

Some mRNP components can be deposited on mRNAs during transcription in a sequence-specific or non-specific manner through interaction(s) with RNA polymerase II, and this event may be influenced by the DNA promoter sequence of a gene (Mitchell and Parker, 2014). Additionally, the deposition of nucleophosmin upstream of the polyadenylation site during polyadenylation and deposition of the exon junction complex (EJC) on splice sites during splicing are other examples of proteins deposited on mRNAs during mRNA processing events (Mitchell and Parker, 2014; Muller-McNicoll and Neugebauer, 2013). The mammalian EJC remains bound to the mRNA after splicing and throughout nuclear export, playing an important role in mRNA quality control by marking mRNAs with premature stop codons for nonsense-mediated mRNA decay

(NMD) (Mitchell and Parker, 2014; Muller-McNicoll and Neugebauer, 2013). Other mRNP components that can influence the subcellular localization of an mRNP are added in the cell nucleus; these components can also ensure that the mRNA does not undergo translation prior to reaching its final subcellular destination (Mitchell and Parker, 2014; Muller-McNicoll and Neugebauer, 2013). As an mRNA matures, it undergoes both common and mRNA-specific transitions, which alter the mRNP composition (Mitchell and Parker, 2014). The remodeling of mRNPs occurs via multiple mechanisms, including the following: mRNAs can be modified by direct enzymatic modification, proteins can be released from mRNAs via the activity of localized modification complexes and DEAD-box helicases, cytoplasmic mRNPs can have proteins removed by the RAN-GTPase gradient and can have proteins and ncRNAs removed during translation (Mitchell and Parker, 2014).

Several unresolved questions exist regarding eukaryotic mRNPs, some of which will be briefly summarized here. Regarding the dynamics of mRNPs in cells, little is known about the stability of protein and ncRNA interactions with mRNA, e.g. whether transient or unstable interactions exist between an mRNA and its binding partners, and if such interactions can affect function, the on- and off-rates for various mRNP components and what these rates indicate about the roles of mRNP stability and kinetics in the determination mRNP composition, which, if any, components remain bound throughout the mRNA “life cycle,” and the role of individual mRNP components in determining the fate of an mRNA (Chen and Shyu, 2014; Mitchell and Parker, 2014; Muller-McNicoll and Neugebauer, 2013). Each mRNP component could act independently, and mRNA fate could be determined by a simple summation of these effects, or individual mRNP components could augment or diminish one another’s effects, making it more difficult to determine the contributions of the individual mRNP components to mRNA fate (Mitchell and Parker, 2014). The range of diversity of mRNPs, both generated from the mRNAs encoded by a single gene that undergo differential splicing and mRNPs generated from

the mRNAs of different genes, is not fully understood, nor how such diversity in composition might influence the fate of individual mRNPs (Mitchell and Parker, 2014). It is possible that every mRNA yields a unique mRNP structure, or that groups of related mRNAs yield subgroups of related mRNPs that are similar in composition (Mitchell and Parker, 2014). Comparison of *in vivo* versus *in vitro* mRNP dynamics also requires further investigation (Mitchell and Parker, 2014).

Little is known about general viral mRNP formation and dynamics. However, the formation of viral mRNPs in IAV-infected cells has been studied to a certain extent (York and Fodor, 2013). Like CoVs, influenza is an RNA virus (Graham et al., 2013; Narayanan et al., 2014; Weiss and Navas-Martin, 2005; York and Fodor, 2013). However, unlike most RNA viruses, replication of the IAV genome and transcription of IAV mRNAs occurs in the cell nucleus, not the cytoplasm, allowing IAV to utilize much of the same process as host mRNAs for the formation, processing, and nuclear export of its mRNAs (York and Fodor, 2013). In fact, the IAV 5' cap structure is identical to that of host mRNAs, as IAV snatches the 5' cap structure from capped host mRNAs to prime the transcription of viral mRNAs by the viral polymerase (York and Fodor, 2013). IAV mRNAs that require splicing also exploit the host splicing machinery (York and Fodor, 2013). Although the IAV 3' poly(A) tail is synthesized by the viral polymerase via a stuttering mechanism which repeatedly copies a relatively short stretch of uridine residues on the viral template RNA, it is identical to the host 5' poly(A) tail structure and interacts with host factors, including nuclear export factors, in a manner that is like that of the host 5' poly(A) tail structure (York and Fodor, 2013). Additionally, IAV mRNAs have internal N6-methyladenosine residues, a sign that IAV mRNAs, like host mRNAs, are transcribed in the cell nucleus (York and Fodor, 2013). These residues set IAV mRNAs apart from the mRNAs of viruses that undergo cytoplasmic transcription (York and Fodor, 2013).

Because CoV mRNA is transcribed, capped, and polyadenylated in the cell cytoplasm (rather than the nucleus) by mechanisms distinct from those of host mRNA synthesis and maturation, it would be reasonable to envision that the composition of CoV mRNPs varies from that of host mRNPs (Weiss and Navas-Martin, 2005). Even though both CoV and cellular mRNAs contain 5' cap and 3' poly(A) tail structures and in the cytoplasm of cells both mRNA species would presumably associate with the same core host machinery, RBPs, and other factors that bind to these structures, CoV mRNAs likely lack the nuclear-derived mRNP components that host mRNPs would contain and would likely not undergo the same interactions with host cell machinery or mRNP remodeling that host mRNPs undergo in the nucleus, or as they are transported from the nucleus to their cytoplasmic translation site. Additionally, the 5' cap and 3' poly(A) tail of TGEV mRNAs may associate with viral, and possibly even host, factors that do not typically associate with host mRNAs, as these structures are added to the viral mRNAs in the cell cytoplasm and synthesized by viral enzymes (Weiss and Navas-Martin, 2005). Variation in the composition of mRNPs from TGEV mRNAs may also be due to the association of CoV mRNAs with TGEV mRNA sequence-specific factors that do not normally associate with host mRNAs, including viral proteins.

It is unknown how TGEV-infection or p9 expression affects the host machinery and factors involved in mRNP formation and processing. Perhaps p9 is able to associate with nuclear mRNPs as it localizes to the nucleus as well as to the cytoplasm (Narayanan et al., 2014). It might also associate with cytoplasmic mRNPs, like viral mRNPs, or it might localize to the cytoplasm as part of a nuclear-derived mRNP that has undergone nuclear export. Perhaps, this would explain how p9 gains access to nuclear-derived mRNAs to inhibit the translation of said mRNAs. It has not been shown whether p9 can affect the translation of mRNAs that are formed in the cytoplasm as well. If p9 can associate with cytoplasmic mRNPs, then p9 might inhibit the translation of viral mRNAs.

The TGEV UTRs did not protect mRNAs from p9-mediated translation inhibition *in vitro* (Chapter 2, Fig. 18).

SARS-CoV mRNAs appear to be affected by SARS-CoV nsp1-mediated translation inhibition (Narayanan et al., 2014). It was previously shown that the TGEV p9 protein could inhibit both host and reporter gene expression of plasmids in multiple cell culture lines, suggesting that p9 is able to inhibit the translation of capped and polyadenylated mRNAs that, like cellular mRNAs, have been transcribed in the nucleus and transported to the cytoplasm (Huang et al., 2011a). However, it was unknown if TGEV mRNAs made in the cell cytoplasm could escape p9-mediated translation inhibition, or if p9 could inhibit the translation of RNAs directly introduced into the cell cytoplasm, which could be considered a surrogate for viral RNAs. Thus, the ability of p9 to inhibit the translation of cytoplasmic mRNAs was tested.

MATERIALS & METHODS

Plasmid constructs

The pRL-SV40 *Renilla* luciferase reporter vector encoding the rLuc gene ORF downstream of the constitutive SV40 promoter was originally purchased from Promega. By replacing the original rLuc ORF of pRL-SV40 with a PCR amplified DNA insert encoding the rLuc gene sequence downstream of the T7 promoter sequence and 5' UTR of human beta-actin mRNA and upstream of a 50-nt-long poly(A) tail, the pALA-SV40 plasmid was generated (Huang et al., 2011b). The pGLA-SV40 and pSMART-TGEV m7 rLuc plasmids are described in chapter 2.

In order to express the SARs-CoV nsp1, CAT, and p9 proteins following plasmid co-transfection, the pCAGGS-SCoV nsp1-myc, pCAGGS-CAT, and pCAGGS-TGEV nsp1-myc plasmids were used, respectively. The pCAGGS-nsp1 plasmid expressing SARS-CoV nsp1 with a C-terminal myc epitope tag was generated by cloning the SARS-

CoV nsp1 ORF into the pCAGGS-MCS vector, as described in Kamitani et al., 2006 (referred to as pCAGGS-SCoV nsp1-myc in Huang et al., 2011a). The pCAGGS-CAT plasmid expressing the CAT protein without a C-terminal epitope tag was generated in like fashion (Huang et al., 2011a). The pCAGGS-TGEV nsp1-myc plasmid is described in chapter 3 (Huang et al., 2011a).

For the generation of *in vitro*-synthesized capped and polyadenylated RNA transcripts, encoding the CAT, SARS-CoV nsp1, and TGEV p9 proteins with a C-terminal myc-His epitope tag, the pcD-CAT, pcD- Nsp1-wt, and pcD-p9-wt plasmids were used, respectively (Huang et al., 2011a; Kamitani et al., 2006; Narayanan et al., 2008). The first two plasmids were constructed, as previously described, by inserting the ORFs of CAT and SARS-CoV nsp1 into the multiple cloning site of a pcDNA™ 3.1/myc-His A expression vector (Invitrogen) (Kamitani et al., 2006; Narayanan et al., 2008). The pcD-p9-wt plasmid was constructed similarly.

RNA constructs

The pcD-CAT, pcD- Nsp1-wt, and pcD-p9-wt plasmids were used to synthesize capped and polyadenylated mRNA transcripts *in vitro*, encoding the CAT, SARS-CoV nsp1, and TGEV p9 proteins, each containing a C-terminal myc-His epitope tag, respectively (Huang et al., 2011a; Narayanan et al., 2008). The GLA and TGEV m7 rLuc mRNAs were synthesized as described in chapter 2. TGEV mRNA6 (m6) encoding the N protein along with a T7 promoter sequence and a 22-nucleotide poly(A) sequence was generated by using TGEV-specific primers to PCR amplify purified m6 cDNA made by reverse transcription of TGEV mRNA isolated from TGEV (Purdue strain)-infected ST cells. Krishna Narayanan generated the TGEV-specific primers and m6 cDNA template. Similarly, the V5-tagged TGEV mRNA 7 (m7-V5) was made by recombinant PCR, to generate TGEV mRNA7 with a T7 promoter sequence, C-terminal V5 epitope tag, and

poly(A) sequence using the same TGEV-specific primers along with additional primers. The m7-V5 PCR product sequence was confirmed by DNA sequencing (GENEWIZ). The pcD plasmids were linearized using the appropriate restriction endonuclease (NEB) and purified, then transcribed with the mMESSAGE mMACHINE T7 Ultra kit (Ambion), as described in chapter 2. The mMESSAGE mMACHINE kit (Ambion) was used to synthesize the capped and polyadenylated m6 (N protein) and m7-V5 RNAs. Kumari Lokugamage generated the m7-V5 PCR product and the *in vitro* transcribed m6 and m7-V5 RNAs used in the experiments for Figs. 25-26.

Antibodies

For Western blot analysis, primary antibodies against the TGEV N protein and the V5 epitope tag were used. The 3D.C10 antibody is a mouse monoclonal antibody specific to the TGEV N protein that was a gift from the laboratory of Luis Enjuanes, PhD of the Spanish National Center for Biotechnology (Jimenez et al., 1986). The rabbit polyclonal antibody directed against the V5 epitope tag was purchased from Abcam. Horseradish peroxidase (HRP)-conjugated goat anti-mouse IgG and goat anti-rabbit IgG secondary antibodies (Santa Cruz Biotechnology) were used to detect the N protein and m7-V5 protein product, respectively.

Plasmid transfection protocol

One day prior to transfection, HEK 293 cells were seeded on 24-well cell culture plates to achieve the desired cell density of 50-70% confluence at the time of plasmid transfection. DNA complexes for plasmid co-transfection were formed in Opti-MEM I Reduced-Serum Medium (Gibco) by combining the reporter and protein expression plasmids (1:10 ratio) with 3 μ L of TransIT-293 Transfection Reagent (Mirus) per 1 μ g of

DNA, and allowing the mixture to incubate at room temperature for 15 minutes. The complexes were added to the cells drop-wise with a micropipette, and distributed evenly by gently rocking the plates. Cell lysates were prepared for rLuc reporter assays at 24 hours post-transfection.

Electroporation protocol

One to two days prior to electroporation, HEK 293 cells were grown (as previously described) in T-75 flasks such that the cells would reach 50-70% confluence on the day of electroporation. Inside a biosafety cabinet, the medium was aspirated from the T-75 flask(s) using a Pasteur pipette, and each flask was rinsed with ~12 mL of PBS. The PBS was then aspirated and ~0.4 mL of 0.25% trypsin-EDTA (Gibco) was added to each flask. The flasks were incubated for 2-5 minutes inside the biosafety cabinet at room temperature to facilitate cell dissociation. Then, the flasks were tapped to further ensure that all cells had detached. To each flask, 10 mL of complete HEK 293 growth medium was added, and the cells were collected in a 50mL conical tube(s) and pelleted by centrifugation at 400x g for 5 minutes at room temperature. The medium was carefully aspirated with a Pasteur pipette following centrifugation, and the cell pellet was gently resuspended in 1 mL of warmed Opti-MEM reduced-serum medium (Gibco) per T-75 flask used. The RNA for each sample was added to a separate tube. In each tube, 1 µg reporter or viral RNA was mixed with 4 µg of protein expression RNA (e.g. CAT/SARS-CoV nsp1/p9) per 100 µL cell suspension. Samples were prepared in triplicate, i.e. 3 µg of reporter or viral RNA plus 12 µg of protein expression RNA in 300 µL cell suspension. The cell suspension and RNA were gently mixed in the tube then transferred to a 0.2 cm Bio-Rad cuvette in the biosafety cabinet. The cells were pulsed using a Gene Pulser Xcell electroporator with CE module (Bio-Rad) using the manufacturer's pre-set protocol for HEK 293 cells. Immediately following the pulse, the

cells were removed from the cuvette, and 100 μ L of each sample was plated in triplicate on a 24-well plate. The plate was gently rocked to evenly distribute the cells. The cells were incubated at 37°C for 24 hours then further processed for downstream assays. Kumari Lokugamage performed the electroporation procedure used to generate the data shown in Figs. 23-26. She generated the data for Figs. 23 and 24, as well as the metabolic labeling data for Fig 25.

Reporter assays

For luciferase reporter assays, the Promega *Renilla* luciferase assay system was used. The medium was aspirated from the cells following the transfection or electroporation protocol described above, and the wells of the plate were washed one time with cold PBS. Next, 150 μ L of 1x reporter lysis buffer (RLB) was added per well. The plate was placed on a shaker for 15 minutes at room temperature before being covered and frozen at -20°C overnight. The following day, the plate was thawed at room temperature, and the samples were collected in individual tubes. The tubes were centrifuged at maximum speed for 1 minute at room temperature in a tabletop microcentrifuge (Eppendorf). An equal volume aliquot of each cell lysate sample (e.g. 5-20 μ L) was added to 100 μ L of prepared substrate, and the rLuc activity was read for each sample with a GloMax® 20/20 Luminometer (Promega), as described in chapter 2.

Metabolic labeling protocol

Cells were prepared per the described electroporation protocol. At 24 hours post electroporation, the medium was replaced with warm methionine-free medium supplemented with dialyzed fetal calf serum, kanamycin and L-glutamine in the biosafety cabinet. The cells were incubated at 37°C for 30 minutes then 75 μ Ci/mL of TRAN35S-

LABEL™ metabolic labeling reagent (1,000 Ci/mmol; MP Biomedicals) was added per well without discarding the methionine-free medium, and the cells were metabolically labeled at 37°C for 1 hour. The cells were washed once with room temperature PBS and collected in 150 µL of 2x SDS (Laemmli) sample buffer, boiled at 100°C for 5 minutes, and stored at -80°C until used for SDS-PAGE.

SDS-PAGE, CCB staining, autoradiography, and WB protocols

For SDS-PAGE, samples were loaded in duplicate on two separate hand cast 12% polyacrylamide gel(s) and run at 100 Volts in a Mini-PROTEAN 3 electrophoresis cell (Bio-Rad) until the dye in the sample buffer reached the bottom of the gel (~1-2 hours). For visualization of total protein, one gel was rinsed three times in deionized water for 5 minutes per wash, then stained with colloidal Coomassie blue (CCB) (Bio-Rad) for 1 hour at room temperature, then destained in deionized water, per the manufacturer's protocol. For autoradiographic detection of metabolically labeled proteins, the second gel was soaked in destaining solution [45% methanol, 10% glacial acetic acid, 45% water] for 1 hour at room temperature then 1M sodium salicylate for 1 hour at room temperature. The gel was then dried using a gel dryer at 80°C, for 1 hour, and an X-ray film was exposed to the dried gel at -80°C for an appropriate amount of time (typically ranging from 3 hours to overnight) before developing the film.

For Western blot analysis, samples were loaded on a precast 4–20% Mini-PROTEAN® TGX™ gel (Bio-Rad) and run at 100 Volts in a Mini-PROTEAN 3 electrophoresis cell (Bio-Rad) for ~1 hour in Tris-glycine running buffer, until the bands of the Dual Color Precision Plus Protein Prestained Standards (Bio-Rad) were well separated and the 10 kDa band was ~1 cm from the bottom of the gel. The proteins were then transferred to a PVDF membrane for 15 minutes at 20 Volts using a Trans-Blot® SD semi-dry transfer cell (Bio-Rad), and the membrane was blocked in 5% non-fat dry

milk (Bio-Rad) in PBS + 0.1% Tween 20 (Sigma) (PBST) for one to three hours at room temperature, or overnight at 4°C depending upon the primary antibody that was used for detection. The membrane was then incubated with primary antibody diluted in blocking buffer at 4°C overnight or at room temperature for 3 hours, respectively. The membrane was then washed thoroughly in PBST before being incubated with horseradish peroxidase (HRP)-conjugated secondary antibody (Santa Cruz), specific for the host species in which the primary antibody was generated, diluted in blocking buffer for 1 hour at room temperature. The membrane was washed thoroughly with PBST after incubation with the secondary antibody, and the protein bands were visualized by incubating the membrane with ECL Plus Substrate (Thermo Scientific Pierce) or ECL Plus Western Blotting Detection reagents (GE HealthCare) per the manufacturers' protocols and exposing the membrane to X-ray film for an appropriate amount of time prior to developing the film. Densitometry analysis was performed using ImageJ software (NIH) to quantify the relative intensity of the protein bands.

RESULTS

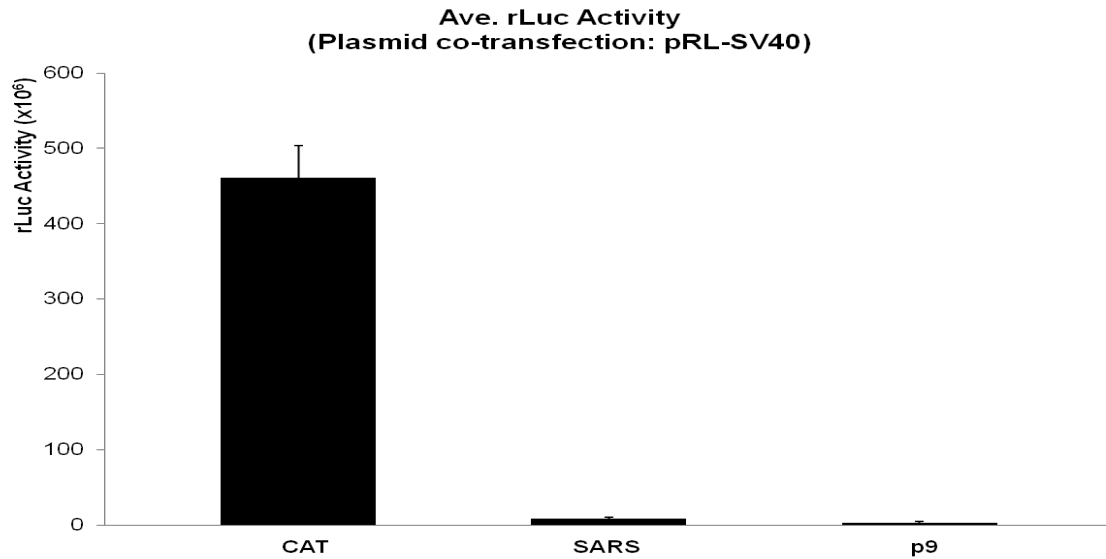


Figure 21: Effect of TGEV p9 on the translation of nuclear-derived rLuc reporter mRNA

HEK 293 cells were co-transfected with the pRL-SV40 rLuc reporter plasmid and one of the following protein expression plasmids: pCAGGS-CAT (CAT), pCAGGS-SCoV nsp1-myc (SARS), or pCAGGS-TGEV nsp1-myc (p9), expressing the CAT, SARS-CoV nsp1, or TGEV p9 proteins, respectively. The latter two proteins both had a C-terminal myc epitope tag. Cell lysates were prepared at 24 hours post-transfection, and a portion of the lysate from each sample was used to measure the rLuc activity. The data represent the average rLuc activity from triplicate samples, with the standard deviation illustrated by the error bars. The average rLuc activity for SARS-CoV nsp1 samples was 2% of GST and p9 samples was 1% of GST (98% and 99% inhibition, respectively); $P < 0.01$ for both SARS-CoV nsp1 and p9. The data shown is representative of three or more independent experiments.

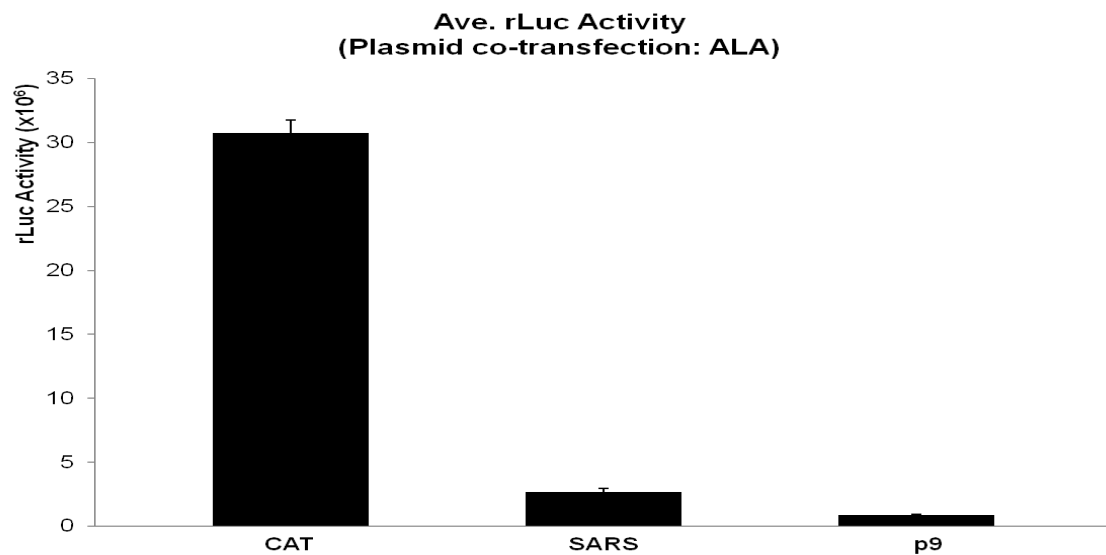


Figure 22: Effect of TGEV p9 on the translation of nuclear-derived ALA reporter mRNA

HEK 293 cells were co-transfected with the pALA-SV40 rLuc reporter plasmid (encoding the rLuc gene ORF downstream of the human beta-actin 5' UTR) and one of the following protein expression plasmids: pCAGGS-CAT (CAT), pCAGGS-SCoV nsp1-myc (SARS), or pCAGGS-TGEV nsp1-myc (p9), expressing the CAT, SARS-CoV nsp1, or TGEV p9 proteins, respectively. The latter two proteins each contained a C-terminal myc epitope tag. Cell lysates were prepared at 24 hours post-transfection, and a portion of the lysate from each sample was used to measure the rLuc activity. The data represent the average rLuc activity from triplicate samples, with the standard deviation illustrated by the error bars. The average rLuc activity for SARS-CoV nsp1 samples was 9% of GST and p9 samples was 3% of GST (91% and 97% inhibition, respectively); $P < 0.01$ for both SARS-CoV nsp1 and p9. The data shown is representative of three or more independent experiments.

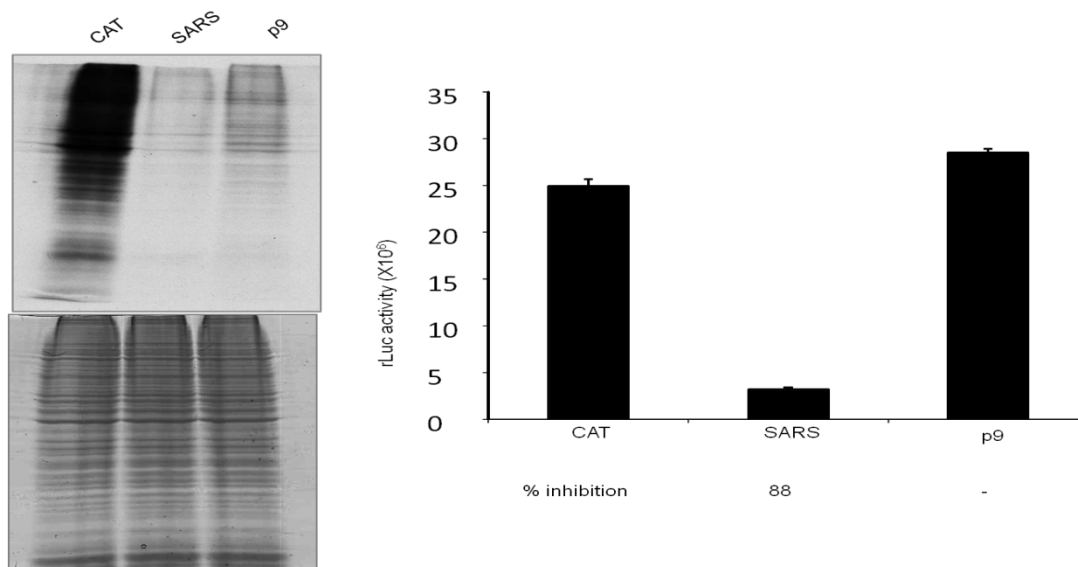


Figure 23: Effect of TGEV p9 on the translation of cytoplasmic GLA mRNA

In vitro-transcribed, capped and polyadenylated RNAs encoding: CAT-myc (lane 1; CAT), SARS-CoV nsp1-myc (lane 2; SARS), or TGEV nsp1-myc RNA (lane 3; p9), were co-introduced into HEK 293 cells together with *in vitro*-transcribed, capped and polyadenylated GLA mRNA using a Gene Pulser Xcell electroporation system (Bio-Rad). At 24 hours post-RNA co-electroporation, cells were metabolically labeled with 75 Ci/ml of [35S]-methionine for 1 hour prior to collection in SDS sample buffer (left figures) or left unlabeled and collected in luciferase assay buffer (right figure), and the cellular lysates, containing equivalent amounts of protein, were resolved by SDS-PAGE then exposed to X-ray film (upper left gel) or stained with colloidal Coomassie blue (lower left gel) to determine host protein synthesis levels (upper left figure; lower left figure serves as loading control) or a luciferase assay to determine luciferase activity levels (right figure). The percent inhibition of luciferase activity relative to CAT (100% activity) is shown below the chart; $P < 0.01$ for SARS-CoV nsp1. Error bars show the standard deviation for triplicate samples. Note that both SARS-CoV and TGEV p9 were able to inhibit host protein synthesis but that only SARS-CoV nsp1 was able to inhibit the translation of the GLA reporter RNA that was introduced into the cell cytoplasm.

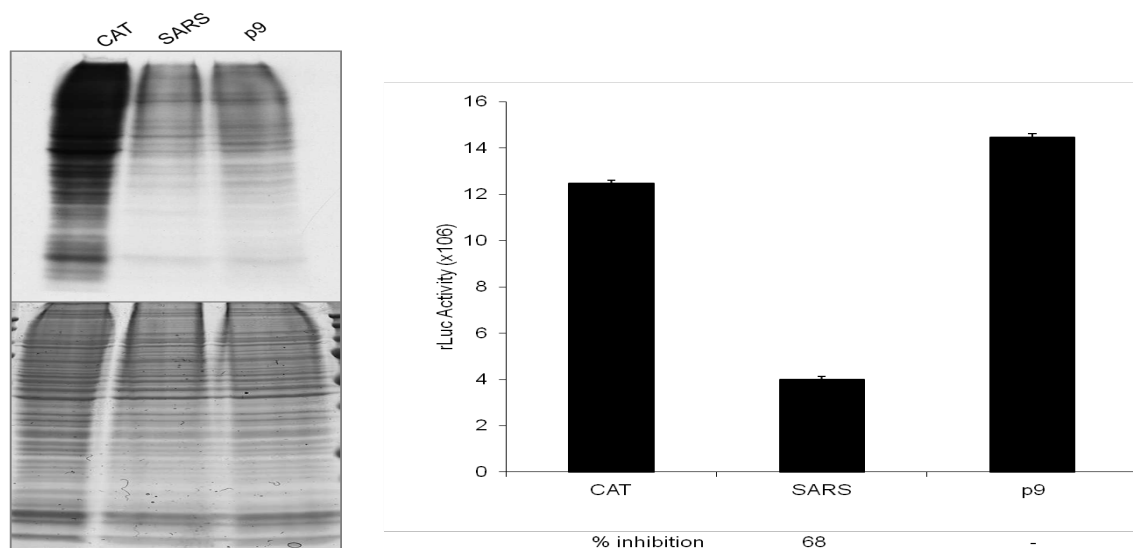


Figure 24: Effect of TGEV p9 on the translation of cytoplasmic m7 rLuc RNA

RNAs were co-electroporated into HEK 293 cells and cellular lysates collected and used as described in the prior figure (Fig. 23), with the TGEV m7 rLuc reporter mRNA in place of GLA mRNA. The percent inhibition of luciferase activity relative to CAT (100% activity) is shown below the chart; $P < 0.01$ for SARS-CoV nsp1. Error bars show the standard deviation for triplicate samples. Note that both SARS-CoV and TGEV p9 were able to inhibit host protein synthesis but that only SARS-CoV nsp1 was able to inhibit the translation of the chimeric TGEV mRNA 7-like reporter RNA that was introduced into the cell cytoplasm.

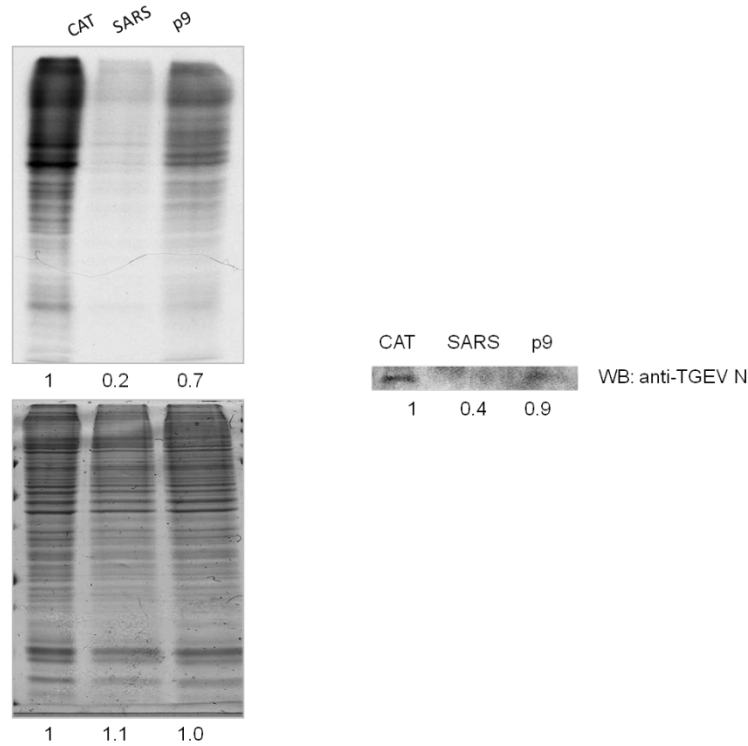


Figure 25: Effect of TGEV p9 on the translation of cytoplasmic TGEV m6

In vitro-transcribed, capped and polyadenylated RNAs encoding: CAT-myc (lane 1; “CAT”), SARS-CoV nsp1-myc (lane 2; “SARS”), or TGEV nsp1-myc RNA (lane 3; “p9”), were co-introduced into HEK 293 cells together with *in vitro*-transcribed, capped and polyadenylated TGEV N protein RNA using a Gene Pulser Xcell electroporation system (Bio-Rad). At 24 hours post-RNA co-electroporation, cells were metabolically labeled with 75 Ci/ml of [35S]-methionine for 1 hour prior to collection in SDS sample buffer, and the cellular lysates, containing equivalent amounts of protein, were resolved by SDS-PAGE then exposed to X-ray film (upper left gel) or stained with colloidal Coomassie blue (lower left gel) to determine host protein synthesis levels (upper left figure; lower left figure serves as loading control), or Western Blot using anti-N primary antibody (laboratory of Luis Enjuanes, PhD) and HRP-conjugated goat anti-mouse IgG secondary antibody (Santa Cruz) to determine N protein expression levels (right figure). Densitometry analysis (ImageJ) was performed to determine the levels of host and N

protein in SARS-CoV nsp1- and p9-expressing cells relative to CAT-expressing cells, as indicated by the numbers below the figures. Note that both SARS-CoV and TGEV p9 were able to inhibit host protein synthesis but that only SARS-CoV nsp1 was able to efficiently inhibit translation of the N protein mRNA that was introduced into the cell cytoplasm.

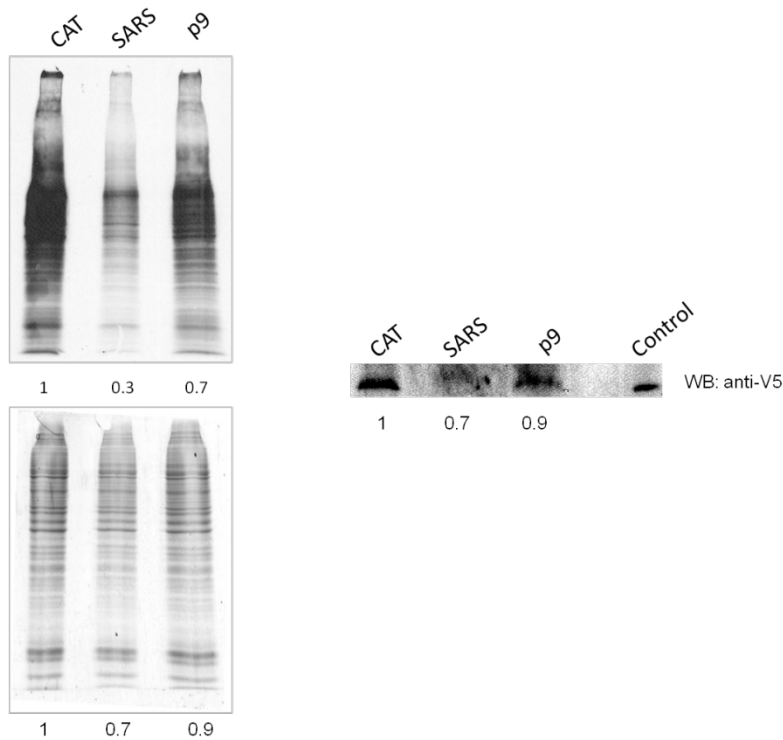


Figure 26: Effect of TGEV p9 on the translation of cytoplasmic TGEV m7-V5

In vitro-transcribed, capped and polyadenylated RNAs encoding: CAT-myc (lane 1; “CAT”), SARS-CoV nsp1-myc (lane 2; “SARS”), or TGEV nsp1-myc RNA (lane 3; “p9”), were co-introduced into HEK 293 cells together with *in vitro*-transcribed, capped and polyadenylated TGEV mRNA 7 containing a V5 epitope tag, as described in Fig. 25, and the cellular lysates, were resolved by SDS-PAGE then exposed to X-ray film (upper left gel) or stained with colloidal Coomassie blue (lower left gel) to determine host protein synthesis levels (upper left figure; lower left figure serves as loading control), or Western Blot using an anti-V5 primary antibody (Abcam) and horseradish peroxidase (HRP)-conjugated goat anti-rabbit IgG secondary antibody (Santa Cruz) to determine the mRNA 7 product expression levels (right figure). The “control” lane in the right figure is a molecular weight marker for the m7-V5 protein. Densitometry analysis (ImageJ) was performed to determine the levels of host protein and m7-V5 protein in SARS-Cov nsp1- and p9-expressing cells relative to CAT-expressing cells, as indicated by the numbers

below the figures. Note that both SARS-CoV and TGEV p9 were able to inhibit host protein synthesis but that only SARS-CoV nsp1 was able to inhibit translation of the V5-tagged mRNA 7 that was introduced into the cell cytoplasm.

As discussed earlier, it was hypothesized that p9 is only able to efficiently access mRNA templates in the context of an mRNP complex that originates in the nucleus of cells *in vivo*, or contains a certain nuclear factor(s) *in vitro*. It is possible that by associating with such mRNPs via a nuclear RBP(s) or other nuclear factor(s), p9 mediates translational suppression in an mRNP-specific manner. Thus, p9 may not be able to access viral mRNAs which are synthesized in the cytoplasm of infected cells, and may not suppress viral translation *in vivo*. To test this hypothesis, the ability of p9 to suppress the translation of mRNAs that were directly introduced into the cytoplasm of cells versus mRNAs transcribed in the cell nucleus was assessed.

HEK 293 cells were co-transfected with a reporter gene expression plasmid and a protein expression plasmid expressing CAT (negative control), SARS-CoV nsp1 (positive control), or p9 protein. At 24 hours post-transfection, reporter gene expression was assessed by rLuc reporter assay, and, as expected, both SARS-CoV nsp1 and p9 were able to efficiently suppress reporter gene expression relative to CAT. This was true for both the parental pRL-SV40 rLuc reporter plasmid (Promega; Fig. 21), as well as for the pALA-SV40 plasmid (Fig. 22). Inhibition of reporter gene expression by p9 and SARS-CoV nsp1 was also observed for all of the reporter plasmids tested, including other reporter plasmids derived from the pRL-SV40 (Promega) and pRL-CMV (Promega) rLuc reporter plasmids (data not shown).

HEK 293 cells were then co-transfected (data not shown) or co-electroporated with *in vitro*-transcribed, capped and polyadenylated reporter mRNA together with a capped and polyadenylated CAT, SARS-CoV nsp1, or p9 protein expressing mRNA. Unlike the results of the plasmid co-transfection studies, at 24 hours post-electroporation, no translation inhibition by p9 of either GLA (Fig. 23, right figure) or m7 rLuc reporter mRNA (Fig. 24, right figure) was observed by luciferase assay. However, SARS-CoV nsp1 was able to strongly inhibit the translation of both electroporated GLA (Fig. 23, right figure) and m7 rLuc reporter mRNA (Fig. 24, right figure). The same was true for

electroporated ALA mRNA as well as reporter mRNAs introduced into the cell cytoplasm by RNA transfection (data not shown). Intriguingly, p9 can inhibit the translation of these same capped and polyadenylated mRNA transcripts *in vitro* in HeLa S10 extract.

To confirm that p9 was expressed and biologically active following electroporation, cells were additionally subjected to metabolic radiolabeling with [³⁵S]-methionine in order to observe the effect of the proteins expressed from the electroporated RNAs on host protein synthesis. Host protein synthesis was inhibited by both SARS-CoV nsp1 and p9 (Figs. 23-24, left figures), indicating that the lack of p9-mediated inhibition of electroporated reporter mRNA translation was not due to a loss of biological activity. Unlike SARS-CoV nsp1, p9 only efficiently suppressed translation of the plasmid-derived reporter protein, which was transcribed in the cell nucleus under the control of a constitutive promoter and translated in the cell cytoplasm following nuclear export, and it failed to suppress the translation of protein expressed from the capped and polyadenylated, *in vitro* transcribed reporter RNA that was directly introduced into the cell cytoplasm. Thus, in accordance with the hypothesis, p9 appears to selectively target mRNAs in nuclear-derived mRNPs for translation inhibition.

To further test the hypothesis that p9 is only able to access and suppress the translation of mRNAs in nuclear-derived mRNPs and not mRNPs containing mRNA templates that have been directly introduced into the cytoplasm, we tested whether p9 could suppress the translation of TGEV mRNA introduced into the cell cytoplasm. The ability of SARS-CoV nsp1 and p9 to inhibit the translation of electroporated, *in vitro* transcribed, capped and polyadenylated TGEV mRNA 6 and V-5 epitope tagged TGEV mRNA 7 was determined using Western blot analysis (Figs. 25-26, right figures, respectively). The biological activity of SARS-CoV nsp1 and p9 was also assessed (Figs. 25-26, left figures). Although the experiments illustrated by Figs. 25-26 require further optimization and replication to yield more conclusive results, it appears that only SARS-

CoV nsp1 can efficiently inhibit the translation of TGEV mRNAs directly introduced into the cell cytoplasm. SARS-CoV nsp1, but not p9, efficiently inhibited the translation of electroporated TGEV m6 RNA (Fig. 25, right figure). It is unclear if SARS-CoV nsp1 was able to inhibit the translation of electroporated TGEV m7-V5 RNA, but p9 did not efficiently inhibit its translation (Fig. 26, right figure). Both SARS-CoV nsp1 and p9 were able to inhibit host protein synthesis in m6 and m7-V5 electroporated cells (Figs. 25-26, left figures), verifying the biological activity of the nsp1s in both experiments.

DISCUSSION

In cells transiently expressing p9, only the translation of host mRNAs and plasmid-derived reporter mRNAs was efficiently suppressed, and the translation of mRNAs introduced into the host cytoplasm was not; therefore, it is important to consider how these three types of mRNAs might differ (e.g. mRNA synthesis or processing, mRNP remodeling or composition). A nuclear process, e.g. transcription, splicing, or nuclear export, could be targeted by p9 *in vivo*, possibly via interaction with its binding partner(s). This might explain why plasmid-derived reporter protein and host protein synthesis is suppressed. p9 might suppress a nuclear process, e.g. transcription or splicing, leading to a decrease in the number of nucleus-derived mRNA transcripts available to undergo translation; additionally, p9 could inhibit the translation of nucleus-derived mRNAs. There is no evidence that convincingly demonstrates that p9 affects nuclear mRNA biogenesis, maturation, or export.

Even if p9 targets a nuclear process *in vivo*, it must still suppress translation (initiation) *in vitro*, including HCV IRES and EMCV IRES-driven translation. In cells, many of the host factors involved with mRNA biogenesis or processing are also players in downstream processes (Eliseeva et al., 2013; Mitchell and Parker, 2014; Muller-McNicoll and Neugebauer, 2013; Natalizio and Wente, 2013). It is not necessary that

such factors be involved in contiguous processes (Muller-McNicoll and Neugebauer, 2013). Perhaps, the factor(s) with which p9 interacts is involved with a nuclear process *in vivo* as well as translation, and remains bound to mRNPs of nuclear origin even after nuclear export. The mRNAs expressed by the pRL vectors (Promega) that were used for DNA transfection would undergo nuclear processes much like host mRNAs, e.g. transcription and splicing, whereas *in vitro* transcribed mRNAs encoding the same proteins would not undergo such nuclear processes when introduced into the cell cytoplasm. This could explain why p9 differentially inhibited the translation of the same proteins depending upon the protein expression system used (i.e. plasmid versus *in vitro* transcribed RNA).

The same *in vitro* transcribed mRNA transcripts whose translation was efficiently inhibited by p9 *in vitro* in HeLa extract, e.g. GLA and m7 rLuc mRNAs, did not have their translation inhibited when they were introduced into the cytoplasm of cells (Chapter 2, Figs. 2, 18; Chapter 4, Figs. 23, 24). Based on the metabolic labeling data, as host protein synthesis was suppressed, it was determined that p9 was expressed from mRNA introduced into the cell cytoplasm in the very same cells, and it was biologically active (Figs. 23-26). Thus, the inability of p9 to efficiently suppress the translation of exogenous, cytoplasmic mRNAs was not simply due to lack of p9 expression or p9 activity *in vivo*. It may be that p9 is unable to efficiently target mRNA transcripts outside of the context of an mRNP complex containing its binding partner(s), which likely associates with mRNAs in the cell nucleus, because p9 accesses mRNAs via said binding partner(s). If the same factor(s) is responsible for p9-mediated translation inhibition as well as allowing p9 to specifically target mRNAs of nuclear origin, then perhaps this is further evidence that p9 interacts with a host factor that typically associates with host mRNP complexes. This information could prove useful in determining the identity of said factor(s).

Based on the *in vitro* reporter assay data, it was determined that the UTRs of TGEV mRNAs do not confer protection against p9-mediated translation inhibition (Chapter 2, Fig. 18). This would suggest that there is another explanation for why the translation of the m7 rLuc, m6, and m7-V5 proteins expressed from mRNAs introduced into the cell cytoplasm was not suppressed. As proposed earlier, it may be unnecessary for the UTRs of TGEV mRNAs to confer protection against p9-mediated translation inhibition *in vivo* because p9 preferentially targets nuclear-derived mRNPs *in vivo*. In TGEV-infected cells, viral mRNAs are synthesized, capped, and polyadenylated in the cell cytoplasm and may lack some of the RBPs or other host factors, including potential p9 binding partner(s), common to nucleus-derived, endogenous mRNPs. Therefore, mRNAs directly introduced into the cell cytoplasm might look more like viral mRNAs, not because of a shared set of UTRs or other RNA sequence, but because of their location within the cell and their mRNP composition.

Chapter 5: Overall Discussion

TGEV p9 suppresses host gene expression by inhibiting mRNA translation (initiation). In this dissertation, new research findings regarding p9 have been presented and discussed in the context of the published findings. In summary, p9-mediated translation inhibition is not absent in RRL, and can be enhanced by increasing the concentration of p9 or the incubation time used for the *in vitro* translation reaction. This finding suggests that p9 could be directly or indirectly targeting one of the canonical eIFs or another ubiquitous host factor, e.g. an RBP, and that the differences in p9 activity in RRL versus HeLa extract may be not be due to a factor(s) that is entirely absent in RRL, rather it may be due to the relative dearth of the factor in RRL and WGE versus HeLa extract and/or the role that the factor(s) plays in translation regulation in the different cell-free *in vitro* translation systems.

Additionally, in WGE, p9 behaves as in RRL—p9-mediated translation inhibition in WGE and RRL is modest relative to p9-mediated translation inhibition in HeLa S10 extract, though p9 activity is increased in WGE and RRL by increasing the concentration of p9 or the incubation time used for the *in vitro* translation reaction. Supplementing WGE with HeLa extract also enhances p9 activity, similar to supplementing RRL with HeLa extract.

As TGEV mRNAs are synthesized in the cell cytoplasm, it may be unnecessary for the TGEV UTRs to contain an element(s) that confers resistance to p9-mediated translation inhibition. The TGEV UTRs, which are a feature shared by all TGEV mRNAs, do not appear to confer mRNAs with resistance to p9-mediated translation inhibition, as inhibition of the chimeric m7 rLuc mRNA was observed *in vitro* in HeLa S10 extract. It is uncertain whether or not this finding holds true for TGEV mRNAs *in vivo* in infected cells. Additional experiments would be required to determine this.

In HEK 293 cells, as well as ST cells (data not shown), p9 was only able to efficiently suppress host protein synthesis and plasmid-driven reporter protein synthesis. It was unable to efficiently inhibit the translation of mRNAs introduced directly into the cytoplasm of cells, even though p9 was able to inhibit the translation of endogenous host mRNAs in the same cells, indicating that biologically active p9 was present in the cells (i.e. the lack of inhibition of cytoplasmic mRNA translation was not due to a loss of p9 function). The same results were obtained regardless of whether the RNAs were introduced into the cytoplasm via electroporation or transfection (data not shown). The inability of p9 to inhibit the translation of cytoplasmic mRNAs may have something to do with cytoplasmic versus nuclear mRNP composition or dynamics. The *in vitro* and *in vivo* findings point to the existence of a host cell factor(s), normally associated with nuclear-transcribed host cell mRNAs (in mRNPs), which is necessary for efficient p9-mediated translation inhibition. This factor(s) may provide p9 with access to mRNAs and/or allow p9 to recognize mRNAs in order to exert its biological activity.

The possibility that p9 affects one or more nuclear processes (e.g. transcription, nuclear export) *in vivo* cannot be ruled out. Another possibility that cannot be ruled out is that p9 lacks intrinsic translation inhibition activity, and that p9 is activating a host factor(s) rather than directly inhibiting translation. Although TGEV (Purdue strain) replication was shown to inhibit host protein synthesis in infected ST cells (between 4-14 hours p.i.), it is unclear whether this inhibition is due solely to p9 (Huang et al., 2011a). It is possible that in infected cells another viral factor(s) contributes to this inhibition, either independently or in conjunction with p9. Additional studies must be performed to confirm that p9 activity, and the host factor(s) that contributes to this activity, is the same *in vitro*, in p9-expressing cells, and in TGEV-infected cells.

Although the host factor(s) believed to interact with p9 was not identified by the studies described in this dissertation, certain findings described within this dissertation help to narrow down the possible identity of this factor(s). As CrPV IRES-mediated

translation was not inhibited by p9, and HCV IRES- and EMCV IRES-mediated translation was inhibited to a lesser extent than cap-mediated translation, the factor(s) may be less essential for IRES-mediated translation than for cap-mediated translation, and unessential in the case of the CrPV IRES. Based on the published literature, the factor is likely not an eIF2 kinase, eIF4E, or PABP (Huang et al., 2011a). Additionally, based on the SGC data discussed in chapter 2, it is unlikely that the factor is eIF5 or eIF5B either, though it may be eIF3 or a component of the ternary complex, e.g. eIF2. It is also possible that p9 does not target one of the canonical translation initiation factors, but that it targets another host factor, most likely an mRNP component involved with translation regulation. For example, although they are not part of the core translation machinery, numerous RBPs have been implicated in the regulation of both cap-dependent and cap-independent translation (Chen and Shyu, 2014; Evdokimova et al., 2006; Martinez-Salas et al., 2015; Mitchell and Parker, 2014; Muller-McNicoll and Neugebauer, 2013; Semler and Waterman, 2008; Svitkin et al., 2009; van Zalen et al., 2015).

The RBP Y-box binding protein 1 (YB-1), is a well described example of a general RBP that can regulate translation. In mature erythrocytes and their precursors, YB-1 is a core component of mRNPs containing beta-globin mRNA, which encodes one of the two main proteins found in mature erythrocytes (van Zalen et al., 2015). In enucleated erythrocytes, in which transcription has ceased to occur but translation remains ongoing, YB-1 is important for the stability of beta-globin mRNAs, though it does not appear to affect the translation of such transcripts [or the transcription of beta-globin mRNA prior to enucleation] (van Zalen et al., 2015). YB-1 is a general repressor of translation (Svitkin et al., 2009). Unlike most other general RBPs, e.g. polypyrimidine tract binding protein (PTB) and La autoantigen, YB-1 is found predominantly in the cell cytoplasm rather than the cell nucleus, which may be important for its role in translational silencing (Evdokimova et al., 2006; Svitkin et al., 2009). YB-1 has been

shown to be a major component of translationally silent mRNPs, even in non-hematopoietic cells (Evdokimova et al., 2006; Svitkin et al., 2009; van Zalen et al., 2015). It is known that in RRL there is a relative dearth of RBPs relative to eIF4F, which accounts for the relative cap-, poly(A) tail-, and PABP-independence of RRL compared to HeLa extract (Mikami et al., 2006b; Svitkin et al., 2009). The addition of the RBP YB-1 to RRL caused translation efficiency in RRL to become dependent upon PABP, demonstrating that YB-1 competes with eIF4G for mRNA binding near the 5' cap, leading to a reduction in the association of eIF4E with the 5' cap and enhancing the responsiveness of the eIF4F-mRNA interaction to modulation by PABP (Svitkin et al., 2009). YB-1 was found to have a greater inhibitory effect on 80S complex formation *in vitro* than the other general RBPs tested (Svitkin et al., 2009). Perhaps, TGEV p9 acts in a similar way as YB-1, either directly or via a binding partner, to silence the translation of specific mRNAs.

The overall goal of this research project was to elucidate the way by which TGEV p9 gains access to and/or recognizes template mRNAs, and the mechanism(s) by which it inhibits translation. The long-term goal of the laboratory is to understand the role(s) of the nsp1s in CoV pathogenicity and virulence. The experiments described in this dissertation, in conjunction with the published literature, help to illustrate that the CoV nsp1s, especially SARS-CoV nsp1 and TGEV p9, share a conserved ability to suppress host gene expression although via divergent mechanisms (Narayanan et al., 2014). The shared ability of these nsp1s to suppress host gene expression, suggests that even given the limited amino acid sequence homology among the CoV nsp1s, the CoV nsp1s possess a common origin (Jansson, 2013; Narayanan et al., 2014). However, the divergence in the mechanisms of action of the nsp1s may point to host species-specific adaptations in nsp1 function(s).

The ability for particular nsp1s to antagonize the innate immune response(s) of a host species may be just one example of such adaptation. CoVs are generally limited in

their host range as well as cellular tropism due to the use of host-specific cellular receptors used to gain entry into host cells (de Groot et al., 2011; Graham et al., 2013; Weiss and Navas-Martin 2005). However, in recent years, numerous emerging zoonotic CoVs capable of causing severe disease in humans have been discovered, notably SARS-CoV and MERS-CoV (Graham et al., 2013; Narayanan et al., 2014). The extent to which the nsp1s of such emerging CoVs influence viral virulence and pathogenesis is of great interest (Narayanan et al., 2014). As these CoVs are thought to have jumped species to infect humans, perhaps their pathogenesis can be partially explained by poor adaptation of these CoVs, including their nsp1s, to their human hosts.

An effort to understand the potential role(s) of the nsp1s of the Alpha- and Beta-CoVs in viral virulence and/or pathogenesis, especially in modulation or evasion of the host immune response, should be made. As few of the CoV nsp1s have been studied in detail, more work remains to be done to determine how nsp1 differs among CoVs of the same and different genera, and to determine if conserved structural and/or functional domains can be identified and characterized. Such information would be useful for predicting the functions of other nsp1s, especially the nsp1s of newly discovered or emergent, pathogenic CoVs. A better understanding of the interplay between the nsp1s and the host immune response would help to further our knowledge of viral immune evasion strategies and would potentially be useful in the rational design of antiviral drugs or vaccines against pathogenic CoVs (Narayanan et al., 2014). Studying the interactions between the nsp1s and host cells could also reveal novel regulators or pathways that are involved in host gene expression (Narayanan et al., 2014).

References

- Almeida, M.S., Johnson, M.A., Herrmann, T., Geralt, M., Wuthrich, K., 2007. Novel beta-barrel fold in the nuclear magnetic resonance structure of the replicase nonstructural protein 1 from the severe acute respiratory syndrome coronavirus. *J Virol* 81(7), 3151-3161.
- Anderson, C.W., Straus, J.W., Dudock, B.S., 1983. Preparation of a cell-free protein-synthesizing system from wheat germ. *Methods Enzymol* 101, 635-44.
- Barton, D. J., E. P. Black, and J. B. Flanagan. 1995. Complete replication of poliovirus *in vitro*: preinitiation RNA replication complexes require soluble cellular factors for the synthesis of VPg-linked RNA. *J Virol* 69(9), 5516-27.
- Bhardwaj, K., Guarino, L., Kao, C.C., 2004. The severe acute respiratory syndrome coronavirus Nsp15 protein is an endoribonuclease that prefers manganese as a cofactor. *J Virol* 78(22), 12218-24.
- Björk, P., Wieslander, L., 2014. Mechanisms of mRNA export. *Semin Cell Dev Biol* 32, 47-54.
- Boisvert, M., Bouchard-Levesque, V., Fernandes, S., Tijssen, P., 2014. Classic nuclear localization signals and a novel nuclear localization motif are required for nuclear transport of porcine parvovirus capsid proteins. *J Virol* 88(20), 11748-59.
- Bordeleau, M.E., Mori, A., Oberer, M., Lindqvist, L., Chard, L.S., Higa, T., Belsham, G.J., Wagner, G., Tanaka, J., Pelletier, J., 2006. Functional characterization of IRESes by an inhibitor of the RNA helicase eIF4A. *Nat Chem Biol* 2(4), 213-20.
- Bredenbeek, P.J., Pachuk, C.J., Noten, A.F., Charite, J., Luytjes, W., Weiss, S.R., Spaan, W.J., 1990. The primary structure and expression of the second open reading frame of the polymerase gene of the coronavirus MHV-A59; a highly conserved polymerase is expressed by an efficient ribosomal frameshifting mechanism. *Nucleic Acids Res* 18(7), 1825-32.

- Brian, D.A., Baric, R.S., 2005. Coronavirus genome structure and replication. *Curr Top Microbiol Immunol* 287, 1-30.
- Brockway, S.M., Denison, M.R., 2005. Mutagenesis of the murine hepatitis virus nsp1-coding region identifies residues important for protein processing, viral RNA synthesis, and viral replication. *Virology* 340(2), 209-23.
- Brockway, S.M., Lu, X.T., Peters, T.R., Dermody, T.S., Denison, M.R., 2004. Intracellular localization and protein interactions of the gene 1 protein p28 during mouse hepatitis virus replication. *J Virol* 78(21), 11551-62.
- Carrington, C.V., Foster, J.E., Zhu, H.C., Zhang, J.X., Smith, G.J., Thompson, N., Auguste, A.J., Ramkissoon, V., Adesiyun, A.A., Guan, Y., 2008. Detection and phylogenetic analysis of group 1 coronaviruses in South American bats. *Emerg Infect Dis* 14(12), 1890-3.
- Castello, A., Alvarez, E., Carrasco, L., 2011. The multifaceted poliovirus 2A protease: regulation of gene expression by picornavirus proteases. *J Biomed Biotechnol* 2011, 369648.
- Chai, W., Burwinkel, M., Wang, Z., Palissa, C., Esch, B., Twardziok, S., Rieger, J., Wrede, P., Schmidt, M.F.G., 2013. Antiviral effects of a probiotic *Enterococcus faecium* strain against transmissible gastroenteritis coronavirus. *Arch Virol* 158(4), 799-807.
- Chan, J.F., To, K.K., Tse, H., Jin, D.Y., Yuen, K.Y., 2013. Interspecies transmission and emergence of novel viruses: lessons from bats and birds. *Trends Microbiol* 21(10), 544-55.
- Chen, C.J., Sugiyama, K., Kubo, H., Huang, C., Makino, S., 2004. Murine Coronavirus Nonstructural Protein p28 Arrests Cell Cycle in G0/G1 Phase. *J Virol* 78(19), 10410-19.
- Chen, C.Y., Shyu, A.B., 2014. Emerging mechanisms of mRNP remodeling regulation. *Wiley Interdiscip Rev RNA* 5(5), 713-22.

- Cheng, A., Zhang, W., Xie, Y., Jiang, W., Arnold, E., Sarafianos, S.G., Ding, J., 2005. Expression, purification, and characterization of SARS coronavirus RNA polymerase. *Virology* 335(2), 165-76.
- Chu, D.K., Peiris, J.S., Chen, H., Guan, Y., Poon, L.L., 2008. Genomic characterizations of bat coronaviruses (1A, 1B and HKU8) and evidence for co-infections in *Miniopterus* bats. *J Gen Virol* 89(Pt 5), 1282-7.
- Clark, M.E., Lieberman, P.M., Berk, A.J., Dasgupta, A., 1993. Direct cleavage of human TATA-binding protein by poliovirus protease 3C *in vivo* and *in vitro*. *Mol Cell Biol* 13(2), 1232-7.
- Connor, R.F., Roper, R.L., 2007. Unique SARS-CoV protein nsp1: bioinformatics, biochemistry and potential effects on virulence. *Trends Microbiol* 15(2), 51-3.
- Das, S., Dasgupta, A., 1993. Identification of the cleavage site and determinants required for poliovirus 3C^{Pro}-catalyzed cleavage of human TATA-binding transcription factor TBP. *J Virol* 67(6), 3326-31.
- de Groot, R.J., Baker, S.C., Baric, R., Enjuanes, L., Gorbalenya, A.E., Holmes, K.V., Perlman, S., Poon, L., Rottier, P.J.M., Talbot, P.J., Woo, P.C.Y., Ziebuhr, J., 2011. Family Coronaviridae, In: King, A.M.Q., Adams, M.J., Carstens, E.B., Lefkowitz, E.J. (Eds.), *Virus taxonomy: classification and nomenclature of viruses: ninth report of the International Committee on Taxonomy of Viruses*. Academic Press, Ltd., London, United Kingdom, pp. 806-828.
- Deming, D.J., Graham, R.L., Denison, M.R., Baric, R.S., 2007. Processing of open reading frame 1a replicase proteins nsp7 to nsp10 in murine hepatitis virus strain A59 replication. *J Virol* 81(19), 10280-91.
- Denison, M.R., Hughes, S.A., Weiss, S.R., 1995. Identification and characterization of a 65-kDa protein processed from the gene 1 polyprotein of the murine coronavirus MHV-A59. *Virology* 207(1), 316-20.
- Denison, M.R., Yount, B., Brockway, S.M., Graham, R.L., Sims, A.C., Lu, X., Baric, R.S., 2004. Cleavage between replicase proteins p28 and p65 of mouse hepatitis virus is not required for virus replication. *J Virol* 78(11), 5957-65.

- Drexler, J.F., Gloza-Rausch, F., Glende, J., Corman, V.M., Muth, D., Goettsche, M., Seebens, A., Niedrig, M., Pfefferle, S., Yordanov, S., Zhelyazkov, L., Hermanns, U., Vallo, P., Lukashev, A., Muller, M.A., Deng, H., Herrler, G., Drosten, C., 2010. Genomic characterization of severe acute respiratory syndrome-related coronavirus in European bats and classification of coronaviruses based on partial RNA-dependent RNA polymerase gene sequences. *J Virol* 84(21), 11336-49.
- Drosten, C., Gunther, S., Preiser, W., van der Werf, S., Brodt, H.R., Becker, S., Rabenau, H., Panning, M., Kolesnikova, L., Fouchier, R.A., Berger, A., Burguiere, A.M., Cinatl, J., Eickmann, M., Escriou, N., Grywna, K., Kramme, S., Manuguerra, J.C., Muller, S., Rickerts, V., Sturmer, M., Vieth, S., Klenk, H.D., Osterhaus, A.D., Schmitz, H., Doerr, H.W., 2003. Identification of a novel coronavirus in patients with severe acute respiratory syndrome. *N Engl J Med* 348(20), 1967-76.
- Ehrenfeld E., Brown, D., 1981. Stability of poliovirus RNA in cell-free translation systems utilizing two initiation sites. *J Biol Chem* 256(6), 2656-61.
- Eliseeva, I.A., Lyabin, D.N., Ovchinnikov, L.P., 2013. *Biochemistry (Mosc)* 78(13), 1377-91.
- Enjuanes, L., Sola, I., Alonso, S., Escors, D., Zuniga, S., 2005. Coronavirus reverse genetics and development of vectors for gene expression. *Curr Top Microbiol Immunol* 287, 161-97.
- Evdokimova, V., Ovchinnikov, L.P., Sorensen, P.H., 2006. Y-box binding protein 1: providing a new angle on translational regulation. *Cell Cycle*. 5(11), 1143-7.
- Everly, D. N., Jr., Feng, P., Mian, I.S., Read, G.S., 2002. mRNA degradation by the virion host shutoff (Vhs) protein of herpes simplex virus: genetic and biochemical evidence that Vhs is a nuclease. *J Virol* 76(17), 8560-71.
- Falsey, A.R., McCann, R.M., Hall, W.J., Criddle, M.M., Formica, M.A., Wycoff, D., Kolassa, J.E., 1997. The "common cold" in frail older persons: impact of rhinovirus and coronavirus in a senior daycare center. *J Am Geriatr Soc* 45(6), 706-11.
- Fan, K., Wei, P., Feng, Q., Chen, S., Huang, C., Ma, L., Lai, B., Pei, J., Liu, Y., Chen, J., Lai, L., 2004. Biosynthesis, purification, and substrate specificity of severe acute

- respiratory syndrome coronavirus 3C-like proteinase. *J Biol Chem* 279(3), 1637-42.
- Fendrick, A. M., Monto, A.S., Nightengale, B., Sarnes, M., 2003. The economic burden of non- influenza-related viral respiratory tract infection in the United States. *Arch Intern Med* 163(4), 487-94.
- Floch, A.G., Palancade, B., Doye, V., 2014. Fifty years of nuclear pores and nucleocytoplasmic transport studies: Multiple tools revealing complex rules. *Methods Cell Biol* 122, 1–40.
- Fraser, C. S., Doudna, J.A., 2007. Structural and mechanistic insights into hepatitis C viral translation initiation. *Nat Rev Microbiol* 5(1), 29-38.
- Gaglia, M.M., Covarrubias, S., Wong, W., Glaunsinger, B.A., 2012. A common strategy for host RNA degradation by divergent viruses. *J Virol* 86(17), 9527-30.
- Galan, C., Enjuanes, L., Almazan, F., 2005. A point mutation within the replicase gene differentially affects coronavirus genome versus minigenome replication. *J Virol* 79(24), 15016-26.
- Gloza-Rausch, F., Ipsen, A., Seebens, A., Gottsche, M., Panning, M., Drexler, J.F., Petersen, N., Annan, A., Grywna, K., Muller, M., Pfefferle, S., Drosten, C., 2008. Detection and prevalence patterns of group I coronaviruses in bats, northern Germany. *Emerg Infect Dis* 14(4), 626-31.
- Gorbalenya, A.E., 2001. Big nidovirus genome. When count and order of domains matter. *Adv Exp Med Biol* 494, 1-17.
- Gorbalenya, A.E., Snijder, E.J., Spaan, W.J., 2004. Severe acute respiratory syndrome coronavirus phylogeny: toward consensus. *J Virol* 78(15), 7863-66.
- Gorlich, D., 1998. Transport into and out of the cell nucleus. *Embo J* 17(10), 2721-27.
- Graham R.L., Donaldson, E.F., Baric, R.S., 2013. A decade after SARS: strategies for controlling emerging coronaviruses. *Nat Rev Microbiol* 11(12), 836-48.

- Guan, B.J., Su, Y.P., Wu, H.Y., Brian, D.A., 2012. Genetic evidence of a long-range RNA-RNA interaction between the genomic 5' untranslated region and the nonstructural protein 1 coding region in murine and bovine coronaviruses. *J Virol* 86(8), 4631-43.
- Gustin, K.M., Guan, B.J., Dziduszko, A., Brian, D.A., 2009. Bovine coronavirus nonstructural protein 1 (p28) is an RNA binding protein that binds terminal genomic cis-replication elements. *J Virol* 83(12), 6087-97.
- Habjan, M., Pichlmair, A., Elliott, R.M., Overby, A.K., Glatter, T., Gstaiger, M., Superti-Furga, G., Unger, H., Weber, F., 2009. NSs protein of Rift Valley Fever Virus induces the specific degradation of the double-stranded RNA-dependent protein kinase. *J Virol* 83(9), 4365-75.
- Han, A.P., Yu, C., Lu, L., Fujiwara, Y., Browne, C., Chin, G., Fleming, M., Leboulch, P., Orkin, S.H., Chen, J.J., 2001. Heme-regulated eIF2alpha kinase (HRI) is required for translational regulation and survival of erythroid precursors in iron deficiency. *EMBO J* 20(23), 6909-18.
- Herold, J., Thiel, V., Siddell, S.G., 1998. Characterization of a papain-like cysteine proteinase encoded by gene 1 of the human coronavirus HCV 229E. *Adv Exp Med Biol* 440, 141-7.
- Hinkley, S., Ambagala, A. P., Jones, C.J., and Srikumaran, S., 2000. A vhs-like activity of bovine herpesvirus-1. *Arch Virol* 145(10), 2027-46.
- Hinnebusch, A.G., 2014. The scanning mechanism of eukaryotic translation initiation. *Annu Rev Biochem* 2014. 83, 779–812.
- Hinnebusch, A.G., Lorsch, J.R., 2012. The mechanism of eukaryotic translation initiation: new insights and challenges. *Cold Spring Harb Perspect Biol* 4(10), pii: a011544.
- Huang, C., Ito, N., Tseng, C.T., Makino, S., 2006a. Severe acute respiratory syndrome coronavirus 7a accessory protein is a viral structural protein. *J Virol* 80(15), 7287-94.

- Huang, C., Narayanan, K., Ito, N., Peters, C.J., Makino, S., 2006b. Severe acute respiratory syndrome coronavirus 3a protein is released in membranous structures from 3a protein-expressing cells and infected cells. *J Virol* 80(1), 210-17.
- Huang, C., Peters, C.J., Makino, S., 2007. Severe acute respiratory syndrome coronavirus accessory protein 6 is a virion-associated protein and is released from 6 protein-expressing cells. *J Virol* 81(10), 5423-6.
- Huang, C., Lokugamage, K.G., Rozovics, J.M., Narayanan, K., Semler, B.L., Makino, S., 2011a. Alphacoronavirus transmissible gastroenteritis virus nsp1 protein suppresses protein translation in mammalian cells and in cell-free HeLa cell extracts but not in rabbit reticulocyte lysate. *J Virol* 85(1), 638-43.
- Huang C., Lokugamage, K.G., Rozovics, J.M., Narayanan, K., Semler, B.L., Makino, S., 2011b. SARS Coronavirus nsp1 Protein Induces Template-Dependent Endonucleolytic Cleavage of mRNAs: Viral mRNAs Are Resistant to nsp1-Induced RNA Cleavage. *PLoS Pathog.* 7(12), e1002433.
- Ikegami T., Peters, C.J., Makino, S., 2005. Rift valley fever virus nonstructural protein NSs promotes viral RNA replication and transcription in a minigenome system. *J Virol* 79(9), 5606-15.
- Ikegami, T., Narayanan, K., Won, S., Kamitani, W., Peters, C.J., Makino, S., 2009. Rift Valley fever virus NSs protein promotes post-transcriptional downregulation of protein kinase PKR and inhibits eIF2alpha phosphorylation. *PLoS Pathog* 5(2), e1000287.
- Imbert, I., Guillemot, J.C., Bourhis, J.M., Bussetta, C., Coutard, B., Egloff, M.P., Ferron, F., Gorbalenya, A.E., Canard, B., 2006. A second, non-canonical RNA-dependent RNA polymerase in SARS Coronavirus. *Embo J* 25(20), 4933-42.
- Isaacs, D., Flowers, D., Clarke, J.R., Valman, H.B., MacNaughton, M.R., 1983. Epidemiology of coronavirus respiratory infections. *Arch Dis Child* 58(7), 500-3.
- Ivanov, K.A., Hertzog, T., Rozanov, M., Bayer, S., Thiel, V., Gorbalenya, A.E., Ziebuhr, J., 2004a. Major genetic marker of nidoviruses encodes a replicative endoribonuclease. *Proc Natl Acad Sci U S A* 101(34), 12694-99.

- Ivanov, K.A., Thiel, V., Dobbe, J.C., van der Meer, Y., Snijder, E.J., Ziebuhr, J., 2004b. Multiple enzymatic activities associated with severe acute respiratory syndrome coronavirus helicase. *J Virol* 78(11), 5619-32.
- Jackson, R.J., Hellen, C.U.T., Pestova, T.V., 2010. The mechanism of eukaryotic translation initiation and principles of its regulation. *Nat Rev Mol Cell Biol* 11(2), 113-27.
- Jan, E., Sarnow, P., 2002. Factorless ribosome assembly on the internal ribosome entry site of cricket paralysis virus. *J Mol Biol* 324(5), 889-902.
- Jansson, A.M., 2013. Structure 1 of alphacoronavirus transmissible gastroenteritis virus nsp1 has implications for coronavirus nsp1 function and evolution. *J Virol* 87(5), 2949-55.
- Jauregui, A.R., Savalia, D., Lowry, V.K., Farrell, C.M., Wathelet, M.G., 2013. Identification of residues of SARS-CoV nsp1 that differentially affect inhibition of gene expression and antiviral signaling. *PLoS One* 8(4), e62416.
- Ji, P., Murata-Hori, M., Lodish, H.F., 2011. Formation of mammalian erythrocytes: chromatin condensation and enucleation. *Trends Cell Biol* 21(7), 409-15.
- Jimenez, G., Correa, I., Melgosa, M.P., Bullido, M.J., Enjuanes, J., 1986. Critical Epitopes in Transmissible Gastroenteritis Virus Neutralization. *J Virol* 60(1), 131-9.
- Kamitani, W., Narayanan, K., Huang, C., Lokugamage, K., Ikegami, T., Ito, N., Kubo, H., Makino, S., 2006. Severe acute respiratory syndrome coronavirus nsp1 protein suppresses host gene expression by promoting host mRNA degradation. *Proc Natl Acad Sci U S A* 103(34), 12885-90.
- Kamitani, W., Huang, C., Narayanan, K., Lokugamage, K.G., Makino, S., 2009. A two-pronged strategy to suppress host protein synthesis by SARS coronavirus Nsp1 protein. *Nat Struct Mol Biol* 16(11), 1134-40.
- Kapp, L. D., Lorsch, J.R., 2004. The molecular mechanics of eukaryotic translation. *Annu Rev Biochem* 73, 657-704.

- Kempf, B.J., Barton, D.J., 2008. Poliovirus 2A(Pro) increases viral mRNA and polysome stability coordinately in time with cleavage of eIF4G. *J Virol* 82(12), 5847-59.
- Koppers-Lalic, D., Rijsewijk, F.A., Verschuren, S.B., van Gaans-Van den Brink, J.A., Neisig, A., Rensing, M.E., Neefjes, J., Wiertz, E.J., 2001. The UL41-encoded virion host shutoff (vhs) protein and vhs-independent mechanisms are responsible for down-regulation of MHC class I molecules by bovine herpesvirus 1. *J Gen Virol* 82(Pt 9), 2071-81.
- Ksiazek, T. G., Erdman, D., Goldsmith, C.S., Zaki, S.R., Peret, T. Emery, S. Tong, S., Urbani, C., Comer, J.A., Lim, W., Rollin, P.E., Dowell, S.F., Ling, A.E., Humphrey, C.D., Shieh, W.J. Guarner, J., Paddock, C.D., Rota, P. Fields, B. DeRisi, J., Yang, J.Y., Cox, N., Hughes, J. M., LeDuc, J.W., Bellini, W. J., Anderson, L.J., 2003. A novel coronavirus associated with severe acute respiratory syndrome. *N Engl J Med* 348(20), 1953-66.
- Kuiken, T., Fouchier, R.A., Schutten, M., Rimmelzwaan, G.F., van Amerongen, G. van Riel, D., Laman, J.D., de Jong, T., van Doornum, G., Lim, W., Ling, A.E., Chan, P.K., Tam, J.S., Zambon, M.C., Gopal, R., Drosten, C., van der Werf, S., Escriou, N., Manuguerra, J.C., Stohr, K., Peiris, J.S., Osterhaus, A.D., 2003. Newly discovered coronavirus as the primary cause of severe acute respiratory syndrome. *Lancet* 362(9380), 263-70.
- Kundu, P., Raychaudhuri, S., Tsai, W., Dasgupta, A., 2005. Shutoff of RNA polymerase II transcription by poliovirus involves 3C protease-mediated cleavage of the TATA-binding protein at an alternative Site: incomplete shutoff of transcription interferes with efficient viral replication. *J Virol* 79(15), 9702-13.
- Kuss S.K., Mata, M.A., Zhang, L., Fontoura, B.M., 2013. Nuclear imprisonment: viral strategies to arrest host mRNA nuclear export. *Viruses* 5(7), 1824-49.
- Lange, A., Mills, R.E., Lange, C.J., Stewart, M., Devine, S.E., Corbett, A.H., 2007. Classical nuclear localization signals: definition, function, and interaction with importin alpha. *J Biol Chem* 282(8), 5101-5.
- Larson, H.E., Reed, S.E., Tyrrell, D.A., 1980. Isolation of rhinoviruses and coronaviruses from 38 colds in adults. *J Med Virol* 5(3), 221-9.

- Law, A.H., Lee, D.C., Cheung, B.K., Yim, H.C., Lau, A.S., 2007. Role for nonstructural protein 1 of severe acute respiratory syndrome coronavirus in chemokine dysregulation. *J Virol* 81(1), 416-22.
- Lee, H.J., Shieh, C.K., Gorbalenya, A.E., Koonin, E.V., La Monica, N., Tuler, J., Bagdzhadzhyan, A., Lai, M.M., 1991. The complete sequence (22 kilobases) of murine coronavirus gene 1 encoding the putative proteases and RNA polymerase. *Virology* 180(2), 567-82.
- Lee, Y.N., Chen, L.K., Ma, H.C., Yang, H.H., Li, H.P., Lo, S.Y., 2005. Thermal aggregation of SARS-CoV membrane protein. *J Virol Methods* 129(2), 152-61.
- Lei, L., Ying, S., Baojun, L., Yi, Y., Xiang, H., Wenli, S., Zounan, S., Deyin, G., Qingyu, Z., Jingmei, L., Guohui, C., 2013. Attenuation of mouse hepatitis virus by deletion of the LLRKxGxKG region of Nsp1. *PLoS One* 8(4), e61166.
- Le May, N., Mansuroglu, Z., Leger, P., Josse, G., Blot, T., Billecocq, A., Flick, R., Jacob, Y., Bonnefoy, E., Bouloy, M., 2008. A SAP30 complex inhibits IFN-beta expression in Rift Valley fever virus infected cells. *PLoS Pathog* 4(1), e13.
- Li, Y., Masaki, T., Yamane, D., McGivern, D.R., Lemon, S.M., 2012. Competing and noncompeting activities of miR-122 and the 5' exonuclease Xrn1 in regulation of hepatitis C virus replication. *Proc Natl Acad Sci U S A* 110(5): 1881-86.
- Lokugamage, K.G., Narayanan, K., Huang, C., Makino, S., 2012. Severe Acute Respiratory Syndrome Virus coronavirus protein nsp1 is a novel eukaryotic translation inhibitor that represses multiple steps of translation initiation. *J Virol* 86(24), 13598-608.
- Lomniczi, B., 1977. Biological properties of avian coronavirus RNA. *J Gen Virol* 36(3), 531-3.
- Lomniczi, B., Kennedy, I., 1977. Genome of infectious bronchitis virus. *J Virol* 24(1), 99-107.
- Martinez-Salas, E., Pacheco, A., Serrano, P., Fernandez, N., 2008. New insights into internal ribosome entry site elements relevant for viral gene expression. *J Gen Virol* 89(Pt 3), 611-26.

- Martinez-Salas, E., Francisco-Velilla, R., Fernandez-Chamorro, J., Lozano, G., Diaz-Toledano, R., 2015. Picornavirus IRES elements: RNA structure and host protein interactions. *Virus Res* pii: S0168-1702(15)00018-0.
- Matthews, J.C., Hori, K., Cormier, M.J., 1977. Purification and properties of *Renilla reniformis* luciferase. *Biochemistry* 16(1), 85-91.
- McCray, P.B., Jr., Pewe, L., Wohlford-Lenane, C., Hickey, M., Manzel, L., Shi, L., Netland, J., Jia, H.P., Halabi, C., Sigmund, C.D., Meyerholz, D.K., Kirby, P., Look, D.C., Perlman, S., 2007. Lethal infection of K18-hACE2 mice infected with severe acute respiratory syndrome coronavirus. *J Virol* 81(2), 813-21.
- Menachery, V.D., Eisfeld, A.J., Schafer, A., Josset, L., Sims, A.C., Proll, S., Fan, S., Li, C., Neumann, G., Tilton, S.C., Chang, J., Gralinski, L.E., Long, C., Green, R., Williams, C.M., Weiss, J., Matzke, M.M., Webb-Robertson, B.J., Schepmoes, A.A., Shukla, A.K., Metz, T.O., Smith, R.D., Waters, K.M., Katze, M.G., Kawaoka, Y., Baric, R.S., 2014. Pathogenic influenza viruses and coronaviruses utilize similar and contrasting approaches to control interferon-stimulated gene responses. *MBio* 5(3), e01174-14.
- Merrick, W.C., 1979. Assays for eukaryotic protein synthesis. *Methods Enzymol* 60, 108-123.
- Mikami, S., Kobayashi, T., Yokoyama, S., Imataka, H., 2006a. A hybridoma-based *in vitro* translation system that efficiently synthesizes glycoproteins. *J Biotechnol* 127(1), 65-78.
- Mikami, S., Masutani, M., Sonenberg, N., Yokoyama, S., Imataka, H., 2006b. An efficient mammalian cell-free translation system supplemented with translation factors. *Protein Expr Purif* 46 (2), 348-57.
- Mikami, S., Kobayashi, T., Masutani, M., Yokoyama, S., Imataka, H., 2008. A human cell-derived *in vitro* coupled transcription/translation system optimized for production of recombinant proteins. *Protein Expr Purif* 62(2), 190-8.
- Minskaia, E., Hertzog, T., Gorbalenya, A.E., Campanacci, V., Cambillau, C., Canard, B., Ziebuhr, J., 2006. Discovery of an RNA virus 3'->5' exoribonuclease that is

- critically involved in coronavirus RNA synthesis. *Proc Natl Acad Sci U S A* 103(13), 5108-13.
- Mitchell, S.F., Parker, R., 2014. Principles and properties of eukaryotic mRNPs. *Mol Cell* 54(4), 547-58.
- Mohr, I., Sonenberg, N., 2012. Host translation at the nexus of infection and immunity. *Cell Host Microbe* 12(4), 470-83.
- Muller-McNicoll, M., Neugebauer, K.M., 2013. How cells get the message: dynamic assembly and function of mRNA-protein complexes. *Nat Rev Genet* 14(4), 275-87.
- Narayanan, K., Huang, C., Lokugamage, K.G., Kamitani, W., Ikegami, T., Tseng, C.T., Makino, S., 2008. Severe acute respiratory syndrome coronavirus nsp1 suppresses host gene expression, including that of type I interferon, in infected cells. *J Virol* 82(9), 4471-9.
- Narayanan, K., Ramirez, S.I., Lokugamage, K.G., Makino, S. 2014. Coronavirus nonstructural protein 1: Common and distinct functions in the regulation of host and viral gene expression. *Virus Res pii: S0168-1702(14)00494-8*.
- Natalizio, B.J., Wente, S.R., 2013. Postage for the messenger: designating routes for nuclear mRNA export. *Trends Cell Biol* 23(8), 365-73.
- Nicholson, B.L., White, K.A., 2014. Functional long-range RNA-RNA interactions in positive-strand RNA viruses. *Nat Rev Microbiol* 12(7), 493-504.
- Parsyan, A., Shahbazian, D., Martineau, Y., Petroulakis, E., Alain, T., Larsson, O., Mathonnet, G., Tettweiler, G., Hellen, C.U., Pestova, T.V., Svitkin, Y.V., Sonenberg, N., 2009. The helicase protein DHX29 promotes translation initiation, cell proliferation, and tumorigenesis. *Proc Natl Acad Sci U S A* 106(52), 22217-22.
- Peiris, J. S., Lai, S.T., Poon, L.L., Guan, Y., Yam, L.Y., Lim, W., Nicholls, J., Yee, W. K., Yan, W.W., Cheung, M.T., Cheng, V.C., Chan, K.H., Tsang, D.N., Yung, R.W., Ng, T.K., Yuen, K.Y., 2003. Coronavirus as a possible cause of severe acute respiratory syndrome. *Lancet* 361(9366), 1319-25.

- Pelham, H.R., Jackson, R.J., 1976. An efficient mRNA-dependent translation system from reticulocyte lysates. *Eur J Biochem* 67(1), 247-56.
- Perlman, S., Dandekar, A.A., 2005. Immunopathogenesis of coronavirus infections: implications for SARS. *Nat Rev Immunol* 5(12), 917-27.
- Perlman, S., Netland, J., 2009. Coronaviruses post-SARS: update on replication and pathogenesis. *Nat Rev Microbiol* 7(6), 439-50.
- Pestova, T. V., Hellen, C.U., Shatsky I.N., 1996. Canonical eukaryotic initiation factors determine initiation of translation by internal ribosomal entry. *Mol Cell Biol* 16(12), 6859-69.
- Pestova, T. V., Lomakin, I.B., Lee, J.H., Choi, S.K., Dever, T.E., Hellen, C.U.T., 2000. The joining of ribosomal subunits in eukaryotes requires eIF5B. *Nature* 403(6767), 332-5.
- Pestova, T.V., Hellen, C.U.T., 2003. Translation elongation after assembly of ribosomes on the Cricket paralysis virus internal ribosomal entry site without initiation factors or initiator tRNA. *Genes Dev* 17(2), 181-6.
- Pestova, T.V., Lomakin, I.B., Hellen, C.U.T., 2004. Position of the CrPV IRES on the 40S subunit and factor dependence of IRES/80S ribosome assembly. *EMBO Rep* 5(9), 906-13.
- Pfefferle, S., Schopf, J., Kogl, M., Friedel, C.C., Muller, M.A., Carbajo-Lozoya, J., Stellberger, T., von Dall'Armi, E., Herzog, P., Kallies, S., Niemeyer, D., Ditt, V., Kuri, T., Züst, R., Pumpor, K., Hilgenfeld, R., Schwarz, F., Zimmer, R., Steffen, I., Weber, F., Thiel, V., Herrler, G., Thiel, H.J., Schwegmann-Wessels, C., Pohlmann, S., Haas, J., Drosten, C., von Brunn, A., 2011. The SARS-coronavirus host interactome: identification of cyclophilins as target for pan-coronavirus inhibitors. *PLoS Pathog* 7(10), e1002331.
- Poon, L.L., Chu, D.K., Chan, K.H., Wong, O.K., Ellis, T.M., Leung, Y.H., Lau, S.K., Woo, P.C., Suen, K.Y., Yuen, K.Y., Guan, Y., Peiris, J.S., 2005. Identification of a novel coronavirus in bats. *J Virol* 79(4), 2001-9.

- Poutanen, S. M., Low, D.E., Henry, B., Finkelstein, S., Rose, D., Green, K., Tellier, R., Draker, R., Adachi, D., Ayers, M., Chan, A.K., Skowronski, D.M., Salit, I., Simor, A. E., Slutsky, A.S., Doyle, P.W., Krajden, M., Petric, M., Brunham, R.C., McGeer, A.J., 2003. Identification of severe acute respiratory syndrome in Canada. *N Engl J Med* 348(20), 1995-2005.
- Prentice, E., McAuliffe, J., Lu, X., Subbarao, K., Denison, M.R., 2004. Identification and characterization of severe acute respiratory syndrome coronavirus replicase proteins. *J Virol* 78(18), 9977-86.
- Reusken, C.B., Lina, P.H., Pielaat, A., de Vries, A., Dam-Deisz, C., Adema, J., Drexler, J.F., Drosten, C., Kooi, E.A., 2010. Circulation of group 2 coronaviruses in a bat species common to urban areas in Western Europe. *Vector Borne Zoonotic Dis* 10(8), 785-91.
- Roberts, A., Deming, D., Paddock, C.D., Cheng, A., Yount, B., Vogel, L., Herman, B.D., Sheahan, T., Heise, M., Genrich, G.L., Zaki, S.R., Baric, R., Subbarao, K., 2007. A mouse-adapted SARS-coronavirus causes disease and mortality in BALB/c mice. *PLoS Pathog* 3(1), e5.
- Rota, P.A., Oberste, M.S., Monroe, S.S., Nix, W.A., Campagnoli, R., Icenogle, J.P., Penaranda, S., Bankamp, B., Maher, K., Chen, M.H., Tong, S., Tamin, A., Lowe, L., Frace, M., DeRisi, J.L., Chen, Q., Wang, D., Erdman, D.D., Peret, T.C., Burns, C., Ksiazek, T.G., Rollin, P.E., Sanchez, A., Liffick, S., Holloway, B., Limor, J., McCaustland, K., Olsen-Rasmussen, M., Fouchier, R., Gunther, S., Osterhaus, A.D., Drosten, C., Pallansch, M.A., Anderson, L.J., Bellini, W.J., 2003. Characterization of a novel coronavirus associated with severe acute respiratory syndrome. *Science* 300(5624), 1394-99.
- Saikatendu, K.S., Joseph, J.S., Subramanian, V., Clayton, T., Griffith, M., Moy, K., Velasquez, J., Neuman, B.W., Buchmeier, M.J., Stevens, R.C., Kuhn, P., 2005. Structural basis of severe acute respiratory syndrome coronavirus ADP-ribose-1"-phosphate dephosphorylation by a conserved domain of nsP3. *Structure (Camb)* 13(11), 1665-75.
- Samady, L., Costigliola, E., MacCormac, L., McGrath, Y., Cleverley, S., Lilley, C.E., Smith, J., Latchman, D.S., Chain, B., Coffin, R.S., 2003. Deletion of the virion host shutoff protein (vhs) from herpes simplex virus (HSV) relieves the viral block to dendritic cell activation: potential of vhs- HSV vectors for dendritic cell-mediated immunotherapy. *J Virol* 77(6), 3768-76.

- Semler, B.L., Waterman, M.L., 2008. IRES-mediated pathways to polysomes: nuclear versus cytoplasmic routes. *Trends Microbiol* 16(1), 1-5.
- Shen, H.B., Chou, K.C., 2010. Virus-mPLOC: a fusion classifier for viral protein subcellular location prediction by incorporating multiple sites. *J Biomol Struct Dyn* 28(2), 175-86.
- Silver, P.A., 1991. How proteins enter the nucleus. *Cell* 64(3), 489-497.
- Smiley, J. R. 2004. Herpes simplex virus virion host shutoff protein: immune evasion mediated by a viral RNase? *J Virol* 78(3), 1063-8.
- Smith, I., Wang, L.F., 2013. Bats and their virome: an important source of emerging viruses capable of infecting humans. *Curr Opin Virol* 3(1), 84-91.
- Snijder, E.J., Bredenbeek, P.J., Dobbe, J.C., Thiel, V., Ziebuhr, J., Poon, L.L., Guan, Y., Rozanov, M., Spaan, W.J., Gorbalenya, A.E., 2003. Unique and conserved features of genome and proteome of SARS-coronavirus, an early split-off from the coronavirus group 2 lineage. *J Mol Biol* 331(5), 991-1004.
- Sonenberg, N., Hinnebusch, A.G., 2009. Regulation of translation initiation in eukaryotes: mechanisms and biological targets. *Cell* 136(4), 731-45.
- Soto Rifo, R., Ricci, E.P., Decimo, D., Moncorge, O., Ohlmann, T., 2007. Back to basics: the untreated rabbit reticulocyte lysate as a competitive system to recapitulate cap/poly(A) synergy and the selective advantage of IRES-driven translation. *Nucleic Acids Res* 35(18), e121.
- Spahn, C.M., Jan, E., Mulder, A., Grassucci, R.A., Sarnow, P., Frank, J., 2004. Cryo-EM visualization of a viral internal ribosome entry site bound to human ribosomes: The IRES functions as an RNA-based translation factor. *Cell* 118(4), 465-75.
- Sturman, L.S., Holmes, K.V., Behnke, J., 1980. Isolation of coronavirus envelope glycoproteins and interaction with the viral nucleocapsid. *J Virol* 33(1), 449-62.
- Su, Y.P., Fan, Y.H., Brian, D.A., 2014. Dependence of Coronavirus RNA Replication on an NH2-Terminal Partial Nonstructural Protein 1 in cis. *J Virol* 88(16), 8868-82.

- Subissi, L., Imbert, I., Ferron, F., Collet, A., Coutard, B., Decroly, E., Canard, B., 2014. SARS-CoV ORF1b-encoded nonstructural proteins 12-16: replicative enzymes as antiviral targets. *Antiviral Res* 101, 122-30.
- Suzutani, T., Nagamine, M., Shibaki, T., Ogasawara, M., Yoshida, I., Daikoku, T., Nishiyama, Y., Azuma, M., 2000. The role of the UL41 gene of herpes simplex virus type 1 in evasion of non-specific host defense mechanisms during primary infection. *J Gen Virol* 81(Pt 7), 1763-71.
- Svitkin, Y.V., Evdokimova, V.M., Brasey, A., Pestova, T.V., Fantus, D., Yanagiya, A., Imataka, H., Skabkin, M.A., Ovchinnikov, L.P., Merrick, W.C., Sonenberg, N., 2009. General RNA-binding proteins have a function in poly(A)-binding protein-dependent translation. *EMBO J* 28(1), 58-68.
- Taddeo, B., Zhang, W., Roizman, B., 2006. The UL41 protein of herpes simplex virus 1 degrades RNA by endonucleolytic cleavage in absence of other cellular or viral proteins. *Proc Natl Acad Sci U S A* 103(8), 2827-32.
- Tanaka, T., Kamitani, W., DeDiego, M.L., Enjuanes, L., Matsuura, Y., 2012. Severe acute respiratory syndrome coronavirus nsp1 facilitates efficient propagation in cells through a specific translational shutoff of host mRNA. *J Virol* 86(20), 11128-37.
- Tang, X.C., Zhang, J.X., Zhang, S.Y., Wang, P., Fan, X.H., Li, L.F., Li, G., Dong, B.Q., Liu, W., Cheung, C.L., Xu, K.M., Song, W.J., Vijaykrishna, D., Poon, L.L., Peiris, J.S., Smith, G.J., Chen, H., Guan, Y., 2006. Prevalence and genetic diversity of coronaviruses in bats from China. *J Virol* 80(15), 7481-90.
- Tesfay, M.Z., Yin, J., Gardner, C.L., Khoretonenko, M.V., Korneeva, N.L., Rhoads, R.E., Ryman, K.D., Klimstra, W.B., 2008. Alpha/Beta Interferon Inhibits Cap-Dependent Translation of Viral but Not Cellular mRNA by a PKR-Independent Mechanism. *J Virol* 82(6), 2620-30.
- Thiel, V., Ivanov, K.A., Putics, A., Hertzog, T., Schelle, B., Bayer, S., Weissbrich, B., Snijder, E.J., Rabenau, H., Doerr, H.W., Gorbalenya, A.E., Ziebuhr, J., 2003. Mechanisms and enzymes involved in SARS coronavirus genome expression. *J Gen Virol* 84(Pt 9), 2305-15.

- Tigges, M. A., Leng, S., Johnson, D.C., Burke, R.L., 1996. Human herpes simplex virus (HSV)-specific CD8+ CTL clones recognize HSV-2-infected fibroblasts after treatment with IFN-gamma or when virion host shutoff functions are disabled. *J Immunol* 156(10), 3901-10.
- Todd, S., J. S. Towner, and B. L. Semler. 1997. Translation and replication properties of the human rhinovirus genome *in vivo* and *in vitro*. *Virology* 229(1), 90-7.
- Tohya, Y., Narayanan, K., Kamitani, W., Huang, C., Lokugamage, K.G., Makino, S., 2009. Suppression of host gene expression by nsp1 proteins of group 2 bat coronaviruses. *J Virol* 83(10), 5282-8.
- Trgovcich, J., Johnson, D., Roizman, B., 2002. Cell surface major histocompatibility complex class II proteins are regulated by the products of the gamma(1)34.5 and U(L)41 genes of herpes simplex virus 1. *J Virol* 76(14), 6974-86.
- Tsang, K. W., Ho, P.L., Ooi, G.C., Yee, W.K., Wang, T., Chan-Yeung, M., Lam, W.K., Seto, W.H., Yam, L.Y., Cheung, T.M., Wong, P.C., Lam, B., Ip, M.S., Chan, J., Yuen, K.Y., Lai, K.N., 2003. A cluster of cases of severe acute respiratory syndrome in Hong Kong. *N Engl J Med* 348(20), 1977-85.
- Tseng, C.T., Huang, C., Newman, P., Wang, N., Narayanan, K., Watts, D.M., Makino, S., Packard, M.M., Zaki, S.R., Chan, T.S., Peters, C.J., 2007. Severe acute respiratory syndrome coronavirus infection of mice transgenic for the human Angiotensin converting enzyme 2 virus receptor. *J Virol* 81(3), 1162-73.
- Vabret, A., Mourez, T., Gouarin, S., Petitjean, J., Freymuth, F., 2003. An outbreak of coronavirus OC43 respiratory infection in Normandy, France. *Clin Infect Dis* 36(8), 985-9.
- Vabret, A., Dina, J., Gouarin, S., Petitjean, J., Tripey, V., Brouard, J., Freymuth, F., 2008. Human (non-severe acute respiratory syndrome) coronavirus infections in hospitalised children in France. *J Paediatr Child Health* 44(4), 176-81.
- van Boheemen, S., de Graaf, M., Lauber, C., Bestebroer, T.M., Raj, V.S., Zaki, A.M., Osterhaus, A.D., Haagmans, B.L., Gorbalenya, A.E., Snijder, E.J., Fouchier, R.A., 2012. Genomic characterization of a newly discovered coronavirus associated with acute respiratory distress syndrome in humans. *MBio* 3(6), pii: e00473-12.

- van der Hoek, L., Pyrc, K., Berkhout, B., 2006. Human coronavirus NL63, a new respiratory virus. *FEMS Microbiol Rev* 30(5), 760-73.
- Van Herwynen, J.F., Beckler, G.S., 1995. Translation using a wheat-germ extract. *Methods Mol Biol* 37, 245-51.
- van Zalen, S., Lombardi, A.A., Jeschke, G.R., Hexner, E.O., Russell, J.E., 2015. AUF-1 and YB-1 independently regulate beta-globin mRNA in developing erythroid cells through interactions with poly(A)-binding protein. *Mech Dev*, pii: S0925-4773(15)00022-2.
- Ventoso, I., MacMillan, S.E., Hershey, J.W., Carrasco, L., 1998. Poliovirus 2A proteinase cleaves directly the eIF-4G subunit of eIF-4F complex. *FEBS Lett* 435(1), 79-83.
- Walsh, D., Mohr, I., 2011. Viral subversion of the host protein synthesis machinery. *Nat Rev Microbiol* 9(12), 860-75.
- Walsh, D., Matthews, M.B., Mohr, I., 2013. Tinkering with translation: protein synthesis in virus-infected cells. *Cold Spring Harb Perspect Biol* 5(1), a012351.
- Wang, L., Ge, C., Wang, D., Li, Y., Hu, J., 2013. The survey of porcine teschoviruses, porcine circovirus and porcine transmissible gastroenteritis virus infecting piglets in clinical specimens in China. *Trop Anim Health Prod* 45(5), 1087-91.
- Wang, X., Li, G.Z., Lu, W.C., 2013. Virus-ECC-mPLoc: a multi-label predictor for predicting the subcellular localization of virus proteins with both single and multiple sites based on a general form of Chou's pseudo amino acid composition. *Protein Pept Lett* 20(3), 309-17.
- Wang, Y., Shi, H., Rigolet, P., Wu, N., Zhu, L., Xi, X.G., Vabret, A., Wang, X., Wang, T., 2010. Nsp1 proteins of group I and SARS coronaviruses share structural and functional similarities. *Infect Genet Evol* 10(7), 919-924.
- Wathelet, M. G., Orr, M., Frieman, M.B., Baric, R.S., 2007. Severe acute respiratory syndrome coronavirus evades antiviral signaling: role of nsp1 and rational design of an attenuated strain. *J Virol* 81(21), 11620-33.

- Weiss, S.R., Navas-Martin, S., 2005. Coronavirus pathogenesis and the emerging pathogen severe acute respiratory syndrome coronavirus. *Microbiol Mol Biol Rev* 69(4), 635-64.
- Wertheim, J.O., Chu, D.K., Peiris, J.S., Kosakovsky Pond, S.L., Poon, L.L., 2013. A case for the ancient origin of coronaviruses. *J Virol* 87(12), 7039-45.
- Wilson, J.E., Pestova, T.V., Hellen, C.U., Sarnow, P., 2000. Initiation of protein synthesis from the A site of the ribosome. *Cell* 102(4), 511-20.
- Woo, P.C., Huang, Y., Lau, S.K., Yuen, K.Y., 2010. Coronavirus genomics and bioinformatics analysis. *Viruses* 2(8), 1804-20.
- Woo, P.C., Lau, S.K., Lam, C.S., Lau, C.C., Tsang, A.K., Lau, J.H., Bai, R., Teng, J.L., Tsang, C.C., Wang, M., Zheng, B.J., Chan, K.H., Yuen, K.Y., 2012. Discovery of seven novel Mammalian and avian coronaviruses in the genus deltacoronavirus supports bat coronaviruses as the gene source of alphacoronavirus and betacoronavirus and avian coronaviruses as the gene source of gammacoronavirus and deltacoronavirus. *J Virol* 86(7), 3995-4008.
- Yarborough, M.L., Mata, M.A., Sakthivel, R., Fontoura, B.M., 2014. Viral subversion of nucleocytoplasmic trafficking. *Traffic* 15(2), 127-40.
- Yi, M., D. E. Schultz, and S. M. Lemon. 2000. Functional significance of the interaction of hepatitis A virus RNA with glyceraldehyde 3-phosphate de- hydrogenase (GAPDH): opposing effects of GAPDH and polypyrimidine tract binding protein on internal ribosome entry site function. *J Virol* 74(14), 6459-68.
- York, A., Fodor, E., 2013. Biogenesis, assembly, and export of viral messenger ribonucleoproteins in the influenza A virus infected cell. *RNA Biology*, 10(8), 1274-82.
- Zaki, A.M., van Boheemen, S., Bestebroer, T.M., Osterhaus, A.D., Fouchier, R.A., 2012. Isolation of a novel coronavirus from a man with pneumonia in Saudi Arabia. *N Engl J Med* 367(19), 1814-20.

- Ziebuhr, J., Thiel, V., Gorbalenya, A.E., 2001. The autocatalytic release of a putative RNA virus transcription factor from its polyprotein precursor involves two paralogous papain-like proteases that cleave the same peptide bond. *J Biol Chem* 276(35), 33220-32.
- Ziebuhr, J., 2005. The coronavirus replicase. *Curr Top Microbiol Immunol* 287, 57-94.
- Ziebuhr, J., Schelle, B., Karl, N., Minskaia, E., Bayer, S., Siddell, S.G., Gorbalenya, A.E., Thiel, V., 2007. Human coronavirus 229E papain-like proteases have overlapping specificities but distinct functions in viral replication. *J Virol* 81(8), 3922-32.
- Zust, R., Cervantes-Barragan, L., Kuri, T., Blakqori, G., Weber, F., Ludewig, B., Thiel, V., 2007. Coronavirus non-structural protein 1 is a major pathogenicity factor: implications for the rational design of coronavirus vaccines. *PLoS Pathog* 3(8), e109.

Vita

Sydney Ilima Ramirez was born on May 14, 1983, in Arcata, California, to Arnold Kei-Ung Chun, M.D. and Marcia Ehinger, M.D. She is married to Bruce Lee Ramirez Cahuachi. They have one daughter, Aliya Elisabeth Ramirez. She graduated summa cum laude from California State University, Sacramento, in Sacramento, California, with her Bachelor of Science Degree. Sydney majored in Biological Sciences with concentrations in Molecular Biology and Microbiology, and a minor in Chemistry. During her undergraduate studies, Sydney became interested in microbiology and biomedical research and participated in a year-long honors program in the laboratory of Christine A. Kirvan, PhD, studying Pediatric Autoimmune Neuropsychiatric Disorders Associated with Streptococcal Infections. Sydney joined the University of Texas Medical Branch (UTMB) M.D.-Ph.D. Combined Degree Program in 2008, where she was able to conduct her PhD research in the UTMB Experimental Pathology Graduate Program under the mentorship of Shinji Makino, D.V.M., Ph.D. While in Dr. Makino's laboratory, Sydney studied Rift Valley fever virus (RVFV) and coronaviruses. Her dissertation focuses on the mechanism used by the non-structural protein 1 (nsp1) of transmissible gastroenteritis virus (TGEV), an alphacoronavirus, to suppress of gene expression.

During her graduate studies at UTMB, Sydney has received several awards and honors. She was recipient of a T32 biodefense training grant from the National Institutes of Health (NIH), which funded her work with RVFV from 2010-2012. She was also a recipient of a Truman Graves Blocker Jr. Research Scholar Minnie and Ward Savage Endowed Award in 2010 and a 2014-2015 Blocker Fellowship in Biomedical Research, which provided support from the Joseph Ferrell York and Mary Belle York Memorial School of Medicine Scholarship Fund and the Harry and Margaret Kelso Endowed

Blocker Scholarship. She received the Edward S. Reynolds award twice, in 2012 and 2013, for her poster presentations at the annual UTMB Department of Pathology's Trainee Research Day. In 2014, she received a Student Travel Grant from the American Society for Virology (ASV) to present her work at the ASV annual meeting.

Education

B.S., May 2008, California State University, Sacramento, Sacramento, California

Publications

Murakami S., Terasaki K., Ramirez S.I., Morrill J.C., Makino S. 2014. Development of a Novel, Single-Cycle Replicable Rift Valley Fever Vaccine. PLoS Negl Trop Dis 8(3): e2746. doi: 10.1371/journal.pntd.0002746

Narayanan, K., Ramirez, S.I., Lokugamage, K.G., Makino, S. 2014. Coronavirus nonstructural protein 1: Common and distinct functions in the regulation of host and viral gene expression. Virus Res. (2014), <http://dx.doi.org/10.1016/j.virusres.2014.11.019>

Summary of Dissertation

Alpha- and betacoronaviruses encode a non-structural protein 1 (nsp1) capable of inhibiting host gene expression, while accumulating data suggest that divergent mechanisms of suppression of host gene expression exist among the nsp1s. Unlike the nsp1 of SARS coronavirus, a group 2b betacoronavirus, the nsp1 of transmissible gastroenteritis virus (TGEV), an alphacoronavirus, inhibits the expression of host genes without associating with the 40S ribosomal subunit or inducing the endonucleolytic

cleavage of mRNAs. In this dissertation, the mechanism of TGEV nsp1-mediated translation inhibition was studied using reporter constructs in *in vitro* cell-free translation systems as well as in expressed cells. The TGEV nsp1 strongly inhibits the translation of capped mRNAs, including those carrying the TGEV 5' and 3' untranslated regions, as well as certain internal ribosome entry site-containing mRNAs, in HeLa S10 extract, but only weakly inhibits the translation of the same mRNAs in rabbit reticulocyte lysate (RRL) or wheat germ extract (WGE). Increasing the amount of TGEV nsp1 protein used for the *in vitro* translation reaction somewhat increased TGEV nsp1 activity in RRL or WGE, or either system supplemented with HeLa extract. Increasing the incubation time also somewhat increased TGEV nsp1 activity in RRL or RRL supplemented with HeLa extract. Immunofluorescence and confocal microscopic analysis showed that TGEV nsp1 localizes to both the nucleus and cytoplasm of expressed cells. TGEV nsp1 may enter the nucleus via passive diffusion because its molecular weight (~9kDa) is below the nuclear pore complex passive diffusion limit. Both TGEV infection and TGEV nsp1 protein expression inhibit cellular protein synthesis. TGEV nsp1 expression strongly inhibits the expression of reporter genes from transfected reporter plasmids. However, it fails to inhibit the translation of exogenous reporter mRNAs directly introduced into the cytoplasm. The findings presented in this dissertation correlate well with the hypothesis that a factor in HeLa extract enhances TGEV nsp1 activity, and suggest that in cells this factor(s) allows TGEV nsp1 to access and inhibit the translation of nuclear-derived mRNAs. In cell extracts or lysates, which lack subcellular compartmentalization, this host factor(s) allows TGEV nsp1 to access certain *in vitro* transcribed mRNAs.

Permanent address: 16810 Hibiscus Lane, Friendswood, TX 77546

This dissertation was typed by Sydney Ilima Ramirez.